

**LIMESTONE SLURRY SCRUBBING - MODELING AND
PARAMETER ESTIMATION**

**APPROVED BY
DISSERTATION COMMITTEE:**

Gary T. Rochelle, Supervisor

Thomas F. Edgar

James R. Fair

James B. Rawlings

Kamy Sepehrnoori

Copyright
by
Rajesh Agarwal
1995

Dedication

To my parents, Rajyashri and Satish Agarwal.

**LIMESTONE SLURRY SCRUBBING - MODELING AND
PARAMETER ESTIMATION**

by

RAJESH SATISH AGARWAL, B. CHEM. ENGG., M.S.

DISSERTATION

Presented to the Faculty of the Graduate School of

The University of Texas at Austin

in Partial Fulfillment

of the Requirements

for the Degree of

DOCTOR OF PHILOSOPHY

THE UNIVERSITY OF TEXAS AT AUSTIN

May, 1995

Acknowledgments

I would like to thank Dr. Rochelle for his patience and encouragement. I have always been impressed and inspired by his ability to quickly and accurately analyze seemingly difficult chemical engineering problems.

Among my colleagues I have found good friends and good people. I wish to thank Todd Carey for making me feel a part of many things American, Shrikar Chakravarti for introducing me to the joy of taking courses at the graduate school, and Mshewa Msafiri for his constant encouragement through the last few months of this dissertation. Some of the best of times have been spent with Harold Johnson, waxing philosophic and savoring the delights of his Indian-American cooking. The years spent in the graduate program would not have been the same without Renae Vandekemp, Francesco Pepe, David Stroud, Jeremy Bednarz, Joseph DeVincentis, Chen Shen, Mark Posey, Lia Arthur, and Phillip Wasserman.

I have never had to look very far to find my heroes. I wish to acknowledge my aunts, Usha, Kamal, and Bharti, and my uncle Anand for being excellent role models. Above all, I wish to thank my parents for their unquestioning faith in my abilities and God Almighty for making all things possible.

LIMESTONE SLURRY SCRUBBING - MODELING AND PARAMETER ESTIMATION

Publication No. _____

Rajesh Satish Agarwal, Ph. D.
The University of Texas at Austin, 1995

Supervisor: Gary T. Rochelle

The Amendments to the Clean Air Act of 1990 require a reduction in the emission of sulfur dioxide (SO_2) into the atmosphere. Electric power utilities are a major source of SO_2 emissions and come under the purview of the Clean Air Act. Limestone slurry scrubbing is the dominant technology for controlling SO_2 emissions generated by these utilities.

The development of a FORTRAN model for simulation of the Limestone Slurry Scrubbing process has been an ongoing effort at the University of Texas at Austin for the past fourteen years. The present investigation is focused on calculating the adjustable parameters in the model. These parameters are calculated using data from bench-scale and pilot-scale absorbers. The estimated parameters can be used to describe mass-transfer characteristics of turbulent contact absorbers operated under similar hydrodynamic conditions, i.e., liquid

velocity, gas velocity and packed height. The uncertainty in the estimated values of the parameters has been quantified using statistics.

The parameters were estimated using Generalized REGression (GREG, Caracotsios, 1986). This FORTRAN program used the Maximum Likelihood Principle to estimate adjustable parameters.

The calculated values indicate that the parameters N_g and k°_L/k_g are similar for both the bench-scale and pilot-scale absorbers under similar hydrodynamic conditions. These estimates were found to be highly dependent on each other, due to the nature of the data and the parameters. More independent estimates could be obtained if the parameter set N_g and $N_g k^{\circ}_L/k_g$ was used.

The effect of liquid phase chemistry on the absorption of SO_2 was also investigated using the model. The investigations show that hydrolysis reaction plays a significant role in the enhancement of SO_2 absorption. The alkalinity due to HCO_3^- and $SO_3^{=}$ does not play a major role below pH of 5. The presence of high concentrations of buffer additives can lead to conditions of gas film control.

Table of Contents

List of Figures	xii
List of Tables	xiv
CHAPTER 1: INTRODUCTION	1
1.1 Background	1
1.2 Other Models	4
1.2.1 FGDPRIISM (Flue Gas Desulfurization Process Integration and Simulation Model)	5
1.2.1.1 Thermodynamic Calculations	5
1.2.1.2 Gas/Liquid Mass Transfer	5
1.2.1.3 Solid/Liquid Mass Transfer	6
1.2.1.4 Hydrodynamic model	6
1.2.1.5 Model Parameters	7
1.2.2 Semi-empirical Model	7
1.3 Previous Work in FGDTX modeling	8
1.3.1 Historical Development of FGDTX	8
1.4 Previous Work in Parameter Estimation	11
1.5 Scope of Investigation	13
1.6 Notation	17
CHAPTER 2: MODEL DESCRIPTION	19
2.1 Introduction	19
2.2 Process Description	19
2.2.1 Scrubber Reactions	22
2.2.2 Hold Tank Reactions	22
2.3 Overall Model Solution	23
2.3.1 General Model Description	23
2.3.1 Convergence Procedure	25
2.3.1.1 Stage Convergence.	26
2.3.1.2 Scrubber and Hold Tank Convergence	26

2.3.1.3 Overall Convergence	26
2.3.1.4 Numerical Procedures and Specified Tolerances	26
2.4 Model Description	28
2.4.1 Solution Thermodynamics	29
2.4.2 Calculation for Gas/Liquid Mass Transfer	32
2.4.3 Solid/Liquid Transport.....	34
2.4.3.1 Limestone Dissolution Model.....	35
2.4.3.2 Crystallization Models	41
2.4.4 Stage Calculations	42
2.5 Modifications	44
2.6 Notation	46
CHAPTER 3: MODEL CHEMISTRY	50
3.1 Introduction.....	50
3.2 Base Case Conditions	51
3.2.1 Calculation of Results	51
3.3 Results.....	55
3.3.1 Effect of Inlet SO ₂	56
3.3.2 Effect of Limestone Utilization	59
3.3.3 Effect of Residence Time in the Hold Tank	63
3.3.4. Effect of Solution Composition	64
3.3.5 Effect of Liquid-to-Gas Ratio	65
3.3.6 Effect of DBA Addition.....	68
3.4 Conclusions.....	72
3.5 Notation	73
CHAPTER 4: PARAMETER ESTIMATION	75
4.1 Introduction.....	75
4.2 Parameters Used For Regression	75
4.3 Data Used For Regression	79
4.4 Method of Regression - GREG Usage.....	86
4.4.2 Objective Function.....	90
4.4.3 Confidence Intervals/Regions and Co-Variance	91

4.4.4 Interpretation of Confidence Intervals/Regions and Co-variance	92
4.4.5 GREG - Sample Input/Output files	94
4.5 Results	95
4.5.1 Transformation of the Dependent Variable	104
4.6 Empirical Correlations	110
4.7 Comparison Between Model Estimates and Experimental Measurements	112
4.7.1 Measurement of N_g and N_L for the EPA/RTP contactor	114
4.7.2 Measurement of N_g for the Shawnee contactor	115
4.7.3 Comparison of the Effects of Wall Area between Shawnee and EPA/RTP contactors	115
4.7.4 Measurement of N_g for a Single-Stage TCA	117
4.7.5 Comparison Between Model Calculations and Experimental Observations	118
4.8 Notation	120
CHAPTER 5: CONCLUSIONS AND RECOMMENDATIONS	123
5.1 Conclusions	123
5.2 Recommendations	125
APPENDIX A: MODEL EQUATIONS	126
A-1 Introduction	126
A-2 Material Balance Equations for the n^{th} Stage	131
A-3 Hold Tank Calculations	142
A-4 Calculation of composition in the Bulk Solution, at the Gas/Liquid Interface and at the Solid Surface	146
A-5 Initial Calculations	155
A-6 Summary	164
A-7 Notation	171
APPENDIX B: CALCULATED RESULTS SHOWING THE EFFECTS OF SOLUTION CHEMISTRY	175
APPENDIX C: SAMPLE CALCULATIONS - DESIGN EXAMPLE	184
C-1 Input file : mdiva.dat	186

C-2 Input file: p_est.dat	190
C-3 Output File : Sample Calculation	192
APPENDIX D: SAMPLE FILES FOR PARAMETER ESTIMATION	198
D-1 Driver routine for calling GREG (p_est.f)	198
D-2 Input file for parameter estimation (EPA/RTP data).	205
D-3 Input file for parameter estimation (Shawnee data).	207
D-4 Output file showing results of regression (EPA/RTP data).....	210
D-5 Calculated values of the H matrix (EPA/RTP data).	216
REFERENCES CITED	217
VITA	

List of Figures

Figure 1.1: Process Flow Diagram of the Limestone Slurry Scrubbing System.....	2
Figure 1.2: Calculated Model Sensitivity to Adjustable Model Parameters.	14
Figure 2.1: Process Flow Diagram Showing a Scrubber and a Hold Tank.	21
Figure 2.2: Axial Mixing Data for a Single Stage TCA (Chen and Douglas, 1968) Versus Theoretical Predictions (Smith, 1981).	43
Figure 3.1: Effect of Change of Inlet SO ₂ Concentration on the Penetration.	58
Figure 3.2: Effects of Limestone Utilization on Penetration and pH at Hold Tank Residence Times of 100 s and 540 s.	60
Figure 3.3: Effect of Constant Inlet pH on Penetration Over a Range of Limestone Utilization.	64
Figure 3.4: Scrubber Performance as a Function of Liquid Rate with a Constant and Variable Number of Gas Phase Transfer Units	66
Figure 3.5: Effect of Dibasic Acid Concentration (ppm) on SO ₂ Penetration (N _g = 2.3, k _L = 200 cc-atm/gmol)	69
Figure 4.1: Measured Values of SO ₂ Penetration for the Large Scale (Shawnee) and Small Scale (EPA/RTP) Contactors (U = 45% to 95%).	83
Figure 4.2: Experimental Data for Large Scale (Shawnee) and Small Scale (EPA/RTP) Contactors (DBA concentration = 0 to 3600 ppm).	85

Figure 4.3: Comparison Between Measured and Predicted (p and pH) Values for the EPA/RTP Contactor.	96
Figure 4.4: Confidence Regions for the N_g and k^o_L/k_g (Response Variable = $-\ln p$, EPA/RTP data).	101
Figure 4.5: Confidence Regions for the N_g and k^o_L/k_g (estimated using $-\ln p$ as the Response Variable for the EPA/RTP data).	103
Figure 4.6: Comparison of Calculated Penetration Values Obtained by Fitting SO_2 Penetration (p) and $-\ln p$ for the EPA/RTP Contactor.	105
Figure 4.7: Comparison of Error (in p) from Fitting the EPA/RTP Data and a Normal Distribution.	106
Figure 4.8: Comparison Between Error (in $-\ln p$) from Fitting EPA/RTP Data and a Normal Distribution.	107

List of Tables

Table 2.1: Material balance equations for stagewise calculations.	44
Table 3.1: Base Case Conditions Used for the Simulation of the TCA Contactor at EPA/RTP.	52
Table 3.2: Effect of Inlet SO ₂ Partial Pressure on Calculated Enhancement Factors (E) and Extent of Gas Film Resistance (K_g/k_g)	57
Table 3.3: Effect of Change of Limestone Utilization (U) and Hold Tank Residence Time ($N_g/\text{stage} = 2.3$, $L/G = 0.2$ L/gmol).	61
Table 3.4: Effect of Change of (L/G) on SO ₂ penetration, Due to Change of Liquid Capacity and Gas Film Mass Transfer Units at $U = 77\%$, $t_{\text{res}}^\dagger = 540$ s.	67
Table 3.5: Effect of DiBasic Acid (DBA) Concentrations on SO ₂ Penetration and Extent of Gas Film Resistance $\frac{K_g}{k_g}$ ($L/G = 0.2$ L/gmol, $U =$ 77%).	70
Table 4.1: Sensitivity of $-\ln p$ to N_g and k°_L/k_g ($N_g = 3$, $N_L = 3$, and $k^\circ_L/k_g = 235$ atm-ml/gmol).	77
Table 4.2: Operating Parameters for Turbulent Contact Absorbers at EPA/RTP (Chang and Dempsey, 1981) and Shawnee (Burbank and Wang, 1981).	80

Table 4.3: Data from EPA/RTP reactor ($L/G = 60$ gal/Mcf, $G = 300$ acfm, $Cl = 500$ ppm, $P_{SO_2} = 2.9e-3$ atm). The calculated values of $-\ln$ p correspond to the values calculated fitting both $-\ln p$ and pH , $-\ln p$, and p	81
Table 4.4: Data from Shawnee Contactor ($L/G = 50$ gal/Mcf, $G = 30000$ acfm, $Cl = 2000$ ppm).	82
Table 4.5: Comparison of the Fits Obtained for the EPA/RTP Data.	97
Table 4.6: Comparison of the Fits Obtained for the Shawnee Data	99
Table 4.7: Parameter estimation Results for a Subset of EPA/RTP Data.	104
Table 4.8: Comparison Between Calculated Residuals ($-\ln p$) and Normal Variables for the EPA/ RTP Data.	108
Table 4.9: Comparison Between Calculated Residuals (SO_2 penetration) and Normal Variables for the EPA/ RTP Data.	109
Table 4.10: Factorial Data from Shawnee Contactor, Showing Effects of L , G in the Presence and Absence of Packing ($Cl^- \sim 6000$ ppm, c.s. area = 32 ft^2 , packing height = 15 inches).	111
Table 4.11: Comparison Between the Experimental Conditions at EPA/RTP and Shawnee and the Conditions in Other Experimental Studies. .	113
Table 4.12: Calculated Areas of the Packing and Wall for the EPA/RTP (Small-scale) and Shawnee (Large-scale) Contactors.	116
Table 4.13: Comparison of the Solution Capacity for Absorption of Ammonia in Water (Douglas, 1964) with Solution Capacity for the Absorption of SO_2 in Na_2CO_3 Solution (Epstein et al., 1973)	120

CHAPTER 1

INTRODUCTION

This chapter begins with a brief background on some of the important factors that motivate reduction of SO₂ emission levels in the atmosphere. Thereafter, previous efforts at modeling limestone slurry scrubbing systems are reviewed. Finally, the scope of this investigation is outlined.

1.1 BACKGROUND

The presence of acidic compounds and their precursors in the atmosphere and in their deposition from the atmosphere present a threat to natural resources, ecosystems, materials, visibility, and public health. The principal sources of acidic compounds and their precursors in the atmosphere are emissions of sulfur and nitrogen oxides generated from the combustion of fossil fuels.

The Clean Air Act amendments of 1990 have focused attention on regulating the emission of sulfur dioxide. By the year 2009, they seek to reduce SO₂ emission levels by a total of ten million tons per annum under the 1980 emission levels. Electric utilities are a major source of SO₂ emissions and come under the purview of the Clean Air Act. Each utility is required to comply annually with a predetermined emission level. The new legislation levies heavy penalties on excessive emissions and also provides incentives for a reduction of emissions over the allotted levels.

Limestone slurry scrubbing is the dominant technology for flue gas desulfurization (Figure 1.1).

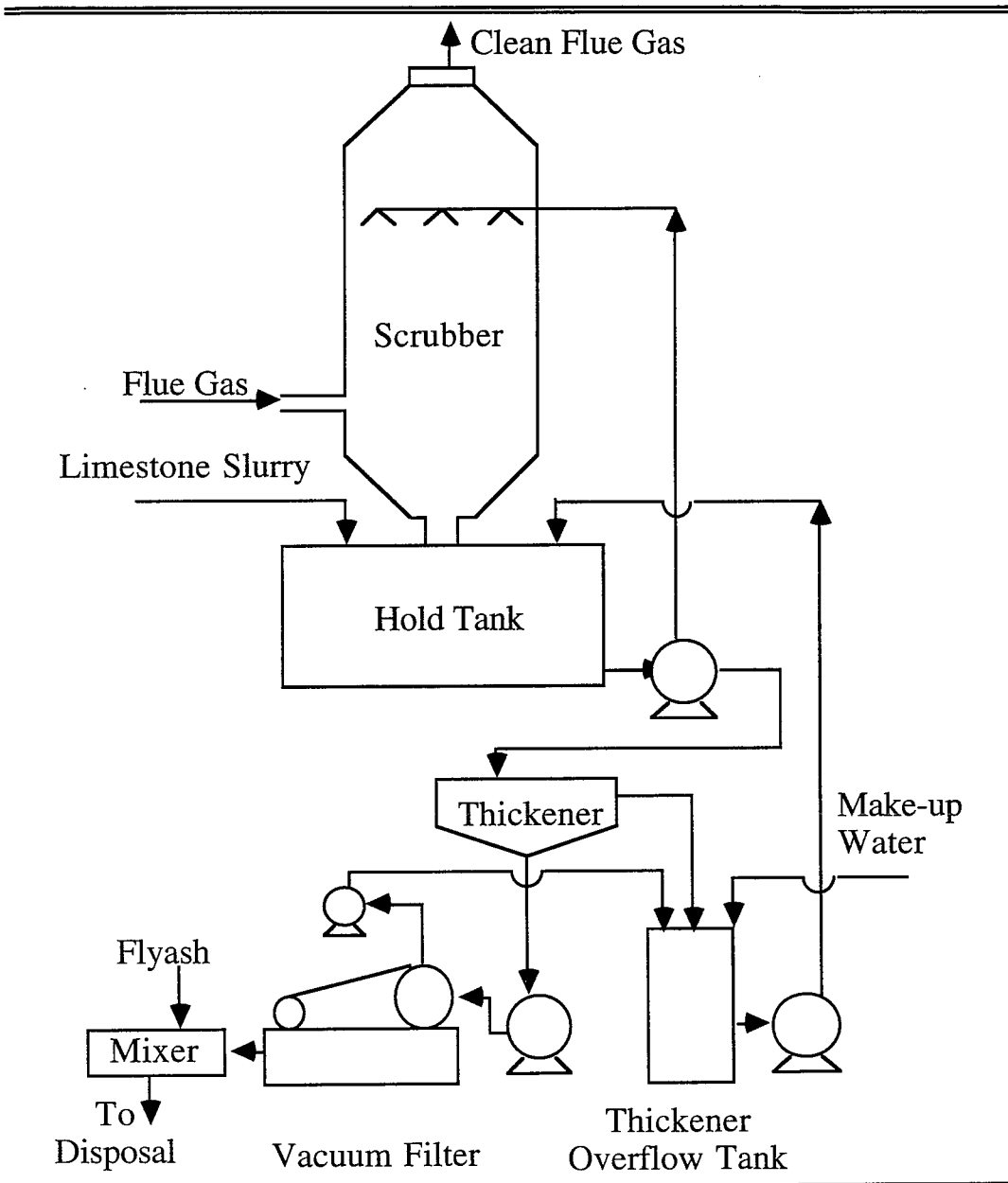


Figure 1.1: Process Flow Diagram of the Limestone Slurry Scrubbing System.

There exists a considerable amount of operating experience with this technology and it has the potential of achieving more than ninety-five percent removal of SO_2 from the flue gas. The limestone slurry scrubbing process consists of two main units - a scrubber and a hold tank. In the scrubber, upward flowing flue gas is brought into counter-current contact with a downward moving aqueous slurry for the primary purpose of SO_2 absorption. The slurry contains CaCO_3 , CaSO_3 and CaSO_4 in the form of suspended solids. The aqueous solution contains ionic species such as $\text{SO}_3^{=}$, HSO_3^- , $\text{CO}_3^{=}$, HCO_3^- , $\text{SO}_4^{=}$, HSO_4^- and Ca^{++} . As a result of absorption of SO_2 , dissolved $\text{CO}_3^{=}/\text{HCO}_3^-$ is converted into $\text{SO}_3^{=}/\text{HSO}_3^-$. The slurry is taken into the hold tank, where sufficient time is provided for solid CaSO_3 to precipitate from the solution. The chemistry of the limestone slurry process as well as the equations used in modeling the process are described in greater detail in Chapter 2.

The absorber can be a spray scrubber, a turbulent contact absorber, or it may consist of a combination of spray headers and trays. The scope of this investigation is limited to turbulent contact absorbers. The turbulent contact absorber is a staged contacting device. Each stage can be understood to consist of the region between two consecutive dual-flow trays. Each tray has up to eighty percent perforated area and does not have downcomers. At each stage, packing of hollow polyethylene spheres is suspended by the upward motion of flue gas. The liquid on each stage is well-mixed (Douglas, 1964) and the gas is plug-flow (see Chapter 2 for explanation). The hold tank is merely a well-mixed

container that provides sufficient residence time for the precipitation of solid CaSO_3 and dissolution of limestone.

The development of a FORTRAN model for simulation of this process has been an ongoing research activity at the University of Texas at Austin for more than fourteen years. The model for simulation of limestone slurry scrubbing systems is called FGDTX[®] and is available under license agreement from the University of Texas at Austin. The goal of modeling is to provide a tool for design/ troubleshooting and to increase knowledge of the various mechanisms that are important to limestone slurry scrubbing.

The present work is focused on validating the existing model over a range of pilot-scale and bench-scale data and developing a parameter estimation procedure by which model parameters can be estimated for limestone slurry scrubbing systems consisting of turbulent contact absorbers.

1.2 OTHER MODELS

In addition to FGDTX there have been two other efforts at modeling flue gas desulfurization. Flue Gas Desulfurization PRocess Integration and Simulation Model (FGDPRISM) has been developed at Radian corporation by Noblett and co-workers (1990, 1991, 1993) with funding from Electric Power Research Institute (EPRI). A semi-empirical model for a pilot-scale absorber (TCA) was also developed by Burbank and Wang (1981).

1.2.1 FGDPRIISM (Flue Gas Desulfurization Process Integration and Simulation Model)

Many of the fundamental principles used in FGDTX have also been incorporated into FGDPRIISM. A comparison between FGDPRIISM and FGDTX is given below.

1.2.1.1 Thermodynamic Calculations

Both of these models use the same database for equilibrium constants (Lowell et al., 1970). The activity coefficients are calculated using a modified Debye-Huckel theory (see Harned and Owen, 1958). The numerical algorithms for convergence of charge and material balances are different for the thermodynamic models. The calculation scheme in FGDPRIISM does not use pseudo equilibrium approximations; i.e., unlike FGDTX it retains the entire solution speciation throughout and does not eliminate ion pairs from the equilibria. This leads to an increase of computational load but makes the calculations more rigorous.

1.2.1.2 Gas/Liquid Mass Transfer

The gas/liquid mass transfer sub-models are similar in both the models for SO₂ absorption but different for O₂ and CO₂ absorption. The sub-models used in FGDTX for the calculation of CO₂ and O₂ absorption are more rigorous than those used in FGDPRIISM. These are described in Chapter 2.

1.2.1.3 Solid/Liquid Mass Transfer

The solid/liquid mass transfer models differ in several aspects. The effects of limestone particle size distribution, limestone type, and limestone utilization are taken into account in FGDTX for the calculation of limestone dissolution constant. It also uses a driving force based on composition at the limestone surface and bulk solution to calculate limestone dissolution. The effects of the presence of $\text{SO}_3^{=}$ ions on limestone dissolution flux is taken into account in FGDTX (Gage, 1989). The calculations for the rate of limestone dissolution (in FGDPRISM) are based on the equation shown below.

FGDPRISM:

$$\text{Rate of limestone dissolution} = K [\text{H}^+] (1 - R_{\text{S}_{\text{CaCO}_3}})$$

K = limestone dissolution constant

FGDTX:

$$\text{Rate of limestone dissolution} = K_{\text{CaCO}_3} D_{\text{Ca}^{++}} \Delta C_{\text{Ca}^{++}}$$

K_{CaCO_3} = limestone reactivity parameter

The calculations in FGDPRISM do not account for the crystallization of calcium sulfite and calcium sulfate in the scrubber. The dissolution of calcium sulfite is not modeled in FGDPRISM.

1.2.1.4 Hydrodynamic model

Droplet trajectories for a spray scrubber can be calculated by FGDPRISM. However, it does not account for the agglomeration of droplets between multiple

spray levels. Calculated area is used as an adjustable parameter for predicting effects of multiple spray header levels.

Droplet trajectories are not used to calculate available area for gas/liquid mass transfer in FGDTX. The effect of interfacial area of contact is included in the parameter N_g , for both spray and tray scrubbers.

1.2.1.5 Model Parameters

The model, FGDPRIISM, has been used to simulate scrubber performance alone. There are no reports of hold tank parameters. Three adjustable parameters are used in FGDTX for scrubber simulation, whereas FGDPRIISM uses four parameters.

FGDTX:

$$\frac{k^o_L}{k_g} = \text{ratio of mass transfer coefficients}$$

$$N_g = \text{number of gas film transfer units}$$

$$K_{\text{CaCO}_3} = \text{limestone reactivity parameter}$$

FGDPRIISM:

$$A = \text{area of gas/liquid contact}$$

$$\delta_L = \text{liquid film thickness}$$

$$\delta_g = \text{gas film thickness}$$

$$K = \text{limestone dissolution constant}$$

1.2.2 Semi-empirical Model

A semi-empirical model has been developed based on pilot plant data for the Turbulent Contact Absorber (TCA). The applicability of this model is specific

to the data for the large scale TCA at Shawnee, Kentucky (Burbank and Wang, 1981). This model can be stated as follows:

$$\text{fraction of SO}_2 \text{ removal} = 1 - \exp(-0.064 L^{.76} \exp(0.038h_s + .0177A^{0.5})) \quad (13)$$

where

L = Liquid flow rate (gpm/ft²)

A = Buffer additive concentration (ppm)

h_s = Static height of spherical packing (inches)

1.3 PREVIOUS WORK IN FGDTX MODELING

1.3.1 Historical Development of FGDTX

Mehta (1982), Chan and Rochelle (1983), Gage (1989), Pepe (1993), and Agarwal and Rochelle (1993) have modeled limestone slurry scrubbing for three stage turbulent contact absorbers. Vandekemp (1993) made changes to the calculation scheme in FGDTX to model a spray scrubber.

1) **Mehta** (Mehta, 1982) incorporated the methods of mass-transfer with equilibrium chemical reactions developed by Chang and Rochelle (1980). He also incorporated the limestone dissolution model developed by Chan and Rochelle (1982). He modeled SO₂ mass transfer and CaCO₃ dissolution as a function of changing solution and gas compositions. The model consisted of the absorber (scrubber) unit alone.

2) **Chan** (and **Rochelle**, 1983) extended the model by adding the following features:

a) G/L mass transfer for CO₂, O₂ .

- b) Mass balances at each stage including limestone, gypsum, calcium sulfite, and calcium sulfate hemihydrate. Simple models for sulfite oxidation and crystallization.
- c) Equilibrium calculations using pseudo-diffusivities, pseudo-concentrations, and the pseudo-equilibrium constants.
- d) A hold tank (crystallizer) unit.

3) **Gage** (1989) modeled the following physical phenomenon to simulate the effects of limestone type and grind in the presence of sulfite.

- a) Effects of limestone particle size distribution and CaSO_3 saturation on reactivity of limestone.
- b) Effect of the different types of limestone on reactivity of limestone.

4) **VandeKemp** (VandeKemp, 1993) made changes to the model calculations allowing for simulation of spray and tray sections in the same scrubber.

- a) Contribution of solid/liquid mass transfer (for a spray section) was calculated by averaging the driving forces at the top and bottom of each section.
- b) Gas phase integration for each stage was substituted by a log-mean approximation to calculate SO_2 absorption. Driving force for mass-transfer of CO_2 and O_2 was calculated using an arithmetic average of the driving forces at the top and bottom of each stage.
- c) A comparison between spray and staged contactors was made for the effects of limestone utilization, adipic acid concentrations, and SO_2 inlet concentration.

5) **Pepe** (1993) improved efficiency of model calculations for gas/liquid transport and stage wise material balances. He attempted simulation of forced oxidation conditions for turbulent contact absorbers.

a) Calculation of SO_2 absorption at the gas/liquid interface was changed. The interfacial H^+ was iterated upon instead of flux to obtain mass-balance at the gas/liquid interface. This improved the speed of convergence.

b) Calculation of solution mass balances was done using Newton's method instead of Generalized Reduced Gradient (GRG2; Lasdon, 1986) method.

c) Convergence on solids' compositions was incorporated into the overall convergence scheme of the model.

6) In this study parameter estimation for limestone slurry scrubbing has been done for the first time. Some of the changes made to the model during this process include.

a) Moving the FORTRAN program from the CYBER to the VAX/VMS computing machines. Changing the numerical convergence procedure for the calculation of material balance in solution and debugging the program for a VAX/VMS compatible version.

b) Changing the solids' convergence calculation to prevent numerical convergence problems.

c) Substituting H^+ for Ca^{++} concentration in the material balance calculations at the hold tank .

d) Testing stage wise convergence procedure for solution of material balances and gas phase calculations versus simultaneous convergence of all the streams for the same. Although the latter was expected to be more efficient, it produced better results only for selected cases.

1.4 PREVIOUS WORK IN PARAMETER ESTIMATION

Previous studies in calculating model parameters for FGDPRISM and the UT model have relied on a trial-and-error approach in arriving at parameter estimates. Confidence intervals/regions for estimated parameters have not been reported.

The effects of presence of chlorides and the addition of buffer acids have been simulated for spray scrubbers using FGDPRISM (Noblett et al.; 1990, 1991). It has also been used to study the effect of ratio of liquid to gas flow rates, number of headers, and header height for spray scrubbers (Noblett et al.; 1991, 1993). Dibasic acids (DBA) such as adipic, succinic and glutaric are often added to the scrubbing solution to enhance SO₂ removal. Depending on the concentration of added buffer acids, the enhancement can be sufficient to reach conditions of gas film control. In order to calibrate FGDPRISM, gas film thickness (δ_g) is adjusted to match SO₂ removal at conditions of gas-film control (high dibasic acid concentrations, or Na₂CO₃ solutions). Thereafter, liquid film thickness (δ_L) is adjusted to match experimental data at low removals (in the absence of dibasic acid). The limestone dissolution constant is adjusted if required. If multiple spray header levels are being used, the area calculated by the droplet trajectory model is adjusted in addition to the above mentioned parameters.

Calibration of FGDPRIISM is based on a trial and error procedure and uses scrubber simulations alone. Parameter values obtained in most of these studies have not been reported. In general, prediction of SO₂ removal at different pH (from values used in calibration) and low SO₂ removals results in a greater error in SO₂ removal (absolute error ~ 5 - 10%).

Chan and Rochelle (1983) used the UT model to study effects of chlorides on a small-scale turbulent contact absorber (Chang and Laslo, 1982; Acurex, 1983; Laslo et al., 1983). This turbulent contact absorber was located at Environmental Protection Agency's Research Triangle Park site. For the sake of convenience it will be referred to as the EPA/RTP absorber. Gage (1989) studied the effects of limestone type and grind on the same configuration. Chan and Rochelle (1983) and Gage (1989) used a trial and error approach to arrive at $N_g = 6.9$ for the EPA/RTP contactor (internal diameter = 9 inches). Based on experimental studies of the absorption of CO₂ into Na₂CO₃/NaHCO₃ solutions, k^o_L/k_g was estimated at 200 cc-atm/gmol. Chan and Gage used this value for their simulations.

In the presence of DBA, SO₂ removal was consistently over-predicted (Chan and Rochelle, 1983). They adjusted the DBA concentrations to 0.65 times the reported value to improve model predictions. They also reduced limestone reactivity by an order of magnitude to simulate data under natural oxidation conditions (in the absence of DBA). Gage (1989) adjusted the limestone reactivity for modeling the effect of limestone type for the EPA/RTP data. Gage did not simulate experiments for which DBA was present in the scrubbing slurry.

At low penetrations ($p = 0.015$ to 0.05) the data for SO_2 penetration ($p = 1$ -fractional removal) was consistently over-predicted (Gage, 1989).

Chan also simulated data for a small-scale gas bubbler ($G = 0.02 \text{ m}^3/\text{min}$). The parameter values estimated from the experimental data were: $N_g = 2.2$ and $k^\circ_L/k_g = 280 \text{ cc-atm/gmol}$ (Jarvis et al., 1983). However, at $N_g = 2.2$, Chan and Rochelle (1983) adjusted k°_L/k_g to 900 cc-atm/gmol and reduced limestone reactivity by a factor of 2.3 to predict the observed data using the UT model.

1.5 SCOPE OF INVESTIGATION

The primary focus of this work is to develop a procedure for estimating the adjustable parameters in the model. Based on a sensitivity study of the model parameters (Figure 1.2), $\frac{k^\circ_L}{k_g}$, N_g and limestone reactivity (K_{CaCO_3}) were identified as the parameters that have maximum effect on SO_2 removal.

There are no established correlations for the mass-transfer coefficients of turbulent contact absorbers. Since mass transfer plays an important role in SO_2 absorption, these parameters must be known to model the limestone slurry scrubbing system. The data used in this study did not include a description of the particle size distribution of limestone solids. As limestone reactivity is strongly influenced by particle size distribution, K_{CaCO_3} was estimated to provide a description of limestone grind.

The data used for parameter estimation have been chosen from experimental studies of turbulent contact absorbers. Experimental data from a bench-scale scrubber of 9" diameter and pilot-scale scrubber of $5.6' \times 5.6'$ (32 ft^2)

square cross-section were used in the estimation studies (Chang and Dempsey, 1981; Burbank and Wang, 1981).

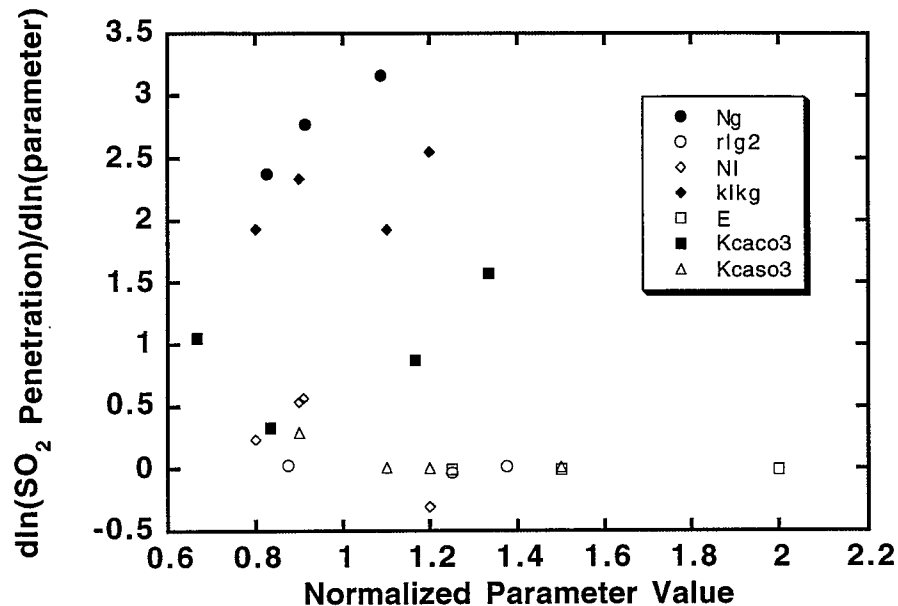


Figure 1.2: Calculated Model Sensitivity to Adjustable Model Parameters.

Parameter Values are Normalized with Respect to a Set of Base Values; $N_g = 6.9$, r_{lg2} (Hold-Tank) = 45 L/gmol, N_L (Hold Tank) = 3, $E = 1$, $K_{CaCO_3} = 3 \times 10^5$ (1/cm²), $K_{CaSO_3} = 3 \times 10^5$ (1/cm²), And $k_L^*/k_g = 200$ cc-atm/gmol. The Conditions are Used to Simulate a Small-Scale Scrubber, $L \sim 17$ Gpm., $G = 275$ acfm (@315°F).

Both sets of data include a fairly wide range of DBA concentrations and limestone utilization resulting in a wide range of pH and SO₂ removal values.

The operating conditions correspond to natural oxidation, i.e., absence of air sparging in the hold tank for oxidation of dissolved sulfite (SO_3^{2-} , HSO_3^-). Under forced oxidation conditions (air sparging in the hold tank) the chemistry of the system is somewhat different, yet the hydrodynamic characteristics of the scrubber trays (in a TCA) remain the same for both modes of operation.

For the purpose of this study, parameter estimation refers to the calculation of the most probable value of the parameters (given a set of experimentally observed data), and determination of their individual confidence intervals and joint confidence regions. The confidence intervals (and regions) are useful in quantifying the extent of uncertainty in the estimated parameters.

Parameter estimation was done using the maximum likelihood estimate method (Box and Draper, 1965; Stewart, 1992). A normal distribution of errors was assumed for both dependent variables of the model (pH and SO_2 penetration). The parameter estimation problem reduces to maximizing the probability density function for the assumed distribution. Simply stated, the optimization problem reduces to locating the minimum of the function shown below by adjusting the model parameters.

$$\ln \sum_{i=1}^n e_{1i}^2 \sum_{i=1}^n e_{2i}^2$$

for $i = 1, 2, \dots, n$ experiments.

e_{1i} and e_{2i} are the errors between the measured and calculated values of SO_2 penetration and pH respectively.

Parameter estimation was repeated using a least-squares objective function with SO₂ penetration as the only dependent variable. The observed pH was matched in each case by adjusting limestone reactivity.

Joint confidence regions and individual confidence intervals are assigned to the estimated parameters, using linear statistics (Ψ^2 statistic). A more detailed description of the method of optimization and the method of calculating confidence intervals is given by Caracotsios (1986). The FORTRAN program Generalized REGression (GREG; Caracotsios, 1986) was used to calculate parameter estimates and confidence intervals.

To reduce co-variance between the estimated parameters, parameter estimation was repeated using N_g and N_L as adjustable parameters. A higher co-variance does not necessarily affect the predictive capabilities of the model, but reduces the physical significance that can be attached to the individual estimates of the parameters.

The method of weighted least-squares was not considered suitable for estimation, as the errors involved with the individual measurements (pH or SO₂ concentration) were not known. Monte-Carlo studies to verify the reliability of linear statistics in prediction of confidence intervals were not done (Bard, 1977; Miller, 1993). This procedure was considered beyond the scope of the project due to the extensive time involved in making such computations. The model predictions for SO₂ removal are fairly linear with respect to the adjustable parameters. It may be expected that linear statistics are applicable to parameter estimates.

The contributions of this work are:

- 1) A robust model for limestone slurry scrubbing validated over a range of limestone utilizations and DBA concentrations.
- 2) Estimation of gas and liquid film mass transfer units for the turbulent contact absorbers operated at EPA/RTP and Shawnee.
- 3) Calculation of contribution of various mechanisms to the enhancement of SO₂ absorption in a typical turbulent contact absorber.

1.6 NOTATION

A	= Area of contact between gas and liquid (cm ² /cc)
C	= Concentration in the liquid phase (gmol/L)
D	= Liquid phase diffusion coefficient (cm ² /s)
E	= Enhancement factor for oxidation (dimensionless)
e ₁	= Error between the measured and calculated value of SO ₂ penetration (dimensionless)
e ₂	= Error between the measured and calculated value of pH (dimensionless)
G	= Gas flow rate (acfm)
h _s	= Static height of spheres (in.)
K _{CaCO₃}	= Dissolution constant for Limestone (1/cm ²)
K _{CaSO₃}	= Dissolution constant for Calcium sulfite (1/cm ²)
k ^o _L /k _g	= Ratio of liquid film mass transfer coefficient to gas film mass transfer coefficient (cc-atm/gmol)
L	= Liquid flow rate (gpm)

N_g	= Number of gas film mass transfer units in the scrubber (dimensionless)
N_L	= Number of liquid film mass transfer units in the hold tank (dimensionless)
p	= sulfur dioxide penetration (dimensionless)
rlg_2	= Ratio of liquid to gas flow rate in the hold tank (L/gmol)
RS_{CaCO_3}	= Relative saturation of limestone in the liquid phase (dimensionless)
Greek Symbols	
Δ	= Difference operator
δ_g	= Gas film thickness (cm)
δ_L	= Liquid film thickness (cm)

CHAPTER 2

MODEL DESCRIPTION

2.1 INTRODUCTION

This chapter includes an introductory discussion of the limestone slurry scrubbing process and a detailed description of the process model used for its simulation. The model description is divided into two parts. An overview of the systems of equations to be solved is presented first, followed by a detailed description of the physical sub-models used for the simulation of solution equilibria, gas/liquid and solid/liquid mass transfer. Experimental data (Chen and Douglas, 1969) on the liquid mixing patterns in a TCA are reviewed in section 2.4 of this chapter.

2.2 PROCESS DESCRIPTION

The objectives of the limestone slurry scrubbing process are two fold:

- 1) To achieve required SO₂ removal,
- 2) To conduct the overall operation in a scale-free manner.

These objectives are conflicting in nature, since the conditions that favor high SO₂ removal (high pH) also lead to precipitation of solid calcium sulfite and calcium sulfate in the scrubber. To achieve efficient system operation most limestone slurry scrubbing systems consist of two units, the scrubber and the hold tank.

A limestone slurry scrubbing system consisting of a scrubber and a hold tank is shown in Figure 2.1. In the scrubber upward flowing flue gas is brought into counter-current contact with the downward moving slurry for the primary purpose of SO_2 absorption. In the hold tank, solids are precipitated and a fresh feed of limestone is added. In systems of interest to this study, the hold tank is merely a large stirred vessel used to provide sufficient residence time for dissolution and precipitation of solids. In other systems the hold tank may also be used for the oxidation of the sulfite in solution to sulfates by air sparging.

Most commercial scrubbers are spray towers or tray towers. The turbulent contact absorber has been used in many experimental studies (Mobley and Chang, 1983; Burbank and Wang, 1981). The TCA column is separated into stages by screens having up to 80% perforated area. In the region between screens, lightweight hollow packing of nitrofoam/polyethylene spheres is fluidized by the upward flowing flue gas. The range of packing size varies from 1-2 inches in diameter and each stage (stage depth = 3-4 ft) can have a settled packing height of upto ten inches. The TCA has the advantage of being able to operate at high gas velocities and low liquid rates. Highly turbulent motion of the packing under these conditions results in high rates of mass transfer (Chen and Douglas, 1968). For limestone slurry systems, fluidized packing is also preferred over fixed packing as it reduces plugging of scrubber internals.

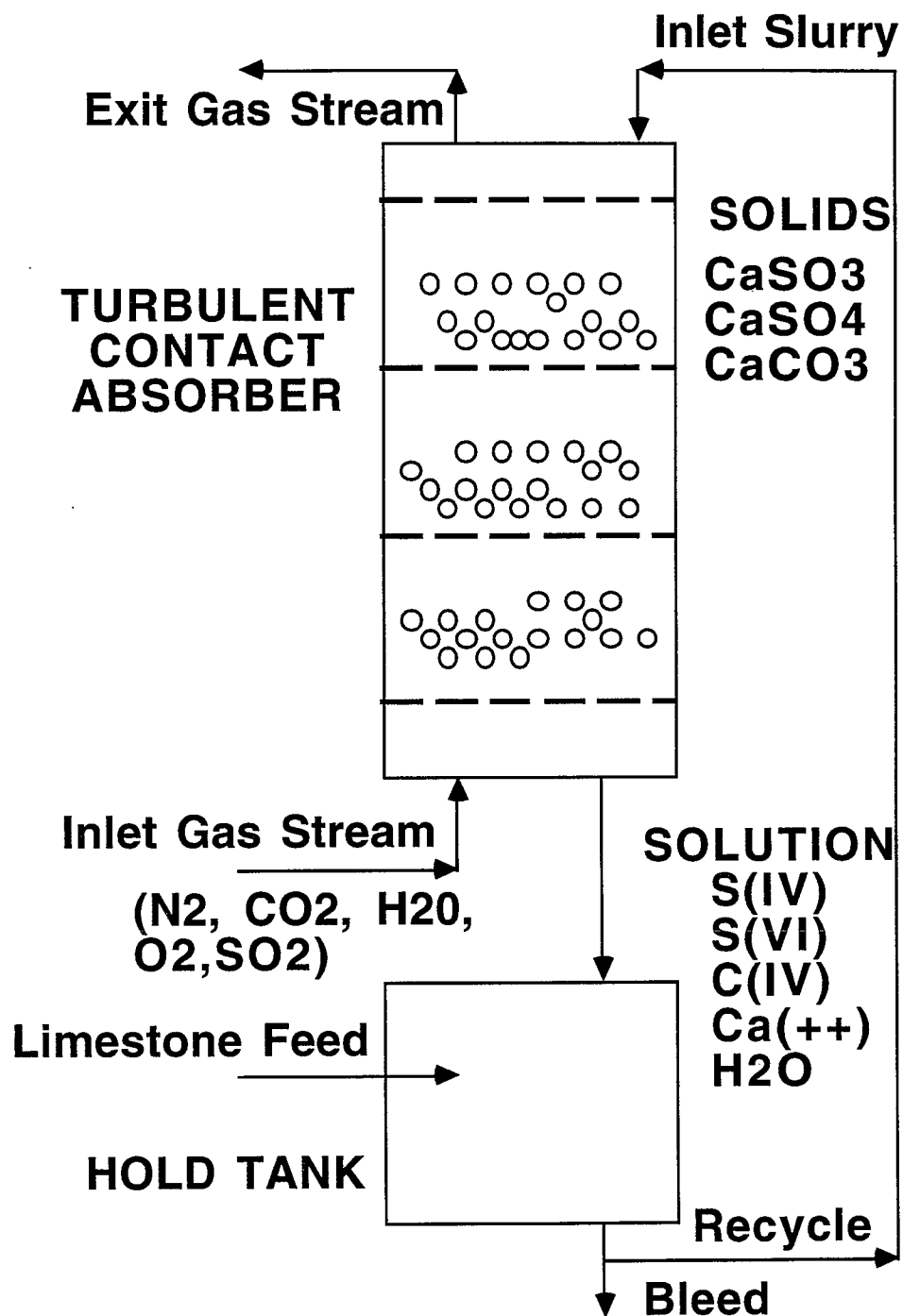
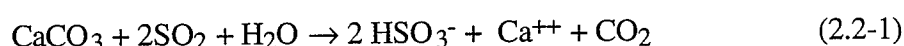


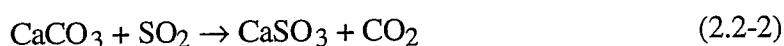
Figure 2.1: Process Flow Diagram Showing a Scrubber and a Hold Tank.

2.2.1 Scrubber Reactions

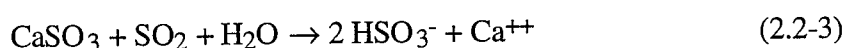
Ideally, half the limestone required stoichiometrically is dissolved in the scrubber:



Excess limestone can result in precipitation of CaSO_3 in the scrubber which often leads to scaling and plugging of scrubber internals.



With insufficient limestone, CaSO_3 dissolves. However, the capacity of the scrubber solution for SO_2 absorption is reduced.



2.2.2 Hold Tank Reactions

The CaSO_3 and CaSO_4 resulting from the reactions in the scrubber should precipitate in the hold tank. A small fraction of slurry is withdrawn from the hold tank and dewatered before disposal as solid waste. A fresh feed of slurried limestone is added to the hold tank and most of the slurry is recycled to the scrubber.



The above reactions are the net effect of detailed equilibria among the ionic species present in the system. A summary of the various equilibria used by the model is presented with the description of the appropriate sub-models.

2.3 OVERALL MODEL SOLUTION

In this section, the overall structure of the model is outlined. A more detailed description of the model in terms of the physical sub-models and used is presented in Section 2.4. A comprehensive list of equations used in the model is presented in Appendix A.

2.3.1 General Model Description

The process model describes the TCA (scrubber) as a staged contactor. At each stage the upward flowing gas is brought into counter-current contact with downward moving slurry. The liquid is assumed to be well-mixed at each stage whereas the gas flows in a plug flow manner.

The gas/liquid mass transfer model accounts for the absorption and desorption of SO_2 , CO_2 and O_2 . The solid/liquid mass transfer model accounts for the dissolution and crystallization of calcium sulfite, dissolution of limestone, and crystallization of gypsum. The hold tank is modeled in the same manner as a scrubber stage with a few changes in the gas phase calculations and mass balance equations.

The model can be understood to consist of the solution of a set of mass balance equations. Overall convergence is established when the calculations predict steady concentration at the inlet to the scrubber between successive iterations. The mass balance equations are solved as a set of constrained non-linear algebraic equations. The calculations nested within the solution of the mass balance equations include the solution of ordinary differential and algebraic

equations for the individual rate based mass transfer models, charge balance, and thermodynamic equilibria.

Scrubber:

The mass balance equations for a stage (n^{th}) can be summarized as follows.

$n = 1, k$ $i = 1, 4$	$X(i)^{n-1} = X(i)^n + f(i) + g(i) \quad (2.3-1)$
-----------------------	---

where

i = i^{th} species (S(IV), S(VI), C(IV) and Ca^{++})

S(IV) = $\text{SO}_3^- + \text{HSO}_3^- + \text{SO}_2$

S(VI) = $\text{SO}_4^- + \text{HSO}_4^-$

C(IV) = $\text{CO}_3^- + \text{HCO}_3^- + \text{CO}_2$

k = Number of stages

$X(i)$ = Concentration of the i^{th} species (gmol/L)

$f(i)$ = $f_i(\mathbf{P}^n, \mathbf{p}, \mathbf{X}^n)$

= $\int f_i' dN_g$

= Change of solution composition due to absorption/desorption of gases over a stage

f_i' = Rate of absorption of i^{th} gaseous species per N_g

\mathbf{P}^n = Partial pressures at the bottom of the n^{th} stage (atm)

= $(P_{\text{SO}_2^n}, P_{\text{CO}_2^n}, P_{\text{O}_2^n})$

$g(i)$ = $g_i(\mathbf{X}^n, \mathbf{q})$

= Change of solution composition due to
dissolution/crystallization of solids over a stage

q, p = Parameter vectors (See Appendix A)

X = Vector of concentrations

Hold Tank:

Similarly mass balance for the hold tank can be written as follows:

$$i = 1, 4$$

$$X(i)^k = X(i)^{k+1} + h(i) + g(i) \quad (2.3-2)$$

where:

$i = S(IV), S(VI), C(IV)$ and H^+ or limestone reactivity

$$h(i) = h_i(P^{k+1}, r, X^{k+1})$$

= Change of solution composition over a stage due to
absorption/desorption of gases.

$$g(i) = g_i(X^{k+1}, s)$$

r, s = parameter vectors (See Appendix A for detailed
description)

2.3.1 Convergence Procedure

The calculations are begun at the top stage based on an initial guess for the
solution ($X^1(i)$) and gas compositions (P^1).

2.3.1.1 Stage Convergence.

1. Based on a guess of the outlet solution ($X^{k+1}(i)$) composition, gas absorption/desorption ($f(i)$) and solids dissolution/crystallization ($g(i)$) are calculated.

2. The iterative procedure of guessing the outlet composition and back calculating the inlet is repeated until the specified inlet is matched.

2.3.1.2 Scrubber and Hold Tank Convergence

3. Steps 1 and 2 are repeated until the bottom stage ($n = k$) is reached. At the bottom stage the calculated and specified SO_2 ($P_{SO_2}^k$) compositions are compared. If the specified tolerances are not met then the gas composition for SO_2 ($P_{SO_2}^k$) is updated and steps 1 through 3 are repeated.

4. Hold tank convergence is calculated in the same manner as individual stage convergence.

2.3.1.3 Overall Convergence

5. Overall convergence is reached when the calculated hold tank outlet concentrations are within the specified tolerance ($X^{k+1}(i) = X^1(i)$). If the required tolerance is not met, then the inlet solution composition (X^1) to the top stage is updated and steps 1 through 5 are repeated.

2.3.1.4 Numerical Procedures and Specified Tolerances

In this section numerical procedures have been outlined sequentially starting at the outermost convergence loop and proceeding to subsequent inner loops.

Overall convergence is assumed when the difference between two successive iterations at the hold tank outlet differ by less than 1% for each of the four solution compositions. The Wegstein method is used to update the successive guess values of inlet solution composition to the scrubber.

Scrubber convergence is established when error between the calculated ($P^{m-1}_{SO_2, in}$) and specified values of the inlet partial pressure of SO_2 ($P_{SO_2, in}$) is within 1% of the specified value. To match the specified value, the exit partial pressure ($P^{m}_{SO_2, out}$) of SO_2 is updated according to the following formula.

$$P^{m}_{SO_2, out} = \frac{P^{m-1}_{SO_2, out} * P_{SO_2, in}}{P^{m-1}_{SO_2, in}} \quad (2.3-3)$$

$P^{m-1}_{SO_2, out}$ = Partial pressure of SO_2 at the top of the scrubber for the (m-1)th numerical iteration (atm.)

$P^{m-1}_{SO_2, out}$ = Partial pressure of SO_2 at the top of the scrubber for the mth numerical iteration (atm.)

$P^{m-1}_{SO_2, in}$ = Partial pressure of SO_2 at the inlet to the scrubber for the (m-1)th iteration (atm.) ($=P^k_{SO_2}$)

This formula assumes that the SO_2 penetration is fairly constant at a specified set of hydrodynamic conditions. The procedures implemented in the current configuration of the model typically require 2-5 iterations for scrubber convergence and 2-10 iterations for overall convergence.

Stage convergence calculations are done using a reduced gradient method with simple bounds on the stage concentrations. The FORTRAN program, GRG2 (Lasdon, 1986) is used to optimize the objective function of the sum of squares of errors between the specified and calculated inlet solution compositions.

$$g = \sum_{i=1}^4 (x_c^{n(i)} - x_g^{n(i)})^2 \times 10^6 \quad (2.3-4)$$

where:

$x_c^{n(i)}$ = Calculated value of $X(i)$ at the n^{th} stage

$x_g^{n(i)}$ = Initial guess for the value of $X(i)$ at the n^{th} stage

Convergence is reached when the objective function has a value less than 10^{-4} , which corresponds to an error of less than 0.01 mM in each of the concentrations (the usual range of concentrations is 0.1-10 mM). Integration of the ordinary differential equations for gas absorption is done using Livermore Solver for Ordinary Differential Equations (LSODE) with the relative tolerance of 10^{-6} on the gas phase pressure. The calculation of the charge balances is done by a procedure that involves iterative solution using the secant method with a specified relative error tolerance of 10^{-6} on the charge balance.

The model calculations typically require 3-5 minutes for convergence of each case on an IBM RS/6000 250/PowerPC running the operating system AIX 3.2.5.

2.4 MODEL DESCRIPTION

A rigorous calculation of the solution equilibria (from initial solution composition) is based on the modified Debye-Huckel theory. The model also calculates simplified pseudo-equilibria based on elimination of ion-pairs for subsequent solution equilibria at each stage. The calculation of the rate-based mass transfer between solid/liquid and gas/liquid phases is based on film theory of mass transfer. A detailed description of these three sub-models is given below.

2.4.1 Solution Thermodynamics

Equilibrium is assumed among ionic species in the bulk liquid as well as solid/liquid and gas/liquid boundary layers. A rigorous calculation of the equilibrium compositions is based on temperature dependent equilibrium constants compiled by Lowell et al.(1970) for 41 FGD species. These calculations are contained in the Bechtel-Modified Radian Equilibrium Program (BMREP) by Epstein et al. (1973). The effect of ionic strength on activity coefficients is calculated using the modified Debye-Huckel theory.

$$\log \gamma_i = A z_i^2 \left[\frac{-I^{1/2}}{1 + B a_i^\circ I^{1/2}} + b_i I \right] + U_i I \quad (2.4-1)$$

$$A = \frac{1.824 * 10^6}{D^{3/2} T^{3/2}} \frac{L^{1/2}}{\text{mole}^{1/2}}$$

$$B = \frac{50.292}{D^{1/2} T^{1/2}} \frac{L^{1/2}}{\text{mole}^{1/2} \text{ A}^\circ}$$

D = liquid phase diffusion coefficient (cm^2/s)

z_i = Charge of the i^{th} species

a_i° , b_i , U_i are constants

The constants a_i° , b_i and U_i have been compiled by Davies (1948), Klotz (1964) and Garrels and Christ (1965) and are summarized by Lowell et al. (1970). The diffusivity values of the individual ionic and non ionic species are based on the work of Mehta and Rochelle (1982), Chan and Rochelle (1982) and Tseng and Rochelle (1986). BMREP is also used to calculate the diffusivities at the temperature of the system using the above diffusivities (measured at 25 °C), and the Stokes-Einstein relationship (2.4-2).

$$D_2 = D_1 \frac{T_2 \mu_1}{T_1 \mu_2} \quad (2.4-2)$$

where:

- T_1 = Reference temperature (298 K)
- T_2 = Temperature of interest (K)
- μ_1 = Solution viscosity at T_1 (cp)
- μ_2 = Solution viscosity at T_2 (cp)
- D_2 = Diffusivity of a given species in solution at T_2 (cm²/s)
- D_1 = Diffusivity (specified) of a given species in solution at T_1 (cm²/s)

The BMREP database does not contain temperature dependent parameters for CaHCO_3^+ ($K_{\text{CaHCO}_3^+}$), CaCO_3° ($K_{\text{CaCO}_3^\circ}$), and the solubility product of calcite (K_c). These parameters were updated by Gage (1989) to the values given by Plummer and Busenberg (1982).

$$\log K_{\text{CaHCO}_3^+} = 1209.12 + 0.31294T - \frac{34765.05}{T} - 478.782 \log T \quad (2.4-5)$$

$$\log K_{\text{CaCO}_3^\circ} = -1228.732 - 0.2944T + \frac{35512.75}{T} + 485.818 \log T \quad (2.4-6)$$

$$\log K_c = -171.9065 - 0.077993T + \frac{2839.319}{T} + 71.595 \log T \quad (2.4-7)$$

Three bisulfite equilibrium constants have also been added by Gage and Rochelle (1992).

$$K_{\text{CaHSO}_3^+} = 0.073$$

$$K_{\text{MgHSO}_3^+} = 0.15$$

$$K_{\text{NaHSO}_3^+} = 2.53$$

Chan and Rochelle (1982) have simplified the solution equilibria and reduced the solution species from 41 to 17 by eliminating ion pairs (CaSO_3° ,

CaCO_3° , etc). The concentrations, diffusivities, and equilibria for the pseudo species are defined on the basis of the individual values of these constants for the component species. For example, the pseudo concentrations, equilibrium constants, and diffusion coefficients for the HCO_3^- pseudo species can be stated as follows:

Pseudo-concentration

$$[\text{HCO}_3^-]_{\text{pseudo}} = [\text{HCO}_3^-] + [\text{CaHCO}_3^+] + [\text{MgHCO}_3^+] \quad (2.4-8)$$

Pseudo-equilibrium constant

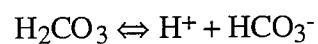
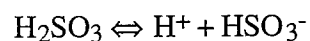
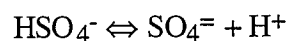
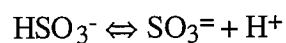
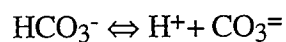
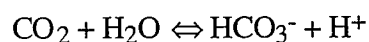
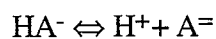
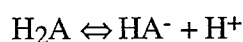
$$K_{\text{pseudo}} = \frac{[\text{H}^+][\text{CO}_3^{=}]_{\text{pseudo}}}{[\text{HCO}_3^-]_{\text{pseudo}}} \quad (2.4-9)$$

Pseudo-diffusivity

$$D_{\text{pseudo}} = \frac{\sum_j D_j C_j}{\sum_j C_j} \quad (2.4-10)$$

$j = \text{HCO}_3^-, \text{CaHCO}_3^+, \text{MgHCO}_3^+$

The other solution equilibria are summarized below:

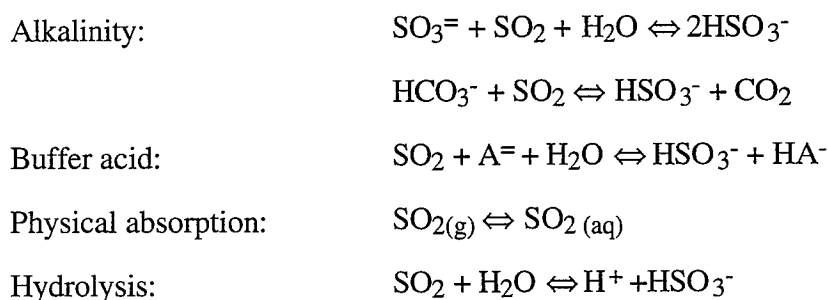


where H_2A is the adipic acid (dibasic buffer additive) species.

These definitions (2.4-8 and 9) include the effects of activity coefficients in the equilibrium constants. This approximation is valid if the ion pair concentrations and the activity coefficients of all the species remain constant (at the input value). This requires that the ionic strength of the solution and the Ca^{++} concentration do not change significantly.

2.4.2 Calculation for Gas/Liquid Mass Transfer

The two-film theory of mass transfer is used for the calculation of gas/liquid mass transfer. In the liquid film, the ionic species are assumed to be at equilibrium. To account for the transport of species having unequal diffusivities an approximation of surface renewal theory is applied to the liquid film (Chang and Rochelle, 1982). The flux is calculated as prescribed by film theory, however the diffusivity (D) is replaced by the square root of its value in film theory (\sqrt{D}). The equilibria that affect the mass transfer of SO_2 are stated below.



The desorption of CO_2 is assumed to be completely liquid film controlled and the hydrolysis reaction of CO_2 is assumed to be at equilibrium (Chan, 1982).



As in the case of CO_2 , the absorption of O_2 is assumed to be liquid phase controlled. Oxygen is assumed to react instantaneously at the G/L interface with

sulfite forming sulfate. The flux of oxygen is enhanced over physical absorption due to its fast reaction in the boundary layer.

$$\text{Flux} = 2E k^{\circ}_L H_{O_2} P_{O_2} \quad (2.4-11)$$

where

E = Enhancement factor for absorption of oxygen

H_{O_2} = Henry's law constant for oxygen (gmol/atm-L)

k°_L = Liquid film mass transfer coefficient in the absence of reaction (cm/s)

The mass-transfer sub-model requires compositions at the gas/liquid interface to calculate the driving force for gas/liquid mass transfer. These are calculated by numerical solution of a set of algebraic equations involving mass balances at the interface (2.4-12), solution equilibria, and assuming zero charge flux at the gas/liquid interface (2.4-14).

The mass balance for SO_2 absorption can be written as:

$$k_g (P_{SO_2,b} - P_{SO_2,i}) = k^{\circ}_L \sum_j (\sqrt{D_j} \Delta C_j / \sqrt{D_{SO_2}}) \quad (2.4-12)$$

where:

$$\Delta C_j = C_{\text{interface},j} - C_{\text{bulk},j}$$

$j = SO_2, SO_3^=, SO_4^=, HSO_3^-, \text{ and } HSO_4^-$.

At the gas/liquid interface, there is no net consumption of the dibasic buffer species.

$$\sum_j \sqrt{D_j} \Delta C_j = 0 \quad (2.4-13)$$

where, $j = H_2A, HA^-, A^=$

The zero charge flux assumption is valid for systems showing small potential gradients in solution (Glasscock and Rochelle, 1989).

$$\sum_k Z_k \sqrt{D_k} \Delta C_k = 0 \quad (2.4-14)$$

where:

Z_k = Charge of the k^{th} ionic species

$k = \text{H}^+, \text{OH}^-, \text{HCO}_3^-, \text{CO}_3^{2-}, \text{HSO}_3^-, \text{SO}_3^{2-}, \text{HSO}_4^-, \text{SO}_4^{2-}, \text{HA}^-, \text{ and } \text{A}^{2-}$

The gas phase absorption/desorption is calculated based on the integration of a set of three ordinary differential equations using the Livermore Solver for Ordinary Differential Equations (LSODE).

$$\begin{aligned} \frac{dP_k}{dN_g} &= \frac{k_L \sum_j \sqrt{D_{jk}} \Delta C_j}{\sqrt{D_{\text{SO}_2}} k_g} \\ &= f'(k) \end{aligned} \quad (2.4-15)$$

$k = \text{SO}_2, \text{CO}_2 \text{ and } \text{O}_2$

$\Delta C = C_{\text{interface}} - C_{\text{bulk}}$

$$N_g = \frac{k_g a ZP}{G} \quad (2.4-16)$$

In case of SO_2

$jk = \text{SO}_2, \text{SO}_3^{2-}, \text{SO}_4^{2-}, \text{HSO}_3^-, \text{HSO}_4^-$

2.4.3 Solid/Liquid Transport

The solid/liquid mass-transfer sub-models calculate the change of solid phase compositions due to the dissolution and precipitation of the solid species. These models account for the dissolution of limestone, dissolution/ precipitation of CaSO_3 and the precipitation of gypsum. Calculations for the dissolution of limestone take into account limestone type and grind, as well as the effect of

sulfite in solution on the surface chemistry of limestone. Precipitation (crystallization) of calcium sulfite solids from solution is calculated using empirical models based on the work of Tseng (1984).

2.4.3.1 Limestone Dissolution Model

Calculation of Limestone Reactivity Parameter

The Limestone dissolution parameter (K_{CaCO_3}) is used to calculate the total dissolution of limestone at a stage as:

$$\Delta CaCO_3 = K_{CaCO_3} [CaCO_3]_{solid} t_{res} D_{Ca} \Delta C_{Ca} \quad (2.4-17)$$

where:

$[CaCO_3]_{solid}$ = Concentration of limestone solid (gmol/l-solution)

t_{res} = Residence time/stage (s)

$\Delta C_{Ca} = C_{Ca,surface} - C_{Ca,bulk}$ (gmol/L)

The derivation for the effect of limestone type and grind on the limestone dissolution parameter has been stated by previous researchers (Gage, 1989; Toprac, 1982). In this work an understanding of the physical relevance of the terms used is explained along with the derivation.

Dissolution rate of a single particle of surface area A is given as

$$\frac{dV_p}{dt} = - \frac{A k_{sL} \Delta C}{\rho_m} \quad (2.4-18)$$

where $\rho_m = 0.027$ gmol/cc is the molar density of solid (limestone).

k_{sL} = Mass transfer coefficient for the dissolution of solid limestone (cm/s)

For a spherical particle of diameter d_p , the above equation can be modified as follows:

$$\frac{dV_p}{dt} = -\frac{\pi d_p^2 k_{sL} \Delta C}{\rho_m} \quad (2.4-19)$$

The mass transfer coefficient can be calculated using the Sherwood number and a correction for the agitation enhancement. In the limit of a small particle in an infinite stagnant medium, a Sherwood number ($N_{Sh} = \frac{k_{sL} d_p}{D}$) of 2 can be assumed. Toprac and Rochelle (1982) suggested the use of the Calderbank and Moo-Young correlation for the effect of enhancement due to liquid phase agitation.

$$k_{sL} = \frac{2D}{d_p} + \beta N_{Sc}^{-2/3} \quad (2.4-20)$$

where β = a term accounting for the agitation force imparted to the solution.

Using the above expression and assuming an initial particle size volume of V_o , the undissolved fraction (f) can be calculated as follows:

$$f = V_p / V_o$$

$$\frac{df}{dt} = \frac{\pi d_p^2 \Delta C \left(\frac{2D}{d_p} + \beta N_{sc}^{-2/3} \right)}{V_o} \quad (2.4-21)$$

For a spherical particle $d_p = (6V_p / \pi)^{1/3}$, a new mass transfer constant can be defined as follows:

$$k_m = \frac{6^{1/3} \pi^{2/3} 2 D \Delta C}{\rho_m} \quad (2.4-22)$$

The fractional dissolution of the single spherical particle can be written as

$$\frac{df}{dt} = - \frac{k_m f^{1/3}}{V_o^{2/3}} - \frac{k_m B f^{2/3}}{D V_o^{1/3}} \quad (2.4-23)$$

where $B = 1.612 \beta N_{sc}^{-2/3} = 765 \text{ cm}^{-1}$ (Gage, 1989)

The above differential equation can be integrated to give the relation between the fraction of a specified particle size (V_o) dissolved versus time. This result has been used to predict the fraction of limestone dissolved for a known initial particle size distribution. Results from batch experiments are predicted well over a range of pH values and sulfite concentrations (Gage, 1989).

$$k_m t = \frac{3}{B^2} [B V_o^{1/3} (1-f^{1/3}) + \ln \frac{1 + B V_o^{1/3} f^{1/3}}{1 + B V_o^{1/3}}] \quad (2.4-24)$$

For a system having a size distribution of particles of volume $V_{o,i}$ each distributed according to size fractions, Φ_i the total fraction remaining (F) is given as follows:

$$F = 1 - U = \sum \Phi_i f_i \quad (2.4-25)$$

The above equations can be used for calculation of the amount of limestone dissolved versus time for a batch system. At each stage of a TCA the liquid is well-mixed. To calculate the dissolution rates at a specified value of F , the above equations need to be scaled for a CSTR time distribution ($P(t)$).

$$P(t) = \frac{1}{\tau} \exp\left(-\frac{t}{\tau}\right)$$

$$F = \Phi_i \frac{1}{k_m \tau} \int_1^0 \frac{f_i \exp\left(-\frac{k_m t}{k_m \tau}\right)}{\frac{df_i}{d(k_m t)}} df_i \quad (2.4-26)$$

An iterative procedure is used to calculate $k_m \tau$ so that the calculated values of F (fraction remaining) match the specified utilization (U) in equation 2.4-26. This value of $k_m \tau$ can be understood to be an average driving force required to achieve the specified utilization (U). The limestone dissolution constant is defined as the ratio of the total solids dissolved to the average driving force required to reach the specified dissolution.

$$K_{\text{CaCO}_3} = \frac{6^{1/3} \pi^{2/3} 2}{\rho_m} \frac{U}{k_m \tau (1-U)} \quad (2.4-27)$$

The total dissolution of limestone at a particular stage is calculated as in (2.4-17). Using the definitions for K_{CaCO_3} and $k_m \tau$ from 2.4-17 and 2.4-22, total dissolution of limestone can be calculated as follows:

$$\Delta \text{CaCO}_3 = \frac{U C_t [\text{CaCO}_3]_{\text{solid}} D_{\text{Ca}^{++}} \Delta C_{\text{Ca}^{++}} t_{\text{res}}}{(1-U) C_t (D \Delta C)_{\tau} \tau} \quad (2.4-28)$$

where:

$$\Delta C_{\text{Ca}^{++}} = C_{\text{Ca}^{++}, \text{surface}} - C_{\text{Ca}^{++}, \text{bulk}}$$

The " $D_{\text{Ca}^{++}} \Delta C_{\text{Ca}^{++}}$ " term in the numerator represents the driving force for dissolution at a stage, whereas the term in the denominator represents driving force required to reach the total specified dissolution $U C_t$. The ratio of the driving forces is used to determine the total dissolution at a particular stage. The other terms involving $\frac{t_{\text{res}}}{\tau}$ and $\frac{[\text{CaCO}_3]}{(1-U) C_t}$ normalize the residence time and the solid concentration of CaCO_3 on a stage to the values calculated for the total dissolution. Hence, by using a dissolution parameter we have assumed that the dissolution is dependent on the driving force at the stage and that the area

available for the dissolution is the same throughout, i.e., equal to the ratio of the total dissolution to the average total driving force.

An alternative approach to understanding the role of the parameter $k_m \tau$ is to compare the reactivity model versus the mass transfer model.

Limestone dissolution for a particle size distribution of area A per liter of solution, can be written as

$$\Delta \text{CaCO}_3 = k_{sL} A \Delta C t_{\text{res}} \quad (2.4-29)$$

If the specific average area per mole of limestone solid present is \underline{a} , then $A = \underline{a} [\text{CaCO}_3]_{\text{solid}}$, and

$$\Delta \text{CaCO}_3 = k_{sL} \underline{a} \Delta C t_{\text{res}} [\text{CaCO}_3]_{\text{solid}} \quad (2.4-30)$$

For the film theory, k_{sL} can be simplified as the ratio of diffusivity D of the species controlling diffusion to the average film thickness (δ_{ave}). The specific surface area can be expressed as an inverse of an effective diameter (d_{eff}) for the particle size distribution.

$$\Delta \text{CaCO}_3 = \frac{D_{\text{Ca}^{++}} \Delta C_{\text{Ca}^{++}} t_{\text{res}} [\text{CaCO}_3]_{\text{solid}}}{\delta_{\text{ave}} d_{\text{eff}}} \quad (2.4-31)$$

Thus the relation of $k_m \tau$ to the film thickness and effective particle diameter can be stated as:

$$\frac{1}{d_{\text{eff}} \delta_{\text{ave}}} = \frac{6^{1/3} \pi^{2/3} 2}{\rho_m} \frac{U}{(1-U) k_m \tau} \quad (2.4-32)$$

Calculation of Total Dissolution of Limestone and Calcium Sulfite

The calculation of $D_{\text{Ca}^{++}} \Delta C_{\text{Ca}^{++}}$ at a stage is dependent on the stage solution composition. In the absence of sulfite the solubility product of the limestone particle is matched at the surface of limestone, whereas in the presence

of sulfite the surface-reaction model developed by Gage (1992) is used to match the calculated flux.

$$\text{Solubility Product : } K_{sp, \text{CaCO}_3} = [\text{Ca}^{++}]_s [\text{CO}_3^{=}]_s$$

In presence of sulfite :

$$D\Delta C = \delta_{ave} k_c \frac{(\text{CaCO}_3_{eq} - \text{CaCO}_3_s)^{0.5}}{(\text{CaCO}_3_s \text{ CaSO}_3_s)} \quad (2.4-33)$$

where k_c = limestone surface rate constant (dependent on limestone type)

The average film thickness is calculated taking into account the polydisperse distribution of limestone by the method outlined by Gage (1992).

$$\frac{1}{\delta_{ave}} = \frac{2 \sum_{i=1}^n \Phi_i \int_0^1 \frac{e^{(-k_m t/k_m \tau)} df_i}{-1-BV_i^{1/3} f_i^{1/3}}}{\sum_{i=1}^n \Phi_i d_{oi} \int_0^1 \frac{f_i^{1/3} e^{(-k_m t/k_m \tau)} df_i}{-1-BV_i^{1/3} f_i^{1/3}}} + 1.612B \quad (2.4-34)$$

The dissolution of CaSO_3 and limestone is calculated using steady state mass transfer. A constant value is used for the dissolution constant of CaSO_3 . The solubility product of CaSO_3 is satisfied at the boundary of the sulfite particle, where:

$$\text{Solubility product : } K_{sp, \text{CaSO}_3} = [\text{Ca}^{++}]_s [\text{SO}_3^{=}]_s$$

Compositions at the solid/liquid interface for dissolution of CaCO_3 and CaSO_3 are calculated by numerical solution of the algebraic equations involving mass balances, equilibria and assuming zero charge flux at the solid/liquid

interface (Chan and Rochelle, 1982). For limestone dissolution these calculations are stated as follows.

There is no net consumption or generation of the sulfite, sulfate or dibasic acid buffer at the surface of limestone. This results in three mass balance equations:

$$\sum_i D_i \Delta C_i = 0$$

$i = \text{HSO}_3^-, \text{SO}_3^{=}, \text{SO}_2$ for sulfite species

$i = \text{HSO}_4^-, \text{SO}_4^{=}$ for sulfate species

$i = \text{H}_2\text{A}, \text{HA}^-, \text{A}^{=}$ for buffer acid species

Zero charge flux leads to the equation:

$$\sum_{k=1}^n Z_k D_k \Delta C_k = 0$$

where:

Z_k = Charge of k^{th} ionic species

$k = \text{H}^+, \text{OH}^-, \text{HCO}_3^-, \text{CO}_3^{=}, \text{HSO}_3^-, \text{SO}_3^{=}, \text{HSO}_4^-, \text{SO}_4^{=}, \text{HA}^-, \text{Ca}^{++}, \text{and } \text{A}^{=}$

2.4.3.2 Crystallization Models

The empirical crystallization models are based on the work of Tseng and Rochelle (1986), and apply to the crystallization of solid calcium sulfite. CaSO_3 is known to crystallize as hemihydrate ($\text{CaSO}_3 \cdot \frac{1}{2} \text{H}_2\text{O}$) and gypsum crystallizes as both hemihydrate and dihydrate ($\text{CaSO}_4 \cdot 2\text{H}_2\text{O}$) forms.

2.4.4 Stage Calculations

At each stage of the TCA, the liquid is assumed to be well-mixed and the gas is plug-flow.

Chen and Douglas (1969) have studied axial mixing patterns of liquid in a TCA using tracer studies and one-dimensional dispersion models. They used a single stage TCA having 1 ft internal diameter packed to a height of 1 ft with 1" hollow polyethylene spheres for their studies. The measurements from the residence time distribution experiments have been compared to the expected values for well-mixed and plug-flow reactors in Figure 2.2. At gas velocities similar ($U_g = 3.7$ m/s) to those observed for the TCA columns at EPA/RTP and Shawnee (3.7 m/s) and somewhat lower liquid velocities (0.015 m/s versus 0.025 m/s), the liquid mixing pattern of a TCA is close to that of an ideal well-mixed reactor ($N_{Pe} = 2.2$). For the results reported by Chen and Douglas, an increase in liquid rate at constant gas velocity causes a decrease in the Peclet ($N_{Pe} = uL/D_L$) number. It can be expected that TCA behavior resembles a well-mixed reactor more closely (at $U = 0.025$ m/s versus 0.015 m/s) at higher liquid rates.

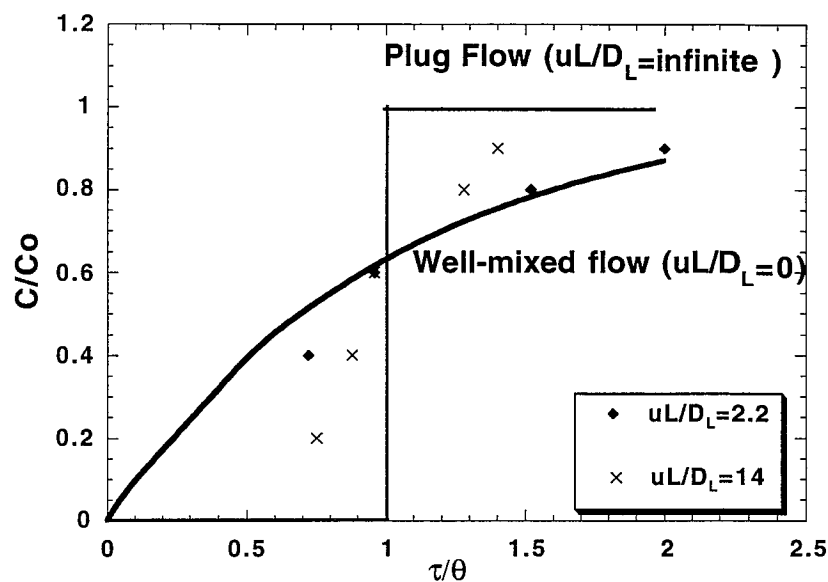


Figure 2.2: Axial Mixing Data for a Single Stage TCA (Chen and Douglas, 1968) Versus Theoretical Predictions (Smith, 1981).

Although there are no studies for gas mixing patterns in TCA, it may be useful to compare the gas mixing patterns for similar contactors at comparable gas velocities. For similar gas velocities Sharma and Doraiswamy (1983) have noted that the Residence Time Distribution (RTD) for gas is suggestive of plug flow for packed columns ($U_g = 0.1-1$ m/s), plate columns without downcomers (0.5-3m/s), bubble cap-columns (0.5-3 m/s) and horizontal pipeline contactors (0.05-3m/s). For plate columns without downcomers and bubble-cap columns, the gas flow

RTD is known to resemble plug flow, and liquid RTD (Sharma and Doraiswamy, 1983) is known to be well-mixed (as assumed for the TCA).

The stagewise material balances are calculated in terms of 4 species and are stated below.

$$\text{Out} - \text{In} = \text{Desorbed/ Absorbed} \pm \text{Crystallized/Dissolved}$$

Table 2.1: Material balance equations for stagewise calculations.

Species	Absorption/Desorption (f(i))	Dissolution-Crystallization (g(i))
S(VI)	$2 \frac{G}{L} (P_{O_2,i} - P_{O_2,o})$	$-K'_{\text{cry1}} (RS_{\text{CaSO}_4} - 1)$
S(IV)	$\frac{G}{L} (P_{\text{SO}_2,i} - P_{\text{SO}_2,o})$ $- 2 \frac{G}{L} (P_{O_2,i} - P_{O_2,o})$	$K_{\text{CaSO}_3} (\sum \Delta_j [\text{SO}_{3,j}])$ OR $- K'_{\text{cry2}} \frac{(RS_{\text{CaSO}_3} - 1)^2}{RS_{\text{CaSO}_4}}$
Ca		$K_{\text{CaCO}_3} (\sum \Delta_j [\text{CO}_{3,j}]) +$ $K_{\text{CaSO}_3} (\sum \Delta_j [\text{SO}_{3,j}])$ OR $- K'_{\text{cry2}} \frac{(RS_{\text{CaSO}_3} - 1)^2}{RS_{\text{CaSO}_4}}$ $- K'_{\text{cry1}} (RS_{\text{CaSO}_4} - 1)$
CO ₂	$\frac{G}{L} (P_{\text{CO}_2,i} - P_{\text{CO}_2,o})$	$K_{\text{CaCO}_3} (\sum \Delta_j [\text{CO}_{3,j}])$

$\text{SO}_{3,j} = \text{S(IV) species} = \text{HSO}_3^-(\text{L}), \text{SO}_3^{2-}(\text{L}) \text{ and } \text{SO}_2(\text{L})$

$\text{CO}_{3,j} = \text{CO}_3^{2-}(\text{L}) = \text{HCO}_3^-(\text{L}) \text{ and } \text{CO}_2(\text{L}); \text{S(VI)} = \text{SO}_4^{2-}, \text{HSO}_4^-$

$\Delta = C_{\text{interface}} - C_{\text{bulk}}$

2.5 MODIFICATIONS

In order to ensure that the model calculations are numerically robust, some modifications were made to the form of the crystallization model for CaSO_3 and

CaSO₄. The original model for sulfite crystallization at a stage had the form of Equation 2.5-1.

$$\frac{\text{CaSO}_3 \text{ (out)} - \text{CaSO}_3 \text{ (in)}}{t_{\text{res}}} = K_{\text{cry}2} \text{ CaSO}_3 \text{ (out)} \frac{(\text{RS}_{\text{CaSO}_3} - 1)^2}{\text{RS}_{\text{CaSO}_4}} \quad (2.5-1)$$

OR

$$\text{CaSO}_3 \text{ (out)} = \frac{\text{CaSO}_3 \text{ (in)}}{1 - \frac{K_{\text{cry}2} (\text{RS}_{\text{CaSO}_3} - 1)^2 t_{\text{res}}}{\text{RS}_{\text{CaSO}_4}}} \quad (2.5-2)$$

The model calculations solved 2.5-2 for the exit concentration of CaSO₃. Due to the form of 2.5-2, certain solution compositions can lead to singularities. The change in solid composition is usually small compared to its absolute value and independent of small changes in the same, so the equation 2.5-1 was modified and CaSO₃ (out) was replaced by CaSO₃ (in) on the right hand side.

In the case of forced oxidation, this modification may not be valid as the concentration of solid (CaSO₃ and CaSO₄) can change significantly.

A similar modification was made in the model for gypsum dissolution and the new model can be stated as

$$\frac{\text{CaSO}_4 \text{ (out)} - \text{CaSO}_4 \text{ (in)}}{t_{\text{res}}} = K_{\text{cry}1} \text{ CaSO}_4 \text{ (in)} (\text{RS}_{\text{CaSO}_4} - 1) \quad (2.5-3)$$

The H⁺ concentration was iterated upon instead of the Ca⁺⁺ to converge the material balance equations in the hold tank. This was found to improve robustness of calculations. This is also a useful calculation as much more data is available on the pH of systems than on the limestone utilization.

For parameter estimation (Chapter 4), pH from the hold tank exit was specified in some cases. In these cases, limestone reactivity was iterated upon instead of H⁺ to converge the material balance equations in the hold tank. The

calculated reactivity at the end of hold tank calculations was used to update the reactivity for scrubber calculations. At a specified limestone particle size distribution and utilization, the reactivity was fairly constant for a specified pH. Hence, if overall convergence was reached for the very first iteration, scrubber calculations were repeated with the updated reactivity value.

2.6 NOTATION

A	= Total interfacial area (cm^2/L)
a	= Interfacial area of contact between gas and liquid (cm^2/cc)
\underline{a}	= Interfacial area of contact between solid and liquid (cm^2/cc)
a_i°	= Activity coefficient parameter (A°)
b_i	= Activity coefficient parameter (dimensionless)
C	= Concentration (gmole/l)
C/C_0	= Ratio of exit/input-step concentration for tracer study (dimensionless)
C_b	= Bulk concentration (gmole/l)
C_s	= Concentration at the solid surface (gmole/l)
C_t	= Total calcium solids' concentration (gmol/l)
D	= Diffusion coefficient (cm^2/s)
d_{eff}	= Effective particle diameter (cm)
D_j	= Diffusivity of j^{th} species in liquid (cm^2/s)
D_L	= Liquid dispersion coefficient (m^2/s)
d_p	= Particle diameter (cm)
E	= Enhancement factor for oxidation (dimensionless)
F	= Fraction of limestone undissolved (dimensionless)
f	= Fraction of SO_2 absorbed (dimensionless)
f_i	= Fraction of undissolved limestone in i^{th} size fraction (dimensionless)
G	= Gas flow rate (gmol/s)

H	= Henry's constant (gmol/L-atm)
I	= Ionic Strength of solution (gmol/L)
K_c	= Equilibrium constant for calcite (gmol/L)
k_c	= Limestone surface constant ($M^{5/2}$ cm/s)
K_{CaCO_3}	= Dissolution constant for $CaCO_3$ ($1/cm^2$)
$K_{CaHCO_3^+}$	= Equilibrium constant for $CaHCO_3^+$ (gmol/L)
$K_{CaHSO_3^+}$	= Equilibrium constant for $CaHSO_3^+$ (gmol/L)
K_{cry1}	= Crystallization constant for gypsum ($1/cm^2$)
K_{cry2}	= Crystallization constant for $CaSO_3$ ($1/cm^2$)
k_g	= Gas side mass transfer coefficient (gmol atm ⁻¹ cm ⁻² s ⁻¹)
k_L°	= Liquid film mass transfer coefficient for gas/liquid absorption (cm-s ⁻¹)
$K_{MgHCO_3^+}$	= Equilibrium constant for $MgHCO_3^+$ (gmol/L)
$K_{MgHSO_3^+}$	= Equilibrium constant for $MgHSO_3^+$ (gmol/L)
k_{mt}	= Limestone reactivity parameter for a batch system (cm ²)
$k_{m\tau}$	= Limestone reactivity parameter for CSTR(cm ²)
K_{NaHSO_3}	= Equilibrium constant for $NaHSO_3$ (gmol/L)
K_{pseudo}	= Pseudo equilibrium constant (L/gmol)
k_{sL}	= Liquid film mass transfer coefficient for solid/liquid dissolution.(cm s ⁻¹)
$K_{sp,CaCO_3}$	= Solubility product of limestone (gmol/L) ²
$K_{sp,CaSO_3}$	= Solubility product of calcium sulfite (gmol/L) ²
L	= Column diameter for calculation of N_{pe} (m)
L	= Liquid flow rate (L/s)
N_g	= Number of gas film transfer units/stage (Scrubber)
N_L	= Number of liquid transfer units (Hold tank)
N_{Sc}	= Schmidt number (dimensionless)
N_{Sh}	= Sherwood number (dimensionless)
P	= Pressure (atm)
$P(t)$	= Distribution function for residence times in a CSTR

$P_{CO_2,i}$	= Partial pressure of CO_2 at the inlet to a stage (atm.)
$P_{CO_2,o}$	= Partial pressure of CO_2 at the exit from a stage (atm.)
$P_{O_2,i}$	= Partial pressure of O_2 at the inlet to a stage (atm.)
$P_{O_2,o}$	= Partial pressure of O_2 at the exit from a stage (atm.)
$P_{SO_2,i}$	= Partial pressure of SO_2 at the inlet to a stage (atm.)
$P_{SO_2,o}$	= Partial pressure of SO_2 at the exit from a stage (atm.)
RS	= Relative Saturation (dimensionless)
t_{res}	= Slurry residence time on a stage (s)
U	= Limestone utilization (dimensionless)
u	= Liquid velocity (m/s)
U_i	= Activity coefficient parameter (Uncharged species only)
U_L	= Liquid velocity (m/s)
V_p	= Particle volume (cm^3)
X	= Concentration in solution (gmol/l)
Z	= Packed height (cm)
Z_i	= Charge on i^{th} species (dimensionless)

Greek Symbols

β	= Term accounting for the agitation force imparted to the solution
ρ	= Density (gmol/cc)
Δ	= Difference operator
δ_{ave}	= Average film thickness (cm)
γ_i	= Activity coefficient of i^{th} species (dimensionless)
Φ_i	= Fraction of particles present in i^{th} size range (dimensionless)
Σ	= Summation

Subscripts and Superscripts

ave	= Average
b	= Bulk phase (liquid or gas)
eff	= Effective
eq	= Equilibrium value

i	= Interface (gas/liquid or solids/liquid)
in	= Stage Inlet
L	= Liquid phase
m	= Molar
out	= Stage exit
pseudo	= Pseudo species
s	= Surface of solid

CHAPTER 3

MODEL CHEMISTRY

3.1 INTRODUCTION

In this chapter, the model has been used to predict the effects of important variables on system performance. The values of inlet SO_2 concentration, limestone utilization, liquid/gas flow rates in the scrubber, inlet solution composition, buffer acid concentration, and residence time in the hold tank are varied about a selected base case. A quantitative explanation of the effects of these variables is offered, using the calculated values of solution compositions and enhancement factors from the model. The data used for parameter estimation show variation in SO_2 concentration, pH, limestone utilization and the ratio of liquid to gas flow rates. Therefore, it is important to understand model predictions of these phenomena.

Chang and Rochelle (1982, 1985) measured and modeled the effect of the hydrolysis reaction and buffer additives on SO_2 enhancement in water and aqueous solutions of buffer additives. Chang and Rochelle (1985) successfully modeled the effect of $\text{SO}_3^{=}$ in NaOH and Na_2SO_3 solutions in a bench-scale stirred cell apparatus. At high pH, in NaOH and Na_2SO_3 solutions, they found that enhancement by $\text{SO}_3^{=}$ dominated SO_2 transport. In aqueous solutions at a pH of 4 to 5, $\text{SO}_3^{=}$ did not contribute significantly to enhancement. Chan and Rochelle (1983) modeled the effects of HCO_3^- on solution chemistry. Although they modeled a three stage scrubber, they did not report calculated enhancement

factors for any of the species at each stage. The contribution of individual enhancement factors for SO_3^- , HCO_3^- , and SO_4^- has not been reported previously for turbulent contact absorbers. The contribution of the enhancement factors can vary significantly over a 3-stage turbulent contact absorber and these species can play an important role in SO_2 absorption.

3.2 BASE CASE CONDITIONS

The base case values for solution composition, solids composition and most operating variables and parameters were obtained from the limestone type and grind study conducted in the EPA/RTP pilot scale absorber (Gage, 1989). A summary of the operating conditions is given in Table 3.1. The details of the experimental run for the above are contained in a progress report by Dempsey et al. (1979). Other details of the base case are described by Gage (1989). A summary of the particle size distribution is included in Appendix B (Table B-6). In the absence of buffer additives the base case conditions lead to a SO_2 penetration ($p = P_{\text{SO}_2,\text{out}}/P_{\text{SO}_2,\text{in}}$) of 0.2 and $\text{pH} = 6.0$ (at the hold tank exit). A sample calculation showing details of the calculated results from FGDTX is presented in Appendix C.

3.2.1 Calculation of Results

The tabulated data (Tables 3.2-3.5) show the calculated values of the enhancement factors as well as some of the important bulk and interfacial concentrations. The values of SO_2 penetration and solution pH shown in Figures 3.1 to 3.5 indicate values calculated by the model.

Table 3.1: Base Case Conditions Used for the Simulation of the TCA Contactor at EPA/RTP.

Operating Conditions	
Number of Stages	3
Residence time in the scrubber (s) [§]	9
Residence time in the hold tank (s)	540
Height of Packing (inches/ stage) ^{§§}	7
Column Diameter (inches)	9
Gas velocity at 430 K [†] (ft/s)	12.5
L/G at 333 K ^{††} (L/gmol)	0.2
Inlet SO ₂ concentration (ppm)	2900
Chloride concentration (ppm)	2000
Adipic Acid concentration (mM)	0.0
Limestone Utilization (%)	77
Limestone type	Fredonia Coarse [‡]
Solids (%)	10
Inlet Slurry Temperature (K)	333
Oxidation (%)	8.4
Model Parameters	
K _{CaSO₄·2H₂O} (Dissolution constant) [gmol/cm ² -s]	3×10 ⁵
K _{CaSO₃·0.5H₂O} (Dissolution constant) [gmol/cm ² -s]	3×10 ⁵
k _L ^o /k _g (cm ³ -atm/gmol)	200
N _g (scrubber)	6.9
N _L (hold tank)	0.6
L/G (hold tank) (L/gmol)	45

[§] The residence time of slurry is calculated based on pressure drop of 8.5", assuming liquid hold-up = pressure drop (Gage, 1989).

^{§§} The packing height was not reported in progress report 31 and is taken from Gage (1989).

[†] 430 K is the temperature of gas before it is brought into contact with scrubber slurry.

^{††} 333 K is the adiabatic saturation temperature of gas in contact with scrubbing slurry.

[‡] The particle size distribution for Fredonia Coarse is given in Appendix B, Table B-6.

For each case (Tables 3.2-3.5), the detailed values of bulk and interfacial solution composition as well as SO₂ partial pressure have been provided in Appendix B (Table B-1 to B-4). A sample calculation for solution containing 200 ppm of DBA is shown in Table B-5 of Appendix B.

The reported values of L/G, t_{res}, Utilization, and N_g are the same for each stage in the scrubber. Any changes in parameters (N_g) or operating conditions (L/G, U, DBA concentrations) from base case conditions (Table 3.1) are noted in the appropriate table. The tabulated values of Y_{SO₂}, H⁺ (interface) and driving force (for SO₂ absorption) have been reported at the inlet conditions to the stage. The enhancement factor (E_k) and fraction of gas film resistance (K_g/k_g) have been calculated using bulk solution compositions at each stage and the bulk gas and interface concentrations at stage inlet.

$$E_k = \sum_k \sqrt{\frac{D_k}{D_{SO_2}}} \frac{(C_{k,i} - C_{k,bulk})}{(C_{SO_2,i} - C_{SO_2,bulk})} \quad (3.2-1)$$

where k = SO₃⁼, HSO₃⁻, SO₄⁼, HSO₄⁻, HA⁻, and SO₂.

$$K_g/k_g = \frac{(P_{SO_2,g} - P_{SO_2,i})}{(P_{SO_2,g} - P_{SO_2,L})}$$

The total enhancement factor is calculated based on the total flux of sulfur species (3.2-1). Equation 3.2-1 can be restated taking into account zero charge flux as shown below.

$$\text{Charge Balance: } \sum_i Z_i \sqrt{D_i} \Delta C_i = 0 \quad (3.2-2)$$

$$i = H^+, CO_3^{=}, HCO_3^-, SO_3^{=}, HSO_3^-, SO_4^{=}, HSO_4^-, A^=, HA^-$$

Expanding 3.2-2 and equating fluxes of negatively and positively charged ions gives 3.2-3. For the sake of convenience the names of the ionic and non ionic compounds will be used to refer to their respective concentrations in the liquid phase.

$$\begin{aligned} \sqrt{D_{H^+}} \Delta H^+ = & 2 (\sqrt{D_{CO_3^{=}}} \Delta CO_3^{=} + \sqrt{D_{SO_3^{=}}} \Delta SO_3^{=} + \\ & \sqrt{D_{SO_4^{=}}} \Delta SO_4^{=} + \sqrt{D_{A^{=}}} \Delta A^{=}) + \\ \sqrt{D_{HCO_3^-}} \Delta HCO_3^- + & \sqrt{D_{HSO_3^-}} \Delta HSO_3^- + \sqrt{D_{HSO_4^-}} \Delta HSO_4^- + \sqrt{D_{HA^-}} \Delta HA^- \end{aligned} \quad (3.2-3)$$

Substituting for HSO_3^- from 3.2-3 in 3.2-1 results in the following expression for the overall enhancement factor

$$\begin{aligned} E_{total} (\sqrt{D_{SO_2}} \Delta SO_2) = & 1 - 2 \sqrt{D_{CO_3^{=}}} \Delta CO_3^{=} - (\sqrt{D_{HCO_3^-}} \Delta HCO_3^- - 2 \sqrt{D_{A^{=}}} \Delta A^{=} \\ & - \sqrt{D_{HA^-}} \Delta HA^- - \sqrt{D_{SO_3^{=}}} \Delta SO_3^{=} - \sqrt{D_{SO_4^{=}}} \Delta SO_4^{=} + \sqrt{D_{H^+}} \Delta H^+ \end{aligned} \quad (3.2-4)$$

$$E_{total} = 1 + E_{CO_3^{=}} + E_{HCO_3^-} + E_{H_2A} + E_{SO_3^{=}} + E_{SO_4^{=}} + E_{H^+} \quad (3.2-5)$$

The individual enhancement factors for H_2A , $CO_3^{=}$, and $SO_3^{=}$ are calculated as shown below. The enhancement factors for H^+ , HCO_3^- and $SO_4^{=}$ are calculated in a manner analogous to $SO_3^{=}$, however E_{H^+} has a positive sign.

$$\begin{aligned} E_{SO_3^{=}} = & - \frac{\sqrt{D_{SO_3^{=}}} \Delta SO_3^{=}}{\sqrt{D_{SO_2}} \Delta SO_2} \\ E_{H_2A} = & -2 \frac{\sqrt{D_{A^{=}}} \Delta A^{=}}{\sqrt{D_{SO_2}} \Delta SO_2} - \frac{\sqrt{D_{HA^-}} \Delta HA^-}{\sqrt{D_{SO_2}} \Delta SO_2} \\ E_{CO_3^{=}} = & -2 \frac{\sqrt{D_{CO_3^{=}}} \Delta CO_3^{=}}{\sqrt{D_{SO_2}} \Delta SO_2} \end{aligned}$$

At the interface, pH is usually between 3 and 4, whereas bulk pH varies between 4.5 and 6. The concentration of HSO_3^- in the bulk liquid is usually the

same order of magnitude as its value at the interface. For the buffer $\text{HSO}_3^-/\text{SO}_3^{=}$ it can be expected that the $\text{SO}_3^{=}$ concentration at the interface is negligible compared to its bulk value.

$$K_a = \frac{a_{\text{H}^+} a_{\text{SO}_3^{=}}}{a_{\text{HSO}_3^-}} = 6.2 \times 10^{-8} \text{ (gmol/L)}$$

Similarly it can be deduced that the interface concentration of HCO_3^- ($K_a = 4.45 \times 10^{-7}$; $\text{CO}_2 + \text{H}_2\text{O} = \text{H}^+ + \text{HCO}_3^-$) is negligible compared to its bulk value. In case of $\text{CO}_3^{=}$ ($K_a = 4.69 \times 10^{-11}$; $\text{H}^+ + \text{CO}_3^{=} = \text{HCO}_3^-$) the concentrations in bulk as well as at the interface are negligible throughout in the range of operating pH values (3-6). Therefore, $\text{ECO}_3^{=}$ has not been reported. Often, bulk concentration values alone can be used to explain enhancement factors for these buffers.

For the limestone slurry scrubbing system, the absolute value of pH should not be used as a measure of the alkalinity in solution. The capacity of the solution for reacting with the absorbed gas depends upon the amount of each buffer present in solution. To the extent that the pH is indicative of the speciation of each buffer, it may be considered to be an indicator of solution capacity.

Results from the first and third stages have been tabulated for each case. Results from the second stage calculations have been omitted from the Tables 3.2-3.5 as the second stage of the contactor has a performance between that of the top and bottom stages. The sum of the reported enhancement factors is less than the total enhancement by ~ 1 (i.e. physical absorption).

3.3 RESULTS

At the simulated conditions it was observed that SO₂ penetration was lower for lower inlet SO₂ partial pressure, lower limestone utilization, higher dibasic acid (DBA) concentration, higher residence time in the hold tank and greater L/G in the scrubber. In most of the above cases it was also observed that the concentration of HCO₃⁻ and SO₃⁼ increased and the HSO₃⁻ concentration decreased when lower penetration was observed. The calculations show that the equilibrium concentration of SO₂ is negligible in the bulk liquid. In most cases SO₂ penetration can be predicted using a simple equation of the form $-\ln p = N_g (K_g/k_g)$. Limestone utilization has a significant effect on the pH and penetration.

3.3.1 Effect of Inlet SO₂

As SO₂ concentration in the gas at the inlet to a stage increases, penetration also increases although the net absorption of SO₂ (ppm) increases. Figure 3.1 shows the effect of inlet SO₂ concentrations of 1900, 3200 and 5000 ppm on penetration (p) and the extent of gas film control (K_g/k_g).

As the partial pressure of SO₂ decreases from 5000 ppm (bottom stage, high inlet SO₂) to 626 ppm (top stage, low inlet SO₂) the total enhancement increases (2.08 to 12.58) and penetration decreases from 0.77 to 0.23. At lower SO₂ partial pressure, the contribution of the enhancement reactions (ΣE_k) is larger in comparison to the contribution of physical absorption (Table 3.2). This is a combination of two factors, a smaller driving force for physical absorption (C_{SO₂,i} = 0.1 mM versus 1.7 mM) and lower levels of H⁺ (0.25 versus 0.76 mM)

and HSO_3^- at the gas liquid interface. Lower levels of H^+ lead to greater enhancement by the hydrolysis reaction as well as by $\text{SO}_3^{=}$ and HCO_3^- .

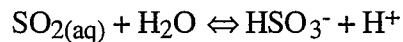


Table 3.2: Effect of Inlet SO_2 Partial Pressure on Calculated Enhancement Factors (E) and Extent of Gas Film Resistance (K_g/k_g); $L/G = 0.2 \text{ L/gmol}$, $N_g/\text{stage} = 2.3$.

Case	Low Inlet SO_2			High Inlet SO_2			Base Case		
U (%)	77			77			77		
t_{res}^\dagger (s)	540			540			540		
Stage	Inlet [‡]	Top	Bottom	Inlet [‡]	Top	Bottom	Inlet [‡]	Top	Bottom
Y_{SO_2}		626	1880		2700	4950		1260	2870
(ppm)									
d.f. ^{††}		304	371		606	612		426	445
(ppm)									
p	0.08	0.23	0.61	0.33	0.60	0.77	0.19	0.43	0.70
pH	6.05	5.49	4.57	5.76	4.84	4.09	5.93	5.24	4.37
H^+_{i} (mM)		0.25	0.48		0.76	0.70		0.49	0.56
$\text{CSO}_{2,\text{i}}$ (mM)		0.10	0.50		0.80	1.70		0.30	0.90
Enhancement Factors									
E_{total}		12.58	3.38		3.81	2.08		6.51	2.52
E_{H^+}		4.35	1.75		2.00	0.88		2.80	1.27
$E_{\text{SO}_3^{=}}$		4.25	0.37		0.39	0.09		1.47	0.21
$E_{\text{HCO}_3^-}$		2.82	0.06		0.14	0.01		0.62	0.02
$E_{\text{SO}_4^{=}}$		1.02	0.22		0.10	0.02		-0.08	0.10
K_g/k_g		0.49	0.19		0.22	0.15		0.33	0.16
p ^{‡‡}		0.32	0.63		0.60	0.76		0.45	0.70
Bulk Compositions (mM)									
HSO_3^-	1.04	3.35	11.00	2.30	9.10	25.00	1.50	5.48	16.67
$\text{SO}_3^{=}$	1.12	1.00	0.42	1.28	0.61	0.30	1.22	0.91	0.37
HCO_3^-	2.28	0.47	0.05	2.48	0.18	0.02	2.41	0.33	0.03
Dissolution (+)/ Precipitation (-), mM									
CaCO_3	6.50	0.36	1.03	13.00	0.99	2.72	8.90	0.53	0.12

CaSO₃	-2.10	0.00	1.30	-21.20	0.82	1.63	-13.50	0.31	1.81
-------------------------	-------	------	------	--------	------	------	--------	------	------

[†]t_{res} = residence time in the hold tank

^{††}d.f. = driving force for SO₂ absorption at the stage inlet.

#Inlet = Overall penetration, pH and solution compositions at scrubber inlet.

##p = exp (-N_gK_g/k_g)

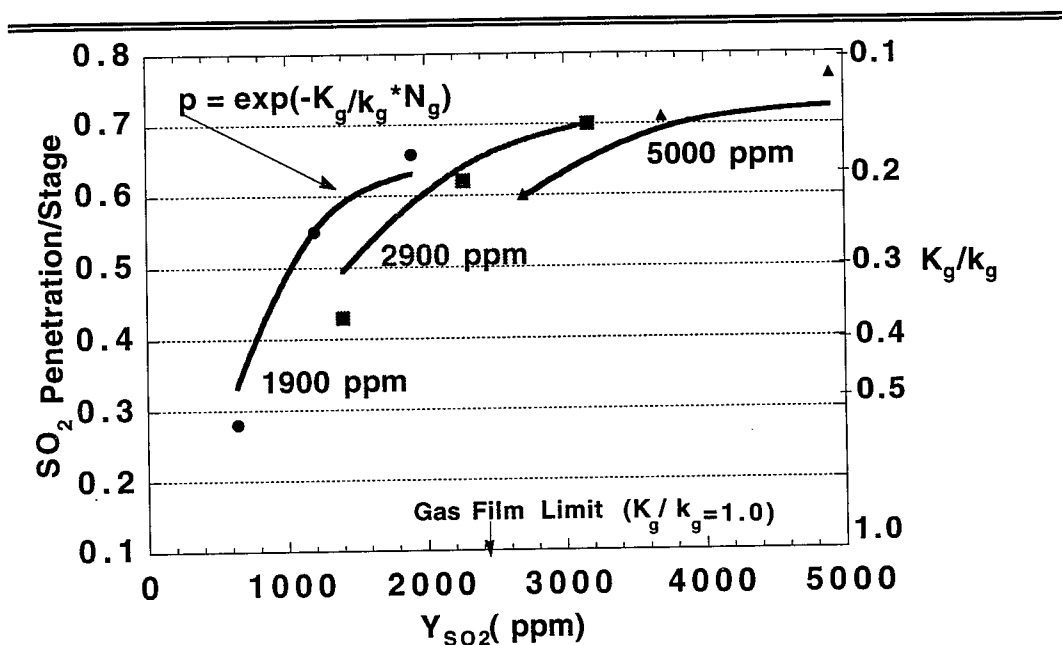


Figure 3.1: Effect of Change of Inlet SO₂ Concentration on the Penetration.

A comparison between model predictions versus predicted SO₂ penetration at stage inlet conditions ($K_g/k_g N_g = -\ln p$) assuming negligible equilibrium partial pressure is also shown. The conditions correspond to EPA/RTP contactor, $N_g = 6.9$, $k_L/k_g = 200$ cc-atm/gmol.

It can be expected that further decrease of SO₂ partial pressure would decrease penetration until the gas film control limit is reached. Figure 3.1 shows this limit at $K_g/k_g = 1.0$ on the Y axis. The equation $K_g/k_g N_g = -\ln p$ accounts for most of the variation in SO₂ penetration, showing that the equilibrium bulk liquid concentration of SO₂ is negligible. This equation can be derived as follows.

$$N_g = \int_{y_1}^{y_2} \frac{dy}{y - y_i^*}$$

$$K_g (P_{SO_2,b} - P_{SO_2,L}^*) = k_g (P_{SO_2,b} - P_{SO_2,i})$$

The ratio $\frac{K_g}{k_g}$ can be expressed in terms of mole fractions (y) instead of pressures (P),

$$N_g = \int_{y_1}^{y_2} \frac{dy}{y - y_i^*} \frac{y - y_i^*}{y - y_L^*} \frac{k_g}{K_g}$$

Neglecting y_L^* and rearranging we get

$$N_g \frac{K_g}{k_g} = \ln \left(\frac{y_2}{y_1} \right)$$

$$N_g \frac{K_g}{k_g} = -\ln p \text{ where } p = \frac{y_1}{y_2}$$

In cases of complete gas film control (as in the presence of high concentrations of DBA) $K_g/k_g = 1.0$, therefore $N_g = -\ln p$.

Total absorption of SO_2 at a stage can be calculated from inlet concentration and penetration, total absorption = $P_{SO_2,b} (1-p)$. Although the penetration increases with increase of $P_{SO_2,b}$ (0.23 versus 0.77), the net absorption of SO_2 (ppm) also increases (482 versus 1138 ppm), this is due to a net increase in the gas phase and liquid phase driving forces (304 versus 612 ppm at stage inlet) at higher partial pressures.

3.3.2 Effect of Limestone Utilization

As the limestone utilization (U) decreases, pH levels rise and the SO_2 penetration decreases (Figure 3.2). Limestone utilization is the moles of SO_2 absorbed per mole of limestone fed to the system.

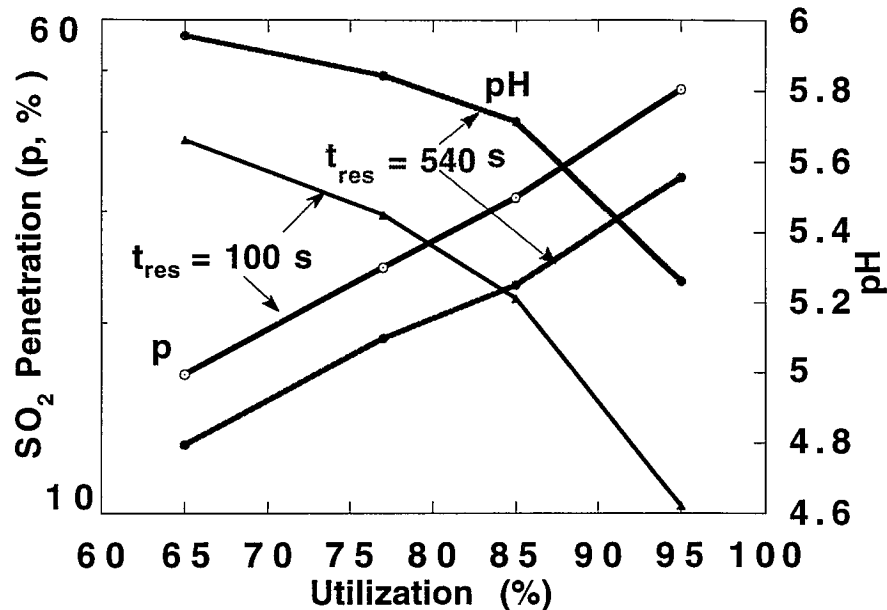


Figure 3.2: Effects of Limestone Utilization on Penetration and pH at Hold Tank Residence Times of 100s and 540s.

The Limestone Particle Size Distribution was Similar to that of Fredonia Coarse (Gage, 1989) for 10% Solids in Slurry.

With a constant slurry solids concentration, decreasing utilization increases the CaCO_3 solids concentration and surface area available for dissolution (the model also accounts for the effect of utilization on the limestone particle size distribution). With increased surface area (lower U), the steady-state pH required to dissolve approximately the same amount of CaCO_3 will be greater throughout the system. Table 3.3 shows that the pH of the scrubber feed increases from 5.32 to 6.06 when the utilization decreases from 95 to 65% and the bulk

solution pH leaving the scrubber also increases by 0.5 pH units over the same range of utilization.

Table 3.3: Effect of Change of Limestone Utilization (U) and Hold Tank Residence Time ($N_g/\text{stage} = 2.3$, $L/G = 0.2$ L/gmol).

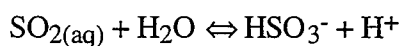
Case I.D.	Low U			High U			Low U, low t_{res}		
U (%)	65			95			65		
t_{res}^{\dagger} (s)	540			540			100		
Stage	Inlet	Top	Bottom	Inlet	Top	Bottom	Inlet	Top	Bottom
Y_{SO_2}		1150	2881		1570	2880		1150	2881
(ppm)									
d.f. ^{††}		432	502		338	362		384	490
(ppm)									
p	0.14	0.36	0.67	0.34	0.62	0.76	0.17	0.43	0.68
pH	6.06	5.41	4.60	5.32	4.65	4.14	5.74	5.25	4.59
H^+_{i} (mM)		0.42	0.59		0.44	0.46		0.40	0.57
Enhancement Factors									
E_{total}		7.95	2.81		3.66	2.1		5.88	2.76
E_{H^+}		3.28	1.35		1.98	1.02		2.88	1.32
$E_{\text{SO}_3^-}$		2.19	0.32		0.51	0.16		1.73	0.33
$E_{\text{HCO}_3^-}$		1.00	0.04		0.09	0.01		0.53	0.00
$E_{\text{SO}_4^-}$		0.00	0.10		0.081	0.08		0.08	0.10
K_g/k_g		0.38	0.18		0.22	0.15		0.33	0.18
p^{\ddagger}	0.41	0.66		0.59	0.70		0.46	0.66	
Bulk Concentration (mM)									
HSO_3^-	1.18	4.68	15.00	5.85	10.80	22.60	2.32	5.80	15.60
SO_3^-	1.24	1.15	0.57	1.15	0.46	0.30	1.23	0.98	0.59
HCO_3^-	2.85	0.49	0.06	0.68	0.08	0.01	1.52	0.32	0.06
Dissolution/ Crystallization (+/-), mM									
CaCO_3	8.40	0.73	1.96	8.96	0.17	0.26	7.50	0.98	1.96
CaSO_3	-12.30	-0.02	0.85	-15.10	1.54	2.99	-11.80	0.13	0.77

$^{\dagger}t_{\text{res}}$ = residence time in the hold tank

†† d.f. = driving force for SO_2 absorption at the stage inlet.

$^{\ddagger}p = \exp(-N_g K_g/k_g)$

Bulk solution pH is an indicator of other processes that lead to a reduction in the bisulfite concentration. Higher pH results in greater precipitation of CaSO_3 (12.30 mM versus 15.10 mM), causing a reduction in HSO_3^- levels (5.85 mM versus 1.18 mM). Bisulfite in the feed solution is reduced from 5.85 mM to 1.18 mM by higher pH at $U = 65\%$ versus $U = 95\%$. Bisulfite in the bottom stage is reduced from 22.6 mM to 15 mM due to the combination of reduced feed bisulfite and reduced dissolution of calcium sulfite. Scrubber bisulfite determines hydrogen ion concentration at the gas/liquid interface through the equilibrium:



The interfacial H^+ concentration determines the contribution of the above hydrolysis reaction to the SO_2 enhancement. The contribution of H^+ to the SO_2 enhancement factor in the bottom stage increases by 34% ($E_{\text{H}^+} = 1.35$ versus 1.02) from 95 to 65% utilization. At the top stage, the combined effect of reduced Y_{SO_2} and reduced bisulfite increases the H^+ contribution by 65% at the top stage ($E_{\text{H}^+} = 3.28$ versus 1.98).

In the scrubber, greater pH increases dissolved alkalinity as sulfite ($\text{HSO}_3^- \rightleftharpoons \text{SO}_3^{2-} + \text{H}^+$). The enhancement due to sulfite in the bottom stage varies from 0.16 (8% of total enhancement) at 95% utilization to 0.32 (10%) at 65% utilization. At the top stage, the combined effect of higher pH and lower interfacial concentration of sulfur dioxide (See Table B-2) results in greater contribution to enhancement 2.19 (27%) at $U = 65\%$ and 1.98 (53%) at $U = 95\%$ by SO_3^{2-} .

In the hold tank greater pH results in greater dissolved alkalinity as bicarbonate, but not as sulfite. Sulfite concentration is reasonably stable at about 1 mM, which is near the saturation value for the calcium sulfite ion pair. Greater bicarbonate alkalinity carries over through the top stage of the scrubber where bicarbonate alkalinity contributes 12% of the SO₂ absorption at 65% utilization, but only 3% at 95% utilization. Even with greater pH, bicarbonate alkalinity is never important in the middle or bottom stages of the scrubber.

3.3.3 Effect of Residence Time in the Hold Tank

The effect of reducing residence time from 540 to 100 seconds in the hold tank is to decrease scrubber feed pH from 6.05 to 5.74, because a greater driving force is needed to dissolve about the same quantity of limestone. The concentration of bicarbonate decreases (2.85 to 1.52 mM) and the bisulfite increases (1.18 mM to 2.32 mM), resulting in somewhat greater SO₂ penetration (0.17 versus 0.14). The decrease of residence time has a significant effect on the performance of the first stage alone, where the penetration is reduced from 0.43 to 0.36. Thereafter, sufficient amounts of limestone are dissolved in the subsequent stages to maintain nearly equal levels of penetration for both cases (100 s versus 540s residence time). At 540 seconds residence time, the hold tank is near equilibrium with respect to limestone dissolution. It can be expected that further increase of the residence time would produce very small changes in penetration and pH.

3.3.4. Effect of Solution Composition

Figure 3.3 demonstrates the effect of solution composition on the SO_2 penetration over a range of limestone utilization values.

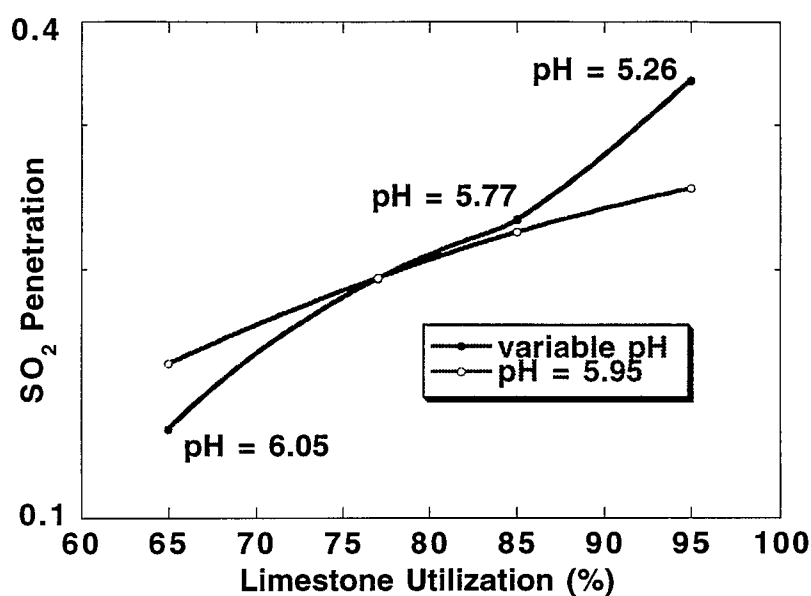


Figure 3.3: Effect of Constant Inlet pH on Penetration Over a Range of Limestone Utilization.

The constant pH curve in Figure 3.3 is calculated by varying the utilization at a constant inlet solution composition (similar to that at $U = 77\%$). The second curve is calculated by varying the limestone utilization and allowing the inlet solution composition to vary. Comparison of the penetration at these conditions shows that the effect of changing utilization without changing solution

composition is about half of the total effect of allowing the hold tank pH and solution composition to change when excess limestone is added. In other words the scrubber performance depends on both the solution (bisulfite, bicarbonate) and solids composition (limestone utilization) of the scrubber feed.

3.3.5 Effect of Liquid-to-Gas Ratio

The effect of liquid-to-gas ratio (L/G) was simulated by adjusting the liquid rate with constant hold tank volume and constant liquid phase residence time of 9 seconds in the scrubber. This is similar to decreasing the gas rate at constant liquid flow rate. Increased L/G reduces SO_2 penetration because it provides additional solution capacity and increases the mass transfer capability of the scrubber. Both of these effects are quantified in Figure 3.4.

With N_g constant at 6.9, only the effect of solution capacity is quantified. With N_g proportional to L/G, the combined effect of both mechanisms is simulated. At low L/G, the two effects appear to be of equal importance. At higher L/G, the effect of L/G on N_g is more significant.

Increase of the L/G causes a decrease in the level of bisulfite at each stage (19.6 versus 14.46 mM for bottom stage) due to the dilution caused by the additional solution present. The decrease of bisulfite levels and greater enhancement due to SO_3^- and H^+ lead to better performance at higher L/G. Table 3.4 shows that both E_{H^+} and $E_{\text{SO}_3^-}$ increase in both the top and bottom stages as the L/G increases.

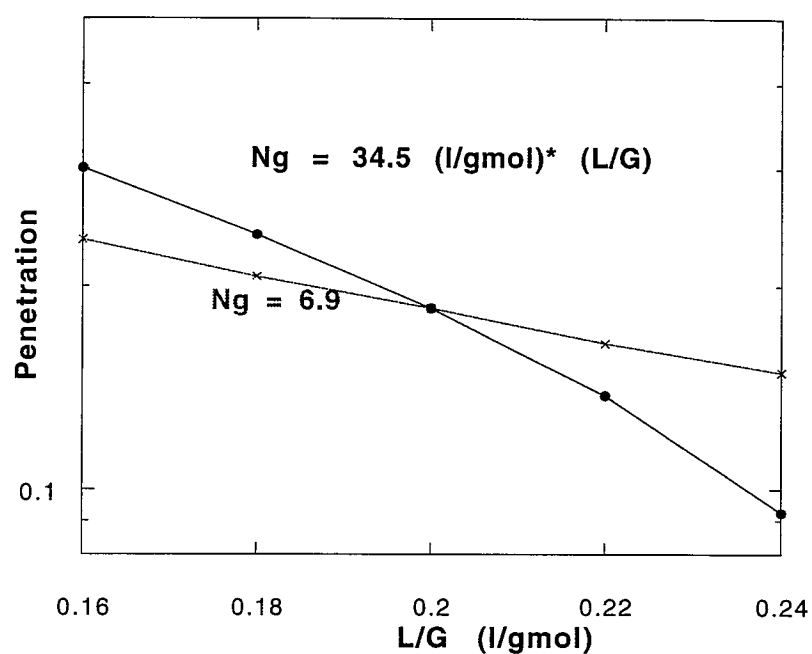


Figure 3.4: Scrubber Performance as a Function of Liquid Rate with a Constant and Variable Number of Gas Phase Transfer Units .

Liquid Rate was Varied by Changing the Ratio of L/G at Constant Gas Velocity and Constant Liquid Hold-up (Residence Time = 9 s).

Table 3.4 shows that decreasing N_g proportionately to L/G causes an increase in the overall penetration at the same L/G (0.31 versus 0.25). The solution capacity for absorption is the slightly better at decreased N_g . As shown in Table 3.4 the HSO_3^- levels are slightly lower for all the stages and the enhancement factors are somewhat higher (5.36 and 2.40 versus 5.18 and 2.35). Decreasing N_g (1.84/stage versus 2.3/stage) causes a reduction in the total mass-

transfer capability of the absorber, which causes higher overall penetration, despite better solution capacity.

Table 3.4: Effect of Change of (L/G) on SO₂ penetration, Due to Change of Liquid Capacity and Gas Film Mass Transfer Units at U = 77%, $t_{res}^{\dagger} = 540$ s.

Case I.D.	Low L/G			High L/G			Low L/G, low N _g		
L/G	0.16			0.24			0.16		
L/gmol									
U (%)	77			77			77		
Stage	Inlet	Top	Bottom	Inlet	Top	Bottom	Inlet	Top	Bottom
Y _{SO₂} (ppm)		1400	2870		1150	2870		1540	2870
d.f. ^{††} (ppm)		396	393		432	483		457	441
p	0.25	0.50	0.74	0.15	0.39	0.68	0.31	0.56	0.74
H ⁺ _i (mM)		0.46	0.50		0.47	0.60		0.54	0.55
pH	5.91	5.08	4.25	5.95	5.34	4.47	5.94	5.14	4.35
Enhancement Factors									
E _{total}		5.10	2.35		7.83	2.78		5.36	2.40
E _{H⁺}		2.57	1.10		3.61	1.40		2.78	1.25
E _{SO₃⁼}		1.06	0.18		1.83	0.23		1.05	0.21
E _{HCO₃⁻}		0.38	0.02		0.85	0.03		0.41	0.02
E _{SO₄⁼}		0.03	0.02		0.09	0.08		0.05	0.05
K _g /k _g		0.28	0.14		0.38	0.18		0.30	0.17
p [‡]		0.52	0.73		0.42	0.66		0.50	0.68
Bulk Compositions (mM)									
HSO ₃ ⁻	1.61	6.76	19.60	1.40	4.57	14.46	1.48	6.27	17.80
SO ₃ ⁼	1.24	0.79	0.34	1.20	0.97	0.41	1.24	0.84	0.38
HCO ₃ ⁻	2.64	0.24	0.02	2.24	0.42	0.04	2.60	0.29	0.03
Dissolution (+)/ Precipitation (-)									
CaCO ₃	10.50	0.64	1.38	8.96	0.17	0.26	9.60	0.59	1.27
CaSO ₃	-16.30	0.55	2.15	-15.10	1.55	2.99	-14.60	0.45	1.81

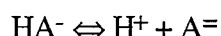
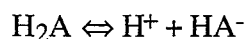
[†]t_{res} = residence time in the hold tank

^{††}d.f. = driving force for SO₂ absorption at the stage inlet.

[‡]p = exp (-N_g K_g/k_g)

3.3.6 Effect of DBA Addition

The addition of dibasic acid (DBA) buffers is often used to improve system performance (Chang and Dempsey, 1982; Chang and Rochelle, 1982).



The buffer species ($\text{A}^{=}$, HA^-) diffuse from the liquid bulk solution to the gas liquid interface and react reversibly with H^+ to give acid species (HA^- , H_2A). The acid species diffuses back to the bulk solution, carrying H^+ in the process. This enhances diffusion of SO_2 as HSO_3^- (Rochelle, 1982).

As the DBA concentration increases from 0 to 3600 ppm there is a drastic reduction of the overall SO_2 penetration from 0.20 to 0.002 (Figure 3.5, Table 3.5). This is due to the enhancing effect of the buffer and is accounted for mostly in the contribution of the $E_{\text{H}_2\text{A}}$ values to the overall concentration.

For the bottom stage the total enhancement increases from 2.87 to 76.8 due to the addition of 3600 ppm of DBA (Table 3.5). The total contribution of enhancement due to DBA increases from 0.6 (20%) to 68 (88% of total enhancement). At the top stage of the TCA, presence of high levels of DBA leads to conditions of gas film control, $K_g/k_g \sim 0.98$ (DBA = 1000, 3600 ppm). At these conditions, the calculated value of $-\ln p \sim 2.3 = N_g/\text{stage}$. In some of the cases with high enhancement factors (top stage, DBA = 1000, 3600 ppm) the stage is practically at gas film control and the interfacial concentration of SO_2 is very low. Practically, enhancement factors above 100 do not make a significant difference

in SO_2 absorption, as the system should be less than 10% liquid film controlled (Since $k_L^\circ/k_g \sim 0.2 \text{ atm/M}$, $H \sim 2 \text{ atm/M}$).

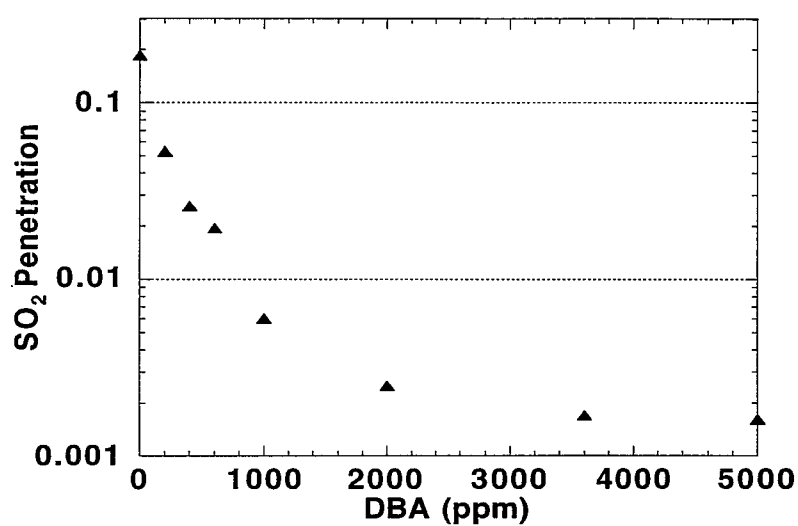


Figure 3.5: Effect of Dibasic Acid Concentration (ppm) on SO_2 Penetration ($N_g = 2.3$, $k_L^\circ/k_g = 200 \text{ cc-atm/gmol}$)

Table 3.5: Effect of DiBasic Acid (DBA) Concentrations on SO₂ Penetration and Extent of Gas Film Resistance $\frac{K_g}{k_g}$ (L/G = 0.2 L/gmol, U = 77%).

Case I.D.	DBA			DBA			DBA		
DBA (ppm)	200			400			1000		
t _{res} (s)	540			540			540		
N _g /stage	2.3			2.3			1		
Stage	Inlet	Top	Bottom	Inlet	Top	Bottom	Inlet	Top	Bottom
Y _{SO₂} (ppm)		967	2920		568	2884		749	2870
d.f. †† (ppm)		533	543		543	631		628	1090
p	0.07	0.20	0.65	0.025	0.12	0.58	.10	.38	.59
pH	5.77	5.28	4.48	5.75	5.51	4.89	5.74	5.54	4.78
C _{SO₂,i} (mM)		2.2e-4	0.98		0.03	0.88		0.01	0.63
H ⁺ _i (mM)		0.23	0.489		0.04	0.42		0.010	0.30
Enhancement Factors									
E _{total}		11.79	2.87		83	3.75		296	8.9
E _{H⁺}		2.29	0.21		2.6	1.02		2.41	1.01
E _{SO₃⁼}		2.68	0.29		18.9	0.37		37	0.78
E _{HCO₃⁻}		1.79	0.03		18.9	0.04		79	0.15
E _{H₂A}		5.18	0.60		45.00	1.41		188	6.31
E _{SO₄⁼}		0.08	0.02		2.88	0.03		9.47	0.11
K _g /k _g		0.41	0.12		0.85	0.20		0.95	0.43
p ‡		0.38	0.74		0.14	0.60		0.38	0.65
Bulk Compositions (mM)									
HSO ₃ ⁻	2.28	6.15	19.1	2.37	4.30	22.30	2.28	3.95	15.70
SO ₃ ⁼	1.311	1.15	0.57	1.30	1.39	0.30	1.31	1.44	1.00
HCO ₃ ⁻	3.01	0.511	.035	3.04	0.84	0.02	3.13	1.20	0.12

Table 3.5, continued

Case I.D.	DBA			DBA		
DBA (ppm)	1000			3600		
L/G (l/gmol)	0.2			0.2		
Utilization (%)	77			77		
t_{res}[†](s)	540			540		
N_g/ stage	2.3			2.3		
Stage	Inlet	Top	Bottom	Inlet	Top	Bottom
Y_{SO2} (ppm)		159	2920		41	2680
d.f.^{††} (ppm)		158	957		39.6	2270
Penetration	0.006	0.10	0.39	0.002	0.11	0.14
pH	5.73	5.82	4.6	5.66	5.76	5.00
C_{SO2,i} (mM)		6.2e-4	0.72		2.9e-4	0.16
H⁺_i (mM)		0.002	0.372		.002	.065
Enhancement Factors						
E_{total}		2857	7.01		4191	76.8
E_{H⁺}		3.98	1.08		12.9	0.77
E_{SO3⁼}		253	0.44		2169	3.3
E_{H2A}		1518	4.6		5861	68
E_{HCO3⁻}		2938	0.06		14712	0.63
E_{SO4⁼}		-342	-0.05		2090	-23
K_g/kg		0.98	0.33		0.98	0.84
p = exp (-N_gK_g/kg)		0.10	0.47		0.10	0.14
Bulk Compositions (mM)						
HSO₃⁻	2.24	2.10	15.5	2.21	1.86	12.80
SO₃⁼	1.26	1.42	0.633	1.21	1.30	1.55
HCO₃⁻	3.063	1.53	0.06	2.96	1.53	0.15

[†]t_{res} = residence time in the hold tank

^{††}d.f. = driving force for SO₂ absorption at the stage inlet.

[‡]p = exp (-N_gK_g/k_g)

3.4 CONCLUSIONS

The addition of buffer additives plays an important role in SO₂ absorption. At high concentrations (3600 ppm) conditions close to gas film control can be expected at each stage of the absorber.

The equilibrium concentration of SO₂ is usually unimportant for most cases and the model $-\ln p = (K_g/k_g) N_g$ can be used to explain most of the data.

Based on the results of Tables 3.2-5 the following conclusions can be drawn about the effect of hydrolysis and the presence of alkalinity in the form of HCO₃⁻ and SO₃⁼. The hydrolysis reaction plays an important role in the absorption of SO₂ under a variety of operating conditions. In the absence of DBA, its contribution is larger than that of other mechanisms and is at least comparable to that of physical absorption. The contribution of alkalinity (HCO₃⁻ and SO₃⁼) is usually significant above pH 5, and is unimportant at the bottom stage of the scrubber.

3.5 NOTATION

A^-	= Adipate ion, $^-OOC(CH_2)_4COO^-$
C_k	= Concentration of k^{th} species (gmol/L)
$C_{k,b}$	= Concentration of the k^{th} species in the bulk liquid solution (gmol/L)
$C_{k,i}$	= Concentration of k^{th} species at the gas/liquid interface species (gmol/L)
$C_{SO_2,i}$	= Total concentration of SO_2 at gas/liquid interface (gmol/L)
D	= Diffusion coefficient in liquid (cm^2/s)
E_k	= Enhancement Factor for k^{th} species (dimensionless)
H^+_i	= Interfacial hydrogen ion concentration (gmol/L)
H_2A	= Adipic Acid
H_{SO_2}	= Henry's Law constant for sulfur dioxide (atm-L/gmol)
K_a	= Equilibrium constant for the acid-base equilibria (gmol/L)
K_g/k_g	= Ratio of overall gas phase mass-transfer coefficient to gas film mass transfer coefficient (dimensionless)
k^o_L/k_g	= Ratio of liquid film to gas film mass transfer coefficients (cc-atm/gmol)
L/G	= Liquid to gas flow rate in the absorber (gal/Mcf)
M	= Concentration in liquid solution (gmol/L)
N_g	= Number of gas film mass-transfer units/stage (dimensionless)
p	= SO_2 penetration (dimensionless)
$P_{SO_2,g}$	= SO_2 partial pressure in bulk gas phase (atm.)
$P_{SO_2,i}$	= SO_2 partial pressure at gas/liquid interface (atm.)
$P_{SO_2,L}$	= SO_2 equilibrium partial pressure in bulk liquid (atm.)
U	= Limestone utilization (%)
y	= Mole fraction of SO_2 in the bulk gas phase (dimensionless)
y_1	= Mole fraction of SO_2 in exit scrubber gas (dimensionless)
y_2	= Mole fraction of SO_2 in inlet scrubber gas (dimensionless)

y_i^*	= Mole fraction of dissolved SO_2 in equilibrium with liquid at interface (dimensionless)
y_L^*	= Mole fraction of dissolved SO_2 in equilibrium with bulk liquid (dimensionless)
Y_{SO_2}	= SO_2 concentration in gas (ppmv)
Z_i	= Charge of i^{th} species
Superscripts and Subscripts	
out	= Exit value (at stage or scrubber)
in	= Inlet value (at stage or scrubber)
L	= Bulk liquid
aq	= Aqueous

CHAPTER 4

PARAMETER ESTIMATION

4.1 INTRODUCTION

In this chapter, results from the estimation of parameters in the model FGDTX are presented. Data from small and large scale absorbers are used for obtaining parameter estimates. The data used for regression cover a wide range of operating conditions with respect to limestone utilization, dibasic acid concentration, and pH. Hence, the estimated parameters should be fairly reliable for turbulent contact absorbers under similar hydrodynamic conditions, i.e., pressure drop, liquid flow rate, gas flow rate, packing height, and packing type.

This chapter begins with a description of the parameters to be estimated. Thereafter, data used for the regression are reviewed along with the method of regression. A discussion of results in terms of parameter estimates, confidence intervals, and joint confidence regions is presented next. Finally, other experimental studies on estimating N_g and k^o_L/k_g are reviewed.

4.2 PARAMETERS USED FOR REGRESSION

Data from large-scale (Burbank and Wang, 1981) and small scale contactors (Chang and Dempsey, 1981) were used for the regression of three parameters, the

number of gas film mass transfer units (N_g), the ratio of liquid to gas film mass transfer coefficients (k_L° / k_g) and the limestone reactivity parameter (K_{CaCO_3}).

$$N_g = \frac{k_g a P_T Z}{G}$$

$$= -\ln(1-f) \text{ at gas film control conditions (dilute gas)}$$

In general, N_g can be used to specify the maximum capacity of absorption for a system under gas film control. N_g values have been reported for three experimental studies on turbulent contact absorbers. The absorption of NH_3 into water has been studied over a range of packing heights, liquid and gas velocities (Douglas, 1964) in a single stage TCA. Measurements of the absorption efficiency of SO_2 into aqueous solutions of Na_2CO_3 have also been used to calculate N_g over a range of packing heights and liquid flow rates for the small-scale three stage TCA at EPA/RTP (Dempsey, 1983). Similar experiments have been conducted for a large-scale three stage TCA at Shawnee using an aqueous solution of Na_2CO_3 for absorbing SO_2 from a gaseous mixture of SO_2 and air (Epstein et al., 1973). Using measurements of SO_2 penetration from the same experiments, $k_g a$ can be estimated if the height of packing (tower), total pressure and gas flow rate are known. N_g is an important parameter for modeling SO_2 penetration. Its effect on model predictions for SO_2 penetration has been explained in Chapter 3 and is also reported as a sensitivity study in Table 4.1.

In general, $k_L^\circ a$ can be measured experimentally under conditions of liquid film control. Values of N_L ($k_L^\circ a Z/L$) have been reported for the three stage TCA at EPA/RTP in the presence of 5" (settled) packing per stage. However, the effect

of the back pressure of CO_2 over Na_2CO_3 solutions has not been accounted for in these experiments. This causes the estimation of k°_L/k_g or $k^\circ_L a$ to be somewhat inaccurate. The parameter k°_L/k_g has a significant effect on SO_2 penetration. The effect of k°_L/k_g on model predictions of SO_2 penetration is reported as a sensitivity study in Table 4.1.

Table 4.1: Sensitivity of $-\ln p$ to N_g and k°_L/k_g ($N_g = 3$, $N_L = 3$, and $k^\circ_L/k_g = 235 \text{ atm-ml/gmol}$).

$-\ln p$ (calc.)	DBA (ppm)	U (%)	$\frac{-d\ln p}{d\ln N_g}$	$\frac{-d\ln p}{d\ln \frac{k^\circ_L}{k_g}}$	$\frac{-d\ln p}{d\ln N_g}$	$\frac{-d\ln p}{d\ln N_L}$
0.66	0	82	0.66	0.66	0.12	0.55
1.23	0	65	1.30	1.10	0.28	1.20
1.59	1000	92	1.00	0.70	0.33	0.63
1.04	1000	91	1.40	0.80	0.55	0.78
1.92	0	45	2.33	1.53	0.65	1.58
2.09	1620	91	1.70	0.60	0.86	0.65
1.53	2200	95	1.90	0.60	1.17	0.61
2.23	1000	84	2.20	0.60	1.29	0.81
2.44	3600	88	2.00	0.30	1.59	0.43
2.36	1000	73	2.60	0.80	1.87	0.71
2.58	1000	68	2.70	0.60	2.01	0.67

Limestone reactivity is calculated on the basis of limestone utilization as well as limestone grind (particle size distribution) and type (Gage, 1989). It is used to calculate the total dissolution of limestone at a scrubber stage as shown in Table 2.1. The effect of limestone utilization (reactivity) on pH and SO_2

penetration, at a fixed particle size distribution is shown in Chapter 3. For the data used in parameter estimation, particle size distribution was not reported.

The limestone reactivity was adjusted using two slightly different procedures. An initial particle size distribution similar to that of Fredonia coarse limestone (54% < 325 mesh, 97% < 70 mesh) was assumed (Gage, 1989) in both cases.

For the bivariate regression (fitting both $-\ln p$ and pH), calculated limestone reactivity was adjusted by dividing limestone reactivity (Fredonia Limestone) for each experimental point, by the same constant (scale1). A greater value of scale1, indicates a lower reactivity. The values of scale1, were calculated by the Generalized REGression program (GREG; Caracotsios, 1986).

For univariate regressions (fitting $-\ln p$ or p alone), calculated limestone reactivity was divided by scale2 to match the observed pH for each case, i.e. $\text{Limestone reactivity} = \text{calculated reactivity (Fredonia limestone)}/\text{scale2}$. Thus a maximum of n values of scale2 resulted for a series of n experiments. In this case, the value of scale2 correspond to the calculated average. The reported confidence intervals were calculated based on the assumption of normality at 95% confidence level ($z_{0.025} = 1.96$).

Some of the other parameters in the model have been specified based on the values used by Gage (1989). These include the oxidation enhancement factor in the scrubber (E), the ratio of liquid to gas flow rates in the hold tank ($RLG2$), the number of liquid film mass transfer units in the hold tank (N_L) and the sulfite

dissolution parameter (K_{CaSO_3}). These are used in the mass balance equations as shown in Table 2.1. A sensitivity study at the specified values was done on all the adjustable parameters in the model, at typical operating conditions (Figure 1.1). It was concluded that model predictions of SO_2 penetration and pH are most sensitive to changes of N_g , k_L°/k_g , and K_{CaCO_3} . The remaining parameters (and their respective models) are not important at the conditions of this regression.

4.3 DATA USED FOR REGRESSION

Data from two absorbers of different sizes were used in this study (Table 4.2). Data from long-term experiments alone were used for parameter estimation (Burbank and Wang, 1981; Chang and Dempsey, 1981). Each experiment lasted two to three days during which steady-state conditions were maintained with respect to operation of the scrubber and the hold tank. The model, FGDTX, does not incorporate the effects of changes in liquid rate, gas rate and packing height on the adjustable parameters. Experiments conducted under constant hydrodynamic conditions were selected for estimating model parameters.

Short term factorial experiments were conducted at Shawnee (Burbank and Wang, 1981) to determine the effect of liquid flow rate, gas flow rate and packing height on scrubber performance in the absence of DBA. These experiments lasted seven to eight hours each. The results from these experiments have been used to calculate empirical correlations for N_g using FGDTX. All the data used in this study corresponds to 'natural oxidation' conditions, i.e., the hold tanks were operated without air sparging.

Table 4.2: Operating Parameters for Turbulent Contact Absorbers at EPA/RTP
(Chang and Dempsey, 1981) and Shawnee (Burbank and Wang, 1981).

Parameter	EPA/RTP	Shawnee
L/G (gal/mcf)	60	50
G (acfm)	300	30000
Diameter (ft)	0.5	5.65 x 5.65 [†]
Packing Height (in)	unknown	15
Hold Tank Residence time (s)	540	540
Scrubber Residence Time (s)	9	9
Slurry Temperature (°K)	333	333
Cl ⁻ concentration (ppm)	500	1000-4000
Total Pressure (atm)	1	1
P _{CO2} (atm)	0.07	0.07

[†]Square cross-section, area = 32 ft²

Some of the operating conditions and data for the EPA/RTP and Shawnee facilities are summarized in Tables 4.2, 4.3, and 4.4. For the small-scale scrubber at EPA/RTP the reported data contain values of DBA concentration, pH at hold tank exit, SO₂ penetration and limestone utilization for each experiment. The ratio of liquid to gas flow rate was maintained constant at 60 gal/Mcf (0.23 L/gmol). Inlet concentration of SO₂ was 2800 ppmv and there were 10% solids in the slurry. Although the presence of three beds of nitrofoam spheres is mentioned, the packing height is not reported. Chang and Laslo (1982) have noted a packing height of four inches per stage while referring to the same experiments at EPA/RTP.

Table 4.3: Data from EPA/RTP reactor ($L/G = 60$ gal/Mcf, $G = 300$ acfm, $Cl = 500$ ppm, $P_{SO_2} = 2.9e-3$ atm). The calculated values of $-\ln p$ correspond to the values calculated fitting both $-\ln p$ and pH, $-\ln p$, and p .

-ln p (obs)	-ln p (calculated)			pH (calc)	scale2	Measured Values		
	Fitted Variables					DBA pH U(%)		
	-ln p	-ln p/pH	p					
				-ln p/ pH				
0.79	0.66	1.18	0.71	5.29	52.6	0	5.0	82
1.04	1.23	1.89	1.22	5.16	21.3	1000	4.8	92
1.2	1.59	1.89	1.52	5.15	11.8	1000	5.0	91
1.27	1.04	1.52	1.20	5.65	76.9	0	5.5	65
1.56	1.92	2.02	1.73	5.14	11.0	1620	5.0	91
1.71	2.09	2.04	1.83	5.08	4.3	2200	5.0	95
1.89	1.53	1.74	1.66	5.91	71.4	0	5.8	45
2.07	2.23	1.91	1.97	5.18	8.5	1000	5.4	84
2.4	2.44	2.13	2.11	5.41	9.5	1000	5.6	73
2.52	2.36	2.18	1.99	5.14	10.0	3600	5.0	88
2.99	2.58	2.18	2.18	5.49	5.0	1000	5.8	68

For the large-scale scrubber at Shawnee, the reported data contain values of DBA concentration, pH, SO_2 penetration, limestone utilization, solution composition at inlet to scrubber, solids' composition, and concentration of SO_2 at the scrubber inlet for each experiment. The column was operated at a liquid to gas flow rate of 50 gal/Mcf and the packing height (settled) was given as five inches per stage. In both cases, the precision of measurement of these quantities is not reported.

Table 4.4: Data from Shawnee Contactor (L/G = 50 gal/Mcf, G = 30000 acfm, Cl = 2000 ppm).

-ln p (obs)	-ln p (calc)		scale2	pH (calc)	Measured Values			
	Fitted Variables				U(%)	DBA (ppm)	PSO2 (ppmv)	pH
	-ln p	-ln p/pH						
1.23	1.00	1.09	4.5	5.62	80	0	2550	5.60
1.38	1.73	1.94	6.7	5.44	84	350	2750	5.65
1.42	1.13	1.26	5.6	5.32	83	0	2300	4.95
1.46	1.73	1.72	3.3	5.48	93	840	1900	5.40
2.52	2.52	2.48	3.7	5.54	80	885	2300	5.45
2.65	2.62	2.52	2.9	4.89	85	1600	2600	5.50
2.65	2.4	2.35	3.4	5.50	75	700	2300	5.30

In this study, the parameters have been adjusted to match SO₂ penetration ($p = \text{SO}_2 \text{ exit concentration} / \text{SO}_2 \text{ inlet concentration}$) or -ln p and exit pH from the hold tank. Variation of SO₂ penetration due to DBA addition and the change of pH as a function of limestone utilization are shown in Figures 4.1 and 4.2 respectively. The experimental data for the small-scale contactor at EPA/RTP and large-scale contactor at Shawnee are presented together in these figures. In both facilities, SO₂ penetration was 0.15 to 0.64 without DBA and decreased to 0.04 to 0.12 with 1000 ppm and 1600 ppm DBA respectively (Figure 4.1).

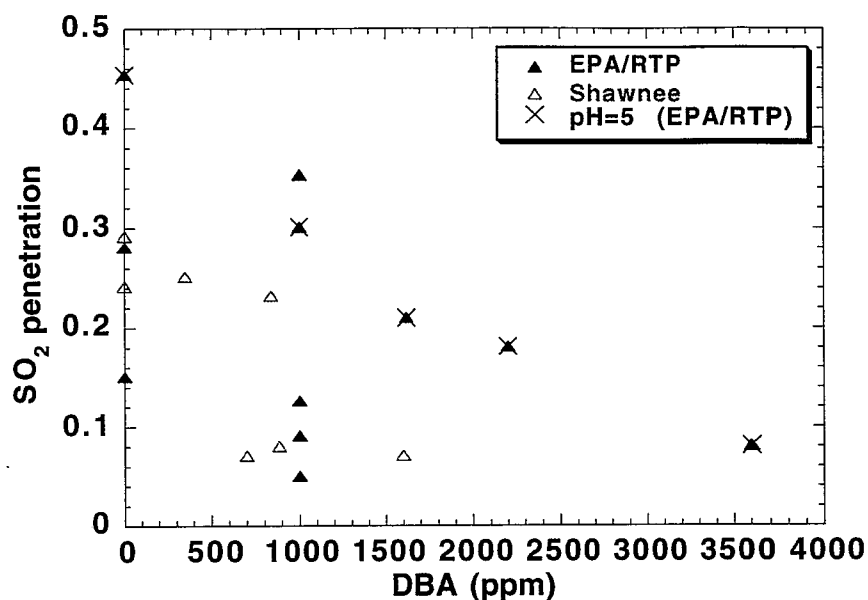


Figure 4.1: Measured Values of SO₂ Penetration for the Large Scale (Shawnee) and Small Scale (EPA/RTP) Contactors ($U = 45\%$ to 95%).

At low SO₂ penetration of 0.05 ($U = 65$, $DBA = 1000$) and 0.08 ($DBA = 3600$ ppm) the experiments correspond to conditions near gas film control $K_g/k_g \sim 1$ (Rochelle, 1982). These conditions are most suitable for estimation of N_g ($N_g \sim -\ln p$), and could be used to specify an upper limit on the value of N_g . At high SO₂ penetration such as 0.45 ($U = 80\%$, $DBA = 0$ ppm) gas film control is less dominant, presenting better conditions for the estimation of k_L° . The model, FGDTX, uses k_L°/k_g as the second adjustable parameter. It may be expected that

under conditions close to liquid film control k_g (or N_g) has a smaller effect on SO_2 penetration, hence the latter set of conditions are more suitable for the estimation of k_L°/k_g . A comparison of model sensitivity to these parameters is presented in Table 4.1. The tabulated sensitivities have been calculated for the EPA/RTP data and verify that the sensitivity to N_g as compared to k_L°/k_g is greatest at high DBA concentration and low SO_2 penetration (high $-\ln p$). In the absence of DBA at high SO_2 penetration (low $-\ln p$), the sensitivity to both the parameters is almost equal. At fixed N_L values, the sensitivity to N_g is lesser than the sensitivity at fixed k_L°/k_g . As expected, the sensitivity to N_L is greater than N_g for the conditions closer to liquid film control.

Figure 4.2 shows the variation in solution pH for the same experiments as in Figure 4.1. At lower limestone utilization ($U = 50, 60\%$) the pH changes more significantly with the change of utilization than at higher utilization ($U = 90, 95\%$). The data also include a range of limestone utilization and pH, which may be suitable for the calculation of limestone reactivity.

The large scale contactor at Shawnee was operated at a higher pH (at equivalent limestone utilization). Subsequently, the SO_2 penetration was lower than the observed SO_2 penetration at similar DBA levels in the EPA/RTP contactor. The increased pH at Shawnee could be due to a more reactive limestone species, i.e. one having a finer grind.

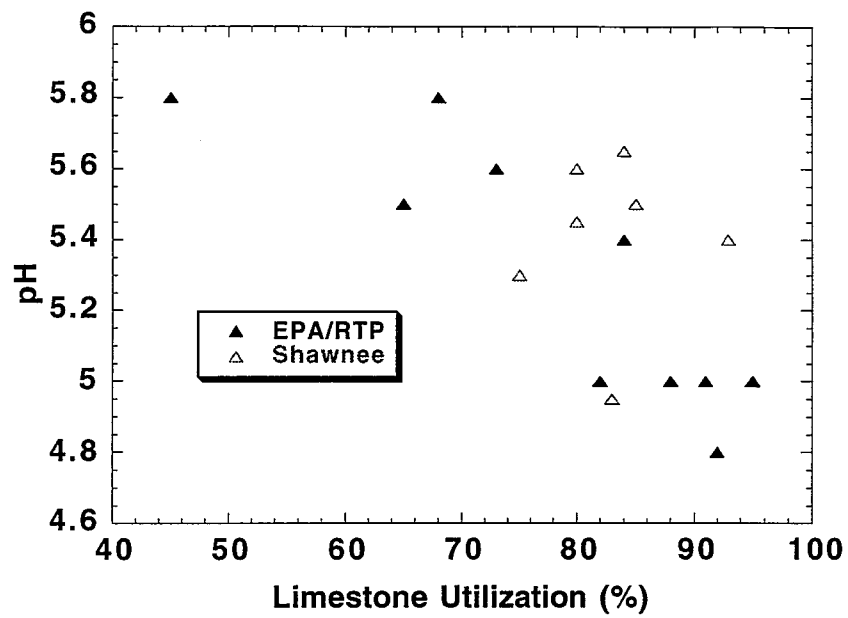


Figure 4.2: Experimental Data for Large Scale (Shawnee) and Small Scale (EPA/RTP) Contactors (DBA concentration = 0 to 3600 ppm).

In calculating model parameters, $-\ln p$ or p were used as dependent variables instead of SO_2 removal. The exit concentration of SO_2 varied from fifty to five percent of the inlet concentration. It can be assumed that gas analyzers at both inlet and exit operated with an error proportional to the magnitude of gas concentration being measured. The absolute error in measurement of the inlet gas concentration could be very substantial compared to the exit concentration of SO_2 , especially at low exit concentration. In this case, a small error in SO_2 removal could disguise a large error in SO_2 penetration or exit concentration. For the data used in regression, gas film control conditions coincide with low SO_2 penetration values. At gas film control conditions, $N_g = -\ln p$. In general, using removal could result in large errors in N_g . The log transformation of penetration was preferred as it produced a better fit at low penetration, resulting in better N_g estimates. The log transformation can result in a loss of normality in the error structure. This could have a significant effect on the accuracy of the calculated confidence intervals based on normality. Normal probability plots have been used in Section 4.5 to check the validity of normality assumptions.

4.4 METHOD OF REGRESSION - GREG USAGE

The problem of parameter estimation using non-linear models for multi-response experiments has been studied by many investigators. Details of the objective function to be used, along with methods of obtaining estimates of confidence intervals and joint confidence region of the parameters have been studied by Box and Draper (1972, 1965), Stewart (1981, 1987, 1992), Caracotsios (1986)

and others. Generalized REGression (GREG), a FORTRAN program written by Caracotsios (1986), has been used to calculate parameter estimates, confidence intervals and regions. This section presents a summary of the assumptions and derivation implemented by Caracotsios (1986) in GREG for determining the objective function to be minimized, confidence interval/region estimates of the parameters, and co-variance between estimated parameters. The results can be used for cases where co-variance structure of data is not known. The derivation has been simplified, and is suitable for a single data structure, i.e., where all the experiments produce measurement errors with the same variance-covariance structure.

Let y_{iu} ($i = 1, 2, \dots, k$; $u = 1, 2, \dots, n$) represent k observations (responses) each, for a set of n experiments. Let x_{iu}^q ($i = 1, 2, \dots, k$; $u = 1, 2, \dots, n$; $q = 1, 2, \dots, r$) represent n sets of observations on each of the r independent variables. Let the k models be represented as

$$y_{iu} = f_i(x_{iu}^q, \theta_h) + \varepsilon_{iu}$$

where:

θ_h ($h = 1, 2, \dots, m$) represent the m unknown model parameters,

f_i are the k models of known form, and

ε_{iu} are random errors such that:

$E(\varepsilon_{iu}) = 0 \forall i, u$, i.e., The average error associated with any variable (ε_{iu}) is 0.

$E(\varepsilon_{iu} \varepsilon_{ju}) = 0 \quad \forall \quad i, j, u \neq v$, i.e., The experimental errors are independent of each other from one experiment to the next.

$E(\varepsilon_{iu}^2) = \sigma_{ii}$; $E(\varepsilon_{iu} \varepsilon_{ju}) = \sigma_{ij}$, i.e., The errors between variables for the same experiment may be correlated.

The probability density function for normal distribution of a single variable (y) having a mean (μ) and standard deviation (σ) can be stated as:

$$p(y) = \frac{1}{\sigma\sqrt{2\pi}} \exp \left[-\frac{1}{2\sigma^2} (y-\mu)^2 \right]$$

Assuming that the y_{iu} follow a multivariate normal distribution, the likelihood function is calculated as shown below, i.e., a joint probability density function for the multivariate distribution.

$$l(\mathbf{y}|\theta, \sigma^{ij}) = (2\pi)^{-1/2nk} |\mathbf{A}|^{1/2n} \exp \left[-\frac{1}{2} \sum_{j=1}^n \sum_{i=1}^n \sigma^{ij} v_{ij} \right]$$

where

$|\mathbf{A}| = \Sigma^{-1}$ is the inverse of the co-variance matrix.

$\Sigma_{ij} = \sigma^{ij}$

$v_{ij} = \sum_{u=1}^n \{y_{iu} - f_i\} \{y_{ju} - f_j\}$

= sum of squares of residuals for n experiments

\mathbf{V} = moment matrix of residuals

= $\{v_{ij}\}$

$\mathbf{y} = \{y_{1u}, y_{2u}, y_{3u}, \dots, y_{ku}\}$

$$\theta = \{\theta_1, \theta_2, \dots, \theta_m\}$$

According to Bayes' theorem (Bard, 1977), we can derive the posterior probability distribution for the parameters after the data have been recorded ($p(\theta|Y, \sigma)$) using the likelihood function, the prior distribution of the parameters and variance.

Bayes' theorem states that:

$$P(A|B) = P(B|A) P(A)/P(B)$$

In the present case, $P(B|A)$ is the likelihood function and $P(A)$ is the prior distribution of parameters and variance, and $P(B)$ is obtained by integration of $P(B|A) P(A)$ over all possible A values. This integral has a constant value. To calculate $p(\theta)$ and $p(\sigma)$ the prior density of the parameters and the variance respectively, we assume a locally uniform prior for θ and use the invariance theory of Jeffreys (1961) for σ :

$$p(\theta) \propto d\theta$$

$$p(\sigma) \propto |A|^{-1/2(k+1)}$$

Combining the prior distribution for θ and σ , with the likelihood, the posterior distribution for θ can be calculated. Maximizing the posterior probability distribution for this case, is equivalent to maximizing the likelihood function.

$$p(\theta, \sigma|y) d\theta \Pi d\sigma \propto (2\pi)^{-1/2nk} |A|^{1/2(n-k-1)} \exp \left\{ -\frac{1}{2} \sum_{j=1}^k \sum_{i=1}^k \sigma^{ij} v_{ij} \right\} d\theta \Pi d\sigma$$

To find the marginal distribution of θ , σ is integrated out, giving:

$$p(\theta|y) \propto |V|^{-1/2n}$$

When the variance-covariance structure of a set of n experiments is the same, the posterior probability density is maximized by maximizing an objective function of the form shown below.

$$\log |V|^{-1/2n}$$

If the data used in the estimation procedure can be divided into several data blocks (N_b), consisting of n_L experiments each, having a different (but unknown) co-variance structure, the objective function to be minimized is as shown below.

$$\sum_{L=1}^{N_b} \log |V_L|^{-1/2 n_L}$$

4.4.2 Objective Function

For Multivariate (bivariate) regression of pH and SO₂ penetration the posterior density is maximized by maximizing an objective function of the form $-\ln |V|$ (or minimizing V). If the errors in the variables are uncorrelated, V is given as in 4.4-1a.

$$V = \begin{bmatrix} \sum_{u=1}^n e_{1u}^2 & 0 \\ 0 & \sum_{u=1}^n e_{2u}^2 \end{bmatrix} \quad (4.4-1-a)$$

If the error in pH and penetration are not independent of each other, the objective function to be used is of the form shown below.

$$\mathbf{V} = \begin{bmatrix} \sum_{u=1}^n e_{1u}^2 & \sum_{u=1}^n e_{1u}e_{2u} \\ \sum_{u=1}^n e_{1u}e_{2u} & \sum_{u=1}^n e_{2u}^2 \end{bmatrix} \quad (4.4-1-b)$$

where:

$$e_{1u} = (-\ln(\text{SO}_2 \text{ penetration})_{\text{measured}} - (-\ln(\text{SO}_2 \text{ penetration})_{\text{calculated}}) \text{ or}$$

$$e_{1u} = (\text{SO}_2 \text{ penetration})_{\text{measured}} - (\text{SO}_2 \text{ penetration})_{\text{calculated}}$$

$$e_{2u} = \text{pH}_{\text{measured}} - \text{pH}_{\text{calculated}}$$

In case of univariate data, the matrix reduces to a single equation least squares.

$$\mathbf{V} = \sum_{u=1}^n e_{1u}^2 \quad (4.4-2)$$

4.4.3 Confidence Intervals/Regions and Co-Variance

The confidence intervals/regions and co-variance between parameters are calculated in GREG as follows.

$$p(\theta, Y) \propto \mathbf{V}$$

$$p_{\max}(\theta^*, Y) \propto \mathbf{V}^*$$

$$\log p(\theta, Y) - \log p_{\max}(\theta^*, Y) = \frac{n}{2} [\log(\mathbf{V}) - \log(\mathbf{V}^*)]$$

$$\log p(\theta, Y) = \log p_{\max}(\theta^*, Y) - \frac{1}{2} (\theta - \theta^*)^T \mathbf{H}^* (\theta - \theta^*)$$

where:

$$\mathbf{H}_{ij}(\theta^*) = \frac{n}{2} \frac{\partial^2 \log \mathbf{V}^*}{\partial \theta_i^* \partial \theta_j^*}$$

$$\log p(\theta, Y) - \log p_{\max}(\theta^*, Y) \propto -\frac{1}{2} \Psi_{\alpha, m}^2$$

$$(\theta - \theta^*)^T \mathbf{H} (\theta - \theta^*) = \Psi_{\alpha, m}^2 \quad (4.4-3)$$

$$\text{Covariance } (\theta_i^*, \theta_j^*) = \frac{H^{-1}_{ij}}{\sqrt{H^{-1}_{ii} H^{-1}_{jj}}} \quad (4.4-4)$$

4.4-3 corresponds to the equation of an ellipsoid in m dimensions. The confidence interval for the i^{th} parameter is calculated as in 4.4-5.

$$(\theta - \theta^*)_i = \frac{U_{\alpha/2}}{H^{*-1}_{(ii)}} \quad (4.4-5)$$

where:

$$U_{\alpha/2} = 1.96$$

4.4.4 Interpretation of Confidence Intervals/Regions and Co-variance

The joint confidence region obtained from minimization of the likelihood function identifies an ellipsoidal solid (equation 4.4-3). If the estimation involves m parameters then the ellipsoid is a solid of m dimensions; when $m = 2$, it is an ellipse. The co-ordinates of each point on the ellipsoid predict data within the $(1-\alpha)$ confidence level. The orientation and shape of the ellipsoid are determined by the left hand side term of equation 4.4-3 (\mathbf{H}). The $\Psi_{\alpha, m}^2$ statistic determines the size

of the ellipsoid. For a fixed value of \mathbf{H} , larger values of $\Psi^2_{\alpha,m}$ would merely result in concentric ellipsoids of larger size.

For linear models, the ellipsoidal confidence regions can be expected to be exact at the stated confidence level (α) if all the distributional assumptions stated in the derivation of the objective function are valid and the model is correct (Donaldson and Schnabel, 1987).

The effect of co-variance can be understood from the geometry of the ellipse. A two dimensional ellipse can be considered for the sake of simplicity. If the co-variance between estimated parameters is zero, the ellipse is oriented along the co-ordinate axes, i.e., θ_i, θ_j . The interval estimates of the parameters (equation 4.4-5) are valid at the estimated parameters θ_i^*, θ_j^* . The presence of the off-diagonal ($h_{ij}, i \neq j$) term in \mathbf{H} changes the orientation of the ellipse so that the major and minor axes of the ellipse are no longer aligned along θ_i, θ_j . In the presence of co-variance, the interval estimates are not valid at θ_i^*, θ_j^* . If the sign of co-variance is negative then the average value of a parameter must decrease if the other increases, in order to remain within the specified confidence region of the ellipse (if the co-variance is positive then the reverse is true). Hence, the individual confidence intervals (4.4-5) are limited in their physical significance as is the parameter value itself.

The elliptical confidence regions for the parameters have been constructed using normal equations as in equation 4.4-3 for the estimation of N_g and k°_L/k_g . The coefficients of the normal equations are obtained from GREG, and are used as:

$$(\Delta N_g')^2 h_{11} + 2 h_{12} (\Delta N_g') \Delta(k^o_L / k_g)' + h_{22} (\Delta(k^o_L / k_g'))^2 = \Psi^2_{0.05,1}$$

where:

$$\mathbf{H} = \begin{bmatrix} h_{11} & h_{12} \\ h_{21} & h_{22} \end{bmatrix}, (h_{21} = h_{12}),$$

N_g' = is the normalized value of N_g

$(k^o_L / k_g)'$ = is the normalized value of k^o_L / k_g

$\Delta \theta_i$ = $\theta_i - \theta_i^*$

θ_i = N_g' or $(k^o_L / k_g)'$

θ_i^* = Value of θ_i at the calculated optimum

The true values of N_g and k^o_L / k_g are used to calculate the elliptical confidence regions after rescaling the above equations (see section 4.5).

A value of $\Psi^2_{0.05,1} = 1.96^2 = 3.84$ was chosen (although, $\Psi^2_{0.05,2} = 5.99$) for the joint confidence regions for the estimation of two parameters. This value allows for comparisons between the individual confidence intervals ($U_{\alpha/2} = 1.96$) and the joint confidence regions.

4.4.5 GREG - Sample Input/Output files

Samples of the input files used for parameter estimation have been shown in Appendix D. These files represent the data used for regression of N_g and k^o_L / k_g (or N_L) for the EPA/RTP and Shawnee contactors. An output file showing the results of the estimation for the EPA/RTP data is also included in Appendix D. The FORTRAN file p_est.f was used to specify the inputs for GREG. This file is also shown in Appendix D. A function tolerance of 1e-2 was specified for the

calculation of $-\ln p$ or p . This corresponds to a relative error of 1% in the calculated function value. The relative tolerance in the parameter value was also specified at 1%. Despite these specifications, the finite difference scheme in GREG calculated derivatives based on a smaller step-size (close to the optimum). The reported values of confidence intervals and confidence regions were re-calculated at the optimum, based on a step-size of 2% with respect to the parameter value. These estimates were calculated at the optimum using the \mathbf{H} matrix based on output from GREG. Examples of these matrices for the EPA/RTP data are shown in Appendix D in the case of estimation based on $-\ln p$ for the parameter sets N_g , k°_L/k_g and N_g, N_L .

4.5 RESULTS

Figure 4.3 shows a comparison between the fitted values obtained from the bivariate objective function and fitted values obtained using the univariate objective function. These results show the difference between the measured and calculated values of pH and $-\ln p$ for the data from the small-scale contactor. For the bivariate case, at lower penetration values ($p \sim 0.05 - 0.11$), pH is consistently over-predicted whereas at higher penetration values ($p \sim 0.16 - 0.45$) pH is under-predicted. This trend in pH results in a somewhat systematic trend in the prediction of SO_2 penetration values. At lower SO_2 penetration, the penetration is under-predicted whereas at higher penetrations it is over-predicted.

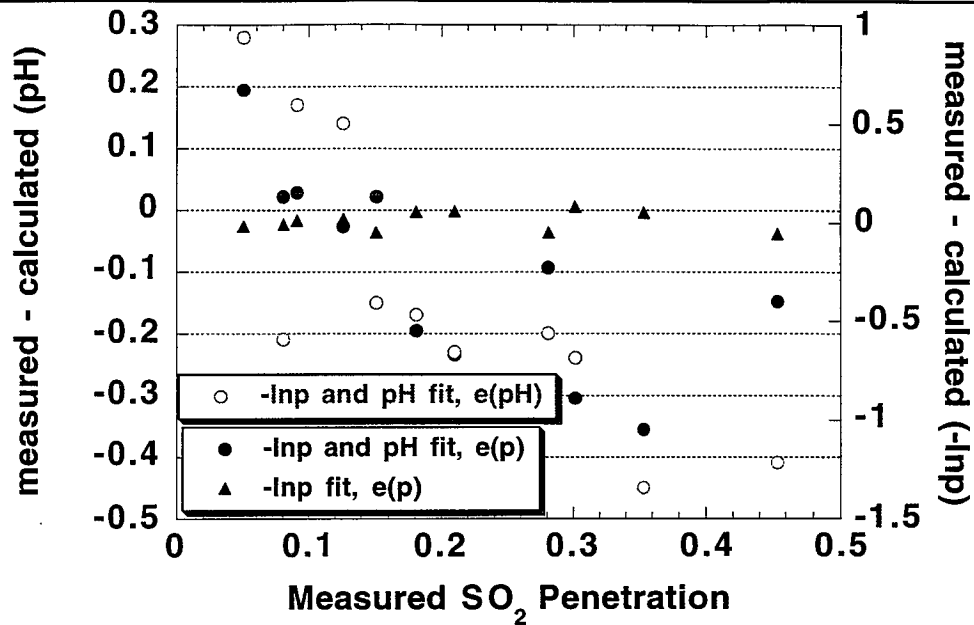


Figure 4.3: Comparison between measured and predicted (p and pH) values for the EPA/RTP contactor.

The parameter values are shown in Table 4.5. The objective functions are shown in equations 1-b and 2. DBA concentration range = 0-3600 ppm, Limestone Utilization range = 45-95%.

Using the univariate fits (matching pH for each experiment) resulted in a more random fit for the penetration as well as smaller error. A comparison between the Sum of Squares Error (SSE) is shown in Table 4.5 and 4.6, ($SSE = \sum V_{ii} (-\ln p) = 2.61$ versus 0.80). This indicates that an accurate estimate of solution composition is required to predict penetration values, and a single value of scale1 (13.5) is not sufficient to predict pH over the wide range of limestone utilization.

Table 4.5: Comparison of the Fits Obtained for the EPA/RTP Data.

Fitted Variables	pH & (-ln p)	(-ln p)	p
N_g	2.40±0.61	2.88±0.55 2.88±0.50	2.4±0.60 2.4±0.60
$\frac{k_L^o}{k_g}$		292±169	434±194
N_L		3.65±1.28	4.53±1.26
scale1	13.5±8.5		
scale2		25.6±76*	25.6±76*
V_{ii} (-ln p)	2.61	0.80	1.13
V_{ii} (pH)	0.69	0	0
V_{ii} (p)	-	0.06	0.022
Co-variance			
$N_g, \frac{k_L^o}{k_g}$	-0.71	-0.87	-0.86
N_g, N_L		-0.68	-0.61
N_g scale1	0.064		
$\frac{k_L^o}{k_g}$ scale1	-0.12		
$\sqrt{\text{MSE}} = \sqrt{\text{var}(V_{ii}(-\ln p), n-p^{\dagger})}$	0.57	0.31	0.36

* scale2 is adjusted for each experimental point, values of scale2 are reported in Table 4.4.
The values reported above correspond to the calculated average and the confidence interval is calculated using the t- statistic ($z_{0.025} = 1.96$).

$^{\dagger}p$ = number of parameters, 3 in case of (-ln p) and pH fits and 2 in all the other cases.

The estimated parameters were different for these two cases
($N_g = 2.88 \pm 0.55$, $k_L^o/k_g = 292 \pm 169$ atm-ml/gmol versus $N_g = 2.40 \pm 0.61$,

$k^{\circ}_L/k_g = 883 \pm 1509$ atm-ml/gmol) due to the difference in the nature of the fits. The average value of scale2 (25.6 ± 76) is about two times greater than the estimated value of scale1 (13.5 ± 8.5) from the multivariate fit) and is spread over a wide range (Table 4.3). The calculated covariance between N_g and k°_L/k_g is negative in both cases, however it has a lower absolute value for the 3-parameter regression (-0.71 versus -0.87), due to the presence of the third parameter (Scale1) which is correlated to k°_L/k_g (co-variance = -0.12) and N_g (co-variance = 0.064).

The mean square error ($MSE = V_{ii}/(n-p)$) can be used to compare the estimated errors in the small and large scale data. ($\sqrt{MSE(-\ln p)} = 0.36$ versus 0.57 , $\sqrt{MSE(pH)} = 0.09$ versus 0.27). For the bivariate case, the large-scale data are matched much better than the small-scale data. The solution composition (pH) is predicted much better for the large scale data. Hence the improvement in going from the bivariate to univariate fit is not as great as in the case of the small scale data. Table 4.6 shows the estimates obtained by using bivariate and univariate objective functions for the Shawnee data (large-scale contactor). The parameters are also more comparable than the small scale data ($N_g = 2.97 \pm 0.54$, $k^{\circ}_L/k_g = 271$ atm-ml/gmol versus $N_g = 2.88 \pm 0.30$, $k^{\circ}_L/k_g = 389$ atm-ml/gmol). The estimated value of scale1 is comparable to the average value of scale2 (3.60 ± 0.50 versus 4.3 ± 2.1).

Table 4.6: Comparison of the Fits Obtained for the Shawnee Data .

Fitted Variables	(-ln p) and pH	-ln p	-ln p
N_g /stage	2.88±0.30	2.97±0.54	2.97±0.63
$\frac{k^o_L}{k_g}$ (atm-ml/gmol)	389	271±103	
N_L			4.04±0.94
scale1	3.65±0.50		
scale2		4.3±2.1*	
V_{ii} (-ln p)	0.53	0.39	
V_{ii} (pH)	0.035	0	
Co-variance		-0.87	
$N_g, \frac{k^o_L}{k_g}$	**		
N_g, N_L			-0.73
N_g *scale1	-0.11		
$\frac{k^o_L}{k_g}$ scale1	**		
$\sqrt{MSE(-ln p)} = \sqrt{\frac{V_{ii}}{n-p^\dagger}}$	0.36	0.28	

* scale2 is adjusted for each experimental point, values of scale2 are reported in Table 4.5. The reported value of scale is the average and its confidence interval is calculated using the normal distribution ($z_{0.025} = 1.96$).

** the confidence interval for k^o_L/k_g was reported as infinity for this case, and the co-variance between k^o_L/k_g and the other parameters was not calculated.

$^\dagger p$ = number of parameters, 3 in case of (-ln p) and pH fits and 2 in all the other cases.

The small and large scale contactors were operated at comparable values of superficial gas and liquid velocities. Using the univariate regression results (Tables 4.5 and 4.6) as a basis for comparison, it is observed that the parameters affected

by hydrodynamic conditions are similar in value ($N_g = 2.88$, $k_L^\circ/k_g = 292$ and $N_g = 2.97$, $k_L^\circ/k_g = 272$ cc-atm/gmol). The average value of scale2 is much higher for the small-scale contactor (scale2 = 25.6 versus 4.3) implying a lower reactivity of limestone. This may be due to a coarser grind of limestone. A wide range in measured total surface area (0.22 m²/g to 2.23 m²/g) has been reported by Gage (1989) due to different limestone grinds. The co-variance between the estimated parameters is the same for both cases, -0.87. For both sets of data the parameter N_g is better estimated, i.e., it has a smaller absolute value of confidence interval relative to its magnitude than k_L°/k_g . This is expected as the model is more sensitive to N_g at the experimental conditions (Table 4.2).

The parameters N_g and k_L°/k_g have a fairly large co-variance, indicating that they cannot be estimated independently of each other. This is to be expected as both these parameters are affected by the gas film coefficient ($N_g = k_g a Z / G$), and the data do not lie clearly in the region of complete gas and liquid film control. The univariate estimations were repeated using N_g and $N_g k_L^\circ/k_g$ as the adjustable parameters. The product $N_g k_L^\circ/k_g$ resembles N_L ($N_L = N_g k_L^\circ/k_g G/L$), the number of liquid film mass transfer units, and is independent of k_g . Tables 4.5 and 4.6 show a comparison between the estimated parameters and confidence interval values for small and large scale data respectively. Using this approach the co-variance was reduced from -0.87 to -0.68 and -0.73 (Table 4.5, 4.6). A reduction in co-variance implies that the parameter estimates are more independent of each other and the confidence intervals are closer to being correct. As the same objective functions have been used, the same minimum is reached and the

parameters have the same values. In general it is possible using canonical transformations (Bard, 1977) to reduce the covariance between linear combinations of parameters to zero. In this case such a linear combination of N_g and k_L^0/k_g would not result in a physically meaningful quantity.

Figure 4.4 shows the elliptical confidence region for N_g and k_L^0/k_g . The ellipse is centered about the estimated values of $N_g = 2.88$ and $k_L^0/k_g = 292$.

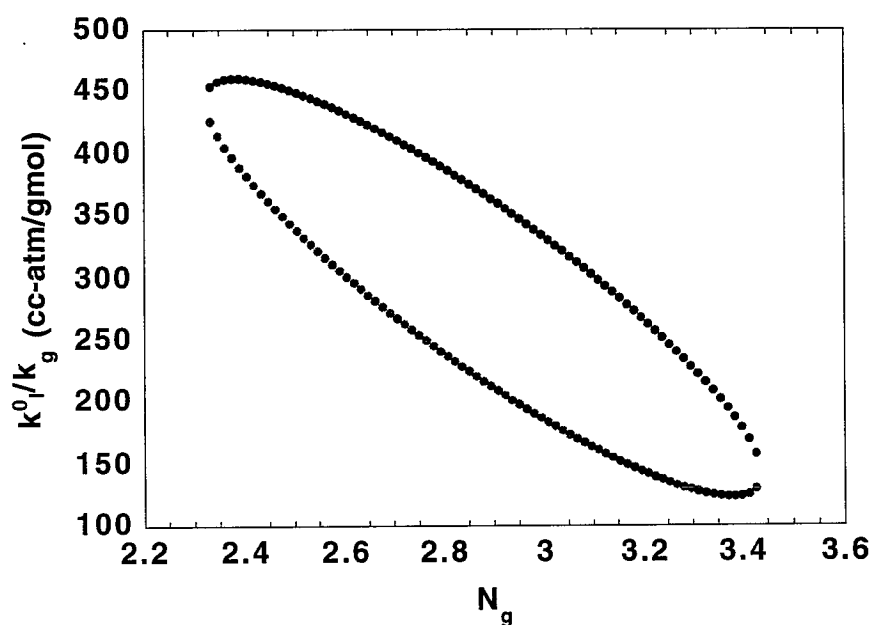


Figure 4.4: Confidence Regions for the N_g and k_L^0/k_g
(Response Variable = $-\ln p$, EPA/RTP data).

The major axis of the ellipse has a negative slope. This is expected as the co-variance has a negative value of -0.87. The individual confidence intervals on N_g and k°_L/k_g define the maximum extent of the ellipse along each axis. Inspection of the ellipse shows that on account of its orientation, the individual confidence intervals are not strictly correct. Although $N_g = 2.88 \pm 0.55$, if a value of $N_g = 2.88 + 0.55$ is used the corresponding value of k°_L/k_g must also be decreased to 123 for the data to be predicted with the same level of confidence.

Figure 4.5 illustrates the effect of co-variance between the estimated parameters for the EPA/RTP data. In order to compare the confidence regions for the parameters sets $N_g, k^{\circ}_L/k_g$ and N_g, N_L the parameters have been normalized about their estimated values.

The values shown in Table 4.5 (for the $-\ln p$ fit) can be normalized as $N_g = 1.00 \pm 0.19$, $k^{\circ}_L/k_g = 1.00 \pm 0.58$ and $N_g = 1.00 \pm 0.17$, $N_L = 1.00 \pm 0.35$. The latter set of confidence intervals are more valid as a result of the orientation of the ellipse. A smaller co-variance results in smaller angle between the major axis of the ellipse and the axis along N_g . An extreme example of this effect would be seen if the major axes of the ellipse were oriented along the axes of N_g and k°_L/k_g . This would lead to the individual confidence intervals (at the center of the ellipse) being correct.

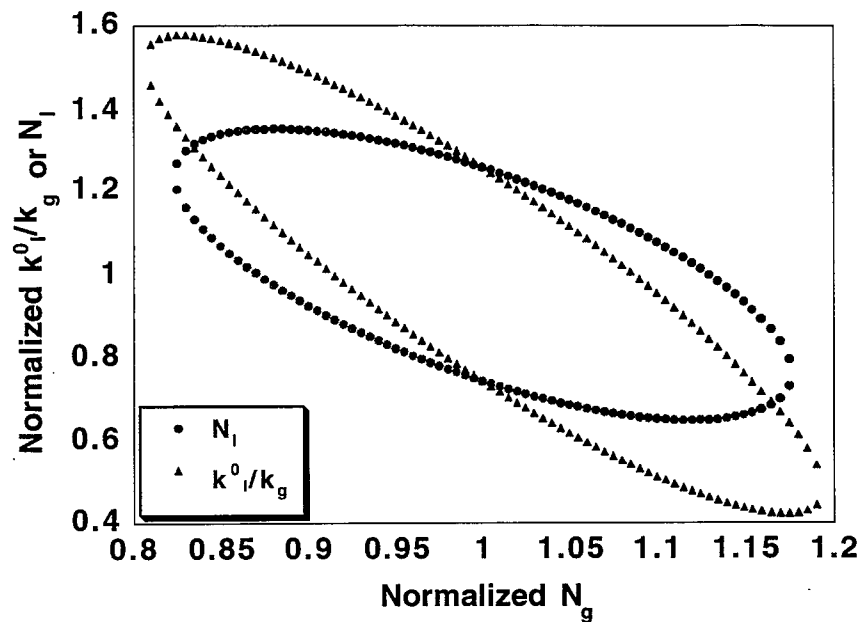


Figure 4.5: Confidence Regions for the N_g and k_L^0/k_g (estimated using $-\ln p$ as the response variable for the EPA/RTP data).

To obtain least correlated parameter estimates, experiments closest to gas and liquid film control were chosen from the available data from EPA/RTP. The 4 points chosen showed the greatest selective sensitivity for N_g and k_L^0/k_g respectively. The results from this estimation are presented in Table 4.7. The estimated confidence intervals are much smaller than those estimated for any other sets of parameters due to small values of errors ($SSE = 0.01$). The parameter set N_g, N_L showed the smallest co-variance, -0.50 .

Table 4.7: Parameter estimation Results for a Subset of EPA/RTP Data.

Variables Fit	-ln p	-ln p
N_g	3.30 ± 0.04	3.30 ± 0.04
$\frac{k_L^o}{k_g}$ (atm-ml/gmol)	308.9 ± 34	
N_L		4.43 ± 0.39
scale2	36 ± 117	
V_{ii} (-ln p)	0.01	
V_{ii} (pH)	0	
Co-variance		
$N_g, \frac{k_L^o}{k_g}$	-0.73	
N_g, N_L		-0.50
$\sqrt{\text{MSE}(-\ln p)} = \sqrt{\frac{V_{ii}}{n-p^\dagger}}$	0.07	

Table 4.7: Continued

(-ln p)	
Observed Values	Calculated Values
1.27	1.29
0.79	0.77
2.99	2.92
2.52	2.60

4.5.1 Transformation of the Dependent Variable

Regression on SO₂ penetration was done using both -ln p as well as p as the dependent variable. The logarithmic transformation resulted in minimizing the ratio

of the measured and calculated exit concentrations of SO_2 whereas the latter minimizes the absolute errors in penetration. Figure 4.6 shows a comparison between $-\ln p$ and p as response variables in terms of the errors in calculated penetration.

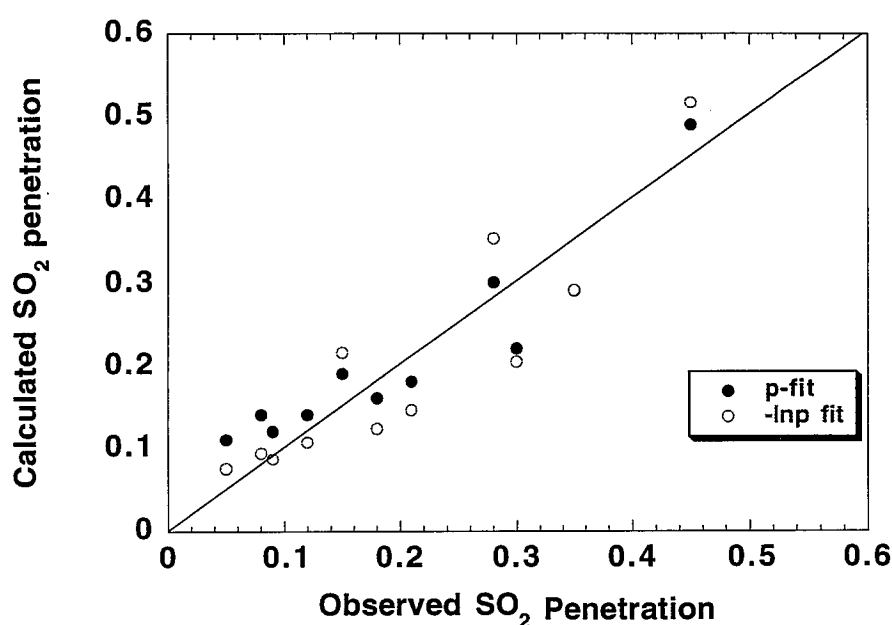


Figure 4.6: Comparison of Calculated Penetration Values Obtained by Fitting SO_2 Penetration (p) and $-\ln p$ for the EPA/RTP Contactor.

The objective function using $-\ln p$ places greater weight on points with low penetration, leading to better fits at lower penetration values. Due to a change in the nature of objective functions, the estimated parameters ($N_g = 2.88 \pm 0.55$,

$k^{\circ}_L/k_g = 292 \pm 169$ versus $N_g = 2.4 \pm 0.60$, $k^{\circ}_L/k_g = 434 \pm 194$) and the sum of squares error have different values.

The log transformation ($-\ln p$) can destroy the normal structure of the errors (if the errors in p are normally distributed). This would seriously affect the distributional assumptions, resulting in erroneous confidence intervals/regions. Normality plots were made for both $-\ln p$ as well as p (Figure 4.7, 4.8; Table 4.8, 4.9).

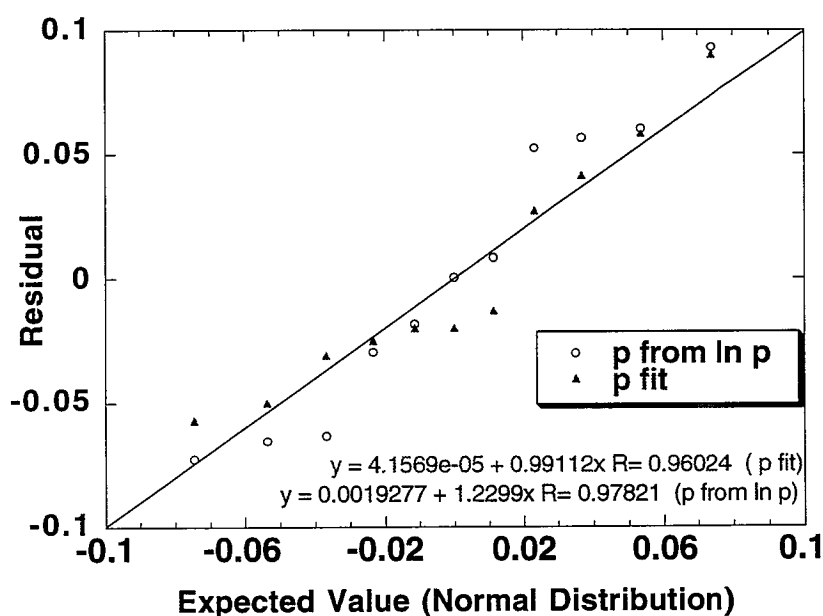


Figure 4.7: Comparison of Error (in p) from Fitting the EPA/RTP Data and a Normal Distribution.

Figure 4.7 compares the residuals in terms of the difference in calculated and observed values of $-\ln p$ versus the variables from a normal distribution. The residuals obtained from using p as dependent variable were transformed in terms of $-\ln p$ in Figure 4.7. Figure 4.8 shows a similar comparison between residuals in terms of p and the variables from a normal distribution.

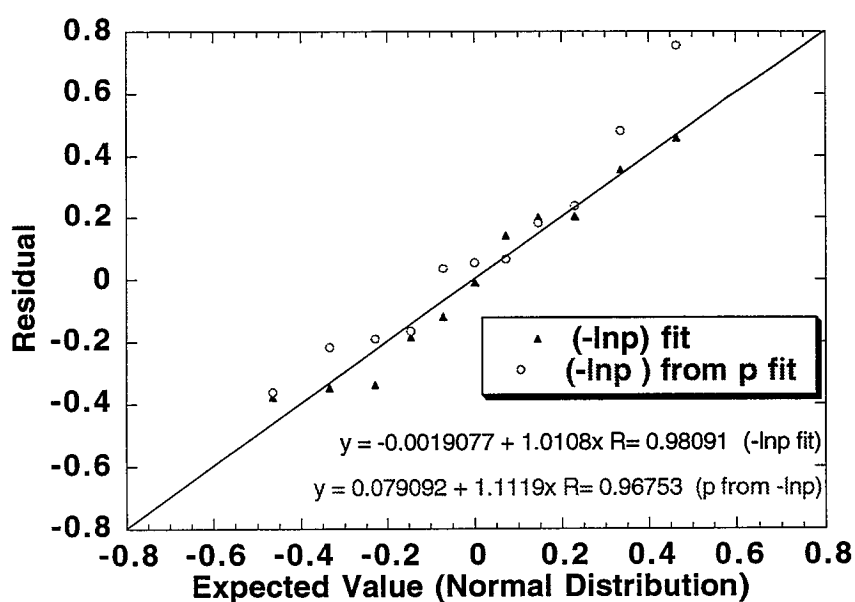


Figure 4.8: Comparison Between Error (in $-\ln p$) from Fitting EPA/RTP Data and a Normal Distribution.

Table 4.8: Comparison Between Calculated Residuals $(-\ln p)$ and Normal Variables for the EPA/ RTP Data.

i	A [†]	Z(A)	(-ln p) ^{††} - fit		p from -ln p	
			$\sqrt{\text{mse}} \cdot z$	ordered residual	$\sqrt{\text{mse}} \cdot z$	ordered residual
1.00	0.06	1.5	0.46	0.46	0.10	0.09
2.00	0.14	1.08	0.33	0.35	0.07	0.06
3.00	0.23	0.74	0.23	0.20	0.05	0.06
4.00	0.32	0.47	0.15	0.20	0.03	0.05
5.00	0.41	0.23	0.07	0.14	0.02	0.01
6.00	0.50	0	0.00	-0.01	0.00	0.00
7.00	0.59	-0.23	-0.07	-0.12	-0.02	-0.02
8.00	0.68	-0.47	-0.15	-0.19	-0.03	-0.03
9.00	0.77	-0.74	-0.23	-0.34	-0.05	-0.06
10.00	0.86	-1.08	-0.33	-0.35	-0.07	-0.07
11.00	0.94	-1.5	-0.46	-0.38	-0.10	-0.07

$$\dagger A = \frac{(i-0.375)}{(n+0.25)}$$

$$\dagger\dagger \sqrt{\text{mse}}(-\ln p) = 0.31$$

Statistical theory has shown that for a normal random variable with mean 0 and estimated standard deviation $\sqrt{\text{MSE}}$, a good approximation of the expected value of the i^{th} smallest observation in a random sample of n is given as below (Neeter et al., 1990).

$$\sqrt{\text{MSE}} \left[z\left(\frac{i-0.375}{n+0.25}\right) \right]$$

where $z(A)$ denotes the $(A) \cdot 100$ percentile of the standard normal distribution.

Table 4.9: Comparison Between Calculated Residuals (SO₂ penetration) and Normal Variables for the EPA/ RTP Data.

i	A [†]	Z(A)	p- fit ^{††}		ln p from p	
			ordered residual	$\sqrt{\text{mse}} \cdot z$	ordered residual	$\sqrt{\text{mse}} \cdot z$
1.00	0.06	1.5	0.09	0.07	0.76	0.53
2.00	0.14	1.08	0.06	0.05	0.48	0.38
3.00	0.23	0.74	0.04	0.04	0.24	0.26
4.00	0.32	0.47	0.03	0.02	0.18	0.17
5.00	0.41	0.23	-0.01	0.01	0.07	0.08
6.00	0.50	0	-0.02	0.00	0.05	0.00
7.00	0.59	-0.23	-0.02	-0.01	0.04	-0.08
8.00	0.68	-0.47	-0.03	-0.02	-0.17	-0.17
9.00	0.77	-0.74	-0.03	-0.04	-0.19	-0.26
10.00	0.86	-1.08	-0.05	-0.05	-0.22	-0.38
11.00	0.94	-1.5	-0.06	-0.07	-0.36	-0.53

$$\dagger A = \frac{(1-0.375)}{(n+0.25)}$$

$$\dagger\dagger \sqrt{\text{mse}(p)} = 0.05$$

Based on the trends in Figure 4.7 and 4.8, it was not possible to reject either response variable. Probably a greater number of data points would lead to a better distinction between the response variables. It can also be noted from Table 4.8 and 4.9 that the maximum residuals (0.458 and 0.090) lie within 2 standard deviations (0.30 and 0.05) of the mean. The assumption of normality cannot be rejected at 95 % confidence.

4.6 EMPIRICAL CORRELATIONS

The model does not incorporate the effects of changes in hydrodynamic parameters such as liquid and gas flow rates as well as height of packing on the adjustable parameters of the model. Factorial experiments were conducted at Shawnee (Head, 1977) to measure the effect of changes in liquid flow rate, gas flow rate and packing height on scrubber performance. Since N_g and k_L°/k_g are highly correlated, N_g was adjusted to match the observed SO_2 penetration in each case (see Table 4.10). The value of k_L°/k_g was fixed at the previously estimated value of 272 atm-ml/gmol. The residence time of slurry in the scrubber was adjusted assuming that pressure drop in the column was equal to the liquid hold-up. The liquid and gas superficial velocities were calculated using a cross-sectional area of 32 ft².

Correlations were obtained by linear regression of $\ln(\text{liquid velocity})$, $\ln(\text{gas velocity})$ against $\ln(N_g)$.

$N_g = 1.08 V_L^{-0.09} V_g^{0.82}$ ($R^2 (\ln N_g) = 0.70$), in the presence of 15" of packing

$N_g = 0.09 V_L^{0.69} V_g^{0.57}$ ($R^2 (\ln N_g) = 0.82$), in the absence of packing

In the presence of packing, the liquid rate has a very minor effect on N_g for the range of liquid rates considered. This may indicate that the packing is wetted and provides most of the contact area for gas/liquid mass transfer. In the absence of packing the liquid rate has a much greater influence on the absorption of SO_2 as it provides both area and solution capacity.

Table 4.10: Factorial Data from Shawnee Contactor, Showing Effects of L, G in the Presence and Absence of Packing ($\text{Cl}^- \sim 6000$ ppm, c.s. area = 32 ft², packing height = 15 inches).

Run -I.D.	p	L (gpm)	G (acfm)	pH	P _{SO2} *1e6 (atm)	ΔP (" water)	N _g [†]
Data for TCA Scrubber in the presence of 15" of packing							
TCA-105	0.08	1200	30000	5.81	2412	9.7	6
TCA-101	0.20	900	30000	5.78	2685	7.2	6.6
TCA-110	0.30	600	30000	5.77	2434	9.2 ^{††}	6.9
TCA-103	0.13	1200	25000	5.88	2669	6	3
TCA-137	0.21	900	25000	5.75	2543	5.3	4.8
TCA-109	0.32	600	25000	5.83	2466	5.5	5.1
TCA-106	0.16	1200	20000	5.8	2589	4.9	4.5
TCA-107	0.26	900	20000	5.77	2520	4.2	4.2
TCA-102	0.29	600	20000	6.11	2700	3.6	5.4
Data for TCA scrubber without packing							
TCA-119	0.30	1200	30000	5.85	2909	2.2	4.2
TCA-115	0.34	900	30000	5.9	2680	1.8	4.65
TCA-123	0.53	600	30000	5.75	2755	1.3	2.7
TCA-117	0.22	1200	25000	6.08	2750	1.6	4.65
TCA-118	0.36	900	25000	6.01	2920	1.2	4.2
TCA-122	0.54	600	25000	5.86	2743	0.7	2.7
TCA-120	0.29	1200	20000	5.84	2920	0.9	3.6
TCA-121	0.37	900	20000	5.89	2725	0.7	3.15
TCA-141	0.48	600	20000	5.84	2554	0.8	2.4

[†]N_g was adjusted for each point to calculate the measured penetration by the model at $\frac{k^{\circ}L}{k_g}$

= 272 atm-ml/gmol.

^{††} A value of $\Delta P = 9.2$ " was obtained from correlations (Head, 1976) although the reported value for this case was 18".

N_g = 1.08 V_L^{-0.09} V_g^{0.82} (R² (lnN_g) = 0.70), in the presence of 15" of packing

N_g = 0.09 V_L^{0.69} V_g^{0.57} (R² (lnN_g) = 0.82), in the absence of packing

4.7 COMPARISON BETWEEN MODEL ESTIMATES AND EXPERIMENTAL MEASUREMENTS

Measured values of N_g have been reported by other investigators at conditions of gas film control for three different sizes of turbulent contact absorbers. At conditions of liquid film control, N_L has been reported for the EPA/RTP contactor. Based on this value, k_L°/k_g was calculated.

Table 4.11 shows a comparison between the operating conditions used in the experimental studies for the three different turbulent contact absorbers. In the case of the experiments used for the parameter estimation study, the gas flow rates were 300 acfm and 30,000 acfm for the small and large scale contactors respectively.

The small scale contactor had a liquid flow rate of 17.5 gpm, whereas the large scale contactor had a liquid flow rate of 1200 gpm. The superficial velocities for the gas and liquid in each case are shown in Table 4.11. The total packing height for the large scale contactor was 15 inches and for the small-scale contactor it was 12 inches. Wherever possible the data obtained from other studies has been extrapolated to match the conditions used in the parameter estimation studies. In the case of the SO_2 -Air- Na_2CO_3 system at Shawnee and Flue Gas- Na_2CO_3 system, the experimental conditions are comparable to those used for parameter estimation.

Table 4.11: Comparison Between the Experimental Conditions at EPA/RTP and Shawnee and the Conditions in Other Experimental Studies.

The scrubbers used packing of 1.5 inch diameter polyethylene or nitrofoam spheres and had dual flow trays with 80% perforated area.

Operating conditions	Conditions used in Parameter Estimation		Experimental Conditions Used in Other Studies		
	Shawnee	EPA/RTP	Shawnee	EPA/RTP	NH ₃ -H ₂ O [‡]
Solute/Solvent	SO ₂ -Flue Gas/ Limestone Slurry		SO ₂ -Air/ Na ₂ CO ₃	SO ₂ -Flue Gas/ Na ₂ CO ₃	NH ₃ - Air/ Water
Liquid Velocity (V_L, m/s)	0.025	0.027	0.025	0.012-0.031	0.003-0.02
Gas Velocity (V_g, m/s)	3.8	3.7	3.6 ^{††}	3.4	1.2-2.2
Solution Temperature (C)	60	60	37	60	30
Cross Sectional Area (ft²)	0.44	32	32	0.44	1
N_g	2.88±0.55	2.97±0.54	3.9	5.2	1.4
Height of Packing/Stage (h_s, in.)	5	4 [†]	0-5	0-7	10-33

[†] Packing height is quoted based on Chang and Laslo (1982).

^{††} Gas velocity is reported at 37 C, adiabatic saturation temperature of gas in contact with solution. Gas velocity is calculated at 60 C for all the other experiments using flue gas.

[‡]Turbulent Contact Absorber used by Douglas (1964).

4.7.1 Measurement of N_g and N_L for the EPA/RTP contactor

For the three stage turbulent contact absorber (Dempsey, 1983), N_g was measured over a range of liquid flow rates (8-20 gpm) and packing heights (0-7"/stage). The absorber was operated under atmospheric pressure and the concentration of SO_2 in the flue gas ranged between 3100 and 4000 ppmv. The concentration of Na_2CO_3 in the inlet solution was maintained at a constant value of 0.54 M, this ensured complete gas film control throughout the range of operating conditions. A constant gas flow rate of 275 acfm (60° C) was maintained for all the experiments. The following correlations were reported for the total N_g .

$$N_g = 0.531 L^{0.58} \text{ (no packing)}$$

$$N_g = 1.54 L^{0.377} \text{ (3" packing/stage)}$$

$$N_g = 2.25 L^{0.329} \text{ (5" packing/stage)}$$

where L = liquid flow rate (gpm)

At a liquid flow rate of 17.5 gpm, the above correlations predict total $N_g = 4.5$ in the presence of 3" packing/stage and $N_g = 5.8$ in the presence of 5" packing/stage. $N_g = 5.2$ was calculated by interpolation, for the presence of 4" packing/stage.

At conditions close to liquid film control, N_L was calculated by measuring CO_2 absorption into an aqueous solution of Na_2CO_3 (constant pH = 9). At a liquid rate of 0.024 m/s (16.5 gpm) the calculated N_L varied from 3.9 to 5.3 due to

changes of CO₂ back pressure. This resulted in a range of $k_L^\circ / k_g = 171\text{-}237$ cc-atm/gmol.

4.7.2 Measurement of N_g for the Shawnee contactor

Absorption of SO₂ from an air-SO₂ mixture into an aqueous solution of Na₂CO₃ was used to measure N_g for the three stage large scale absorber at Shawnee. The experiments were conducted in the presence and absence of packing at a solution temperature of 70°F and gas temperature ranging from 90 to 110°F. The concentration of Na₂CO₃ in the solution at the inlet of the scrubber ranged between 0.027M and 0.22M and the SO₂ concentration in air ranged between 900-1200 ppmv. For gas velocity of 3.6 m/s and at liquid velocity of 0.025 m/s, N_g varied from 2.6 in the absence of packing (or packing support) to 3.9 in the presence of 5 inches packing per stage (Na₂CO₃ = 0.027 M, P_{SO₂} = 900 ppmV).

4.7.3 Comparison of the Effects of Wall Area between Shawnee and EPA/RTP contactors

Some of the differences between the measured values of N_g for the small and large scale contactors may be explained by a comparison of the total area due to the surface area of the wall and the surface area of packing. Table 4.12 shows the contributions of packing area and surface area of the absorber walls. The packing was supported by grids with 80% perforated area. The contribution of surface area provided by these trays can be neglected. There are no measurements available for

the effective interfacial area provided by the gas/liquid dispersion formed in the region between the stages. This has prevented a quantitative analysis of the effects of the same.

Table 4.12: Calculated Areas of the Packing and Wall for the EPA/RTP (small-scale) and Shawnee (large-scale) Contactors.

Contactor	area (ft ² /ft ³)		
	packing [†]	wall	total ^{††}
EPA/RTP	3.36	5.28	8.64
Shawnee	3.34	0.75	4.09

[†] Packing area is calculated based on 1.5" diameter of packing and 5" stagnant packing height.

^{††} The calculated total area does not include the contribution from the G/L dispersion that may be present on a stage.

The ratio of calculated N_g seem to correlate well with ratio of total area for 0", 3" and 5" of packing height in the case of the small-scale contactor. $N_{g,5}/N_{g,3} = 1.27$, $a_5/a_3 = 1.18$; $N_{g,5}/N_{g,0} = 2$, $a_5/a_0 = 1.625$ ($U_g = 3.4$ m/s and $U_L = 0.025$ m/s).

The ratio of total areas in the Shawnee TCA versus the EPA/RTP TCA is 2.1, the ratio of measured N_g for the EPA/RTP contactor versus the Shawnee contactor is 1.48 i.e. the ratio of areas is greater than the ratio of N_g . The measured values of N_g change from 2.6 for the Shawnee contactor without packing to 3.91 in the presence of packing. These differences cannot be explained based on the ratio of total areas. In the absence of packing, N_g for the Shawnee contactor was 2.6.

Under similar conditions the observed N_g for the EPA/RTP contactor was 3.03. The ratio of wall areas for these absorbers is much larger, i.e., 7.04.

The contribution of the area due to the wetted wall of the scrubber seems to correlate well with N_g in the small-scale contactor. However, for the large scale contactor, the walls of the scrubber make a small contribution to the overall effective area of a stage. The analysis based on wall and packing areas does not explain the observed values of N_g for the large scale contactor.

4.7.4 Measurement of N_g for a Single-Stage TCA

Using the NH_3 -air-water system, absorption of NH_3 was measured in a single stage absorber for a range of liquid flow rates, gas flow rates, and packing heights (Douglas, 1964). The absorber had a cross-sectional area of 1 ft² and was packed to a height of 10 to 33 inches with 1.5" diameter hollow polyethylene spheres (4.5 g weight). The concentration of ammonia ranged from 4000 ppmv to 1600 ppmv at inlet and 1000 to 100 ppmv at exit. The experiments were conducted under atmospheric pressure. The concentration of dissolved ammonia in the aqueous stream ranged between 0.02 and 0.09 mole % at the exit of the scrubber. The inlet stream did not contain any dissolved ammonia. At these conditions, absorption of ammonia can be expected to be gas film controlled.

The conditions for the operation of the TCA for ammonia absorption were different from those used at EPA/RTP or Shawnee. Although, liquid velocity (~0.02 m/s versus 0.025 m/s) was comparable in all the three cases, the gas

velocity was much lower (1.2 -2.2 versus 3.8 m/s) The packing height in this TCA was higher (10-33"/stage versus 5-7"/stage). The calculated values of N_g range from 0.9 in the presence of 10 inches of packing to 3.4 in the presence of 18 inches of packing. The data from this study were used to correlate measured N_g with packing height (h_s , m), liquid velocity (U_L , m/s), and gas velocity (U_g , m/s).

$$N_g = 17.4 V_g^{-1.2} V_L^{0.22} h_s^{0.48}$$

At Shawnee conditions, $h_s = 0.128$ m, $U_g = 3.63$ m/s, $U_L = 0.025$ m/s, the calculated values of were $N_g = 0.6/\text{stage}$; $N_g = 1.8$ for a three stage contactor. Correcting for the difference in diffusivity between the molecular species SO_2 and NH_3 , as shown below, gives $N_{g-\text{SO}_2} = 1.4$.

$$\frac{N_{g-\text{SO}_2}}{N_{g-\text{NH}_3}} = \sqrt{\frac{D_{\text{SO}_2-\text{Air}}}{D_{\text{NH}_3-\text{Air}}}} = \sqrt{\frac{1}{1.9}}$$

Douglas (1964) reported non-uniformities in fluidization of spherical packing during the experiments on NH_3 absorption. In the deeper beds (33 in. packing) the spheres tended to move entirely in up-flow on one side and entirely in down-flow on the other. These problems were not observed at bed depths of 10 inches.

4.7.5 Comparison Between Model Calculations and Experimental Observations

Calculated values of N_g show a range from 1.4 for the NH_3 -water system to 5.2 for the SO_2 - Na_2CO_3 system in the small-scale TCA. The values obtained by

parameter estimation lie between these extremes. All of the above values were obtained at similar gas and liquid velocities.

The calculated N_g values are greatest in the presence of the highest concentrations of Na_2CO_3 , where instantaneous reaction with SO_2 is expected. The least value of N_g is observed in the ammonia-water system where no reaction is expected although the equilibrium solubility of ammonia is expected to lead to conditions of gas film control.

Some of these differences may be explained on the basis of a droplet size distribution of liquid. The smaller droplets of liquid would present the maximum surface area per unit volume, as well as higher mass transfer coefficients. The capacity of the smaller droplets is limited by their volume. The concentration of Na_2CO_3 is an order of magnitude higher for the experiments at EPA/RTP as compared to those at Shawnee (0.54 versus 0.027 M). This can lead to a greater capacity for absorption at comparable droplet surface area.

A comparison between the solution capacity in each case has been shown in Table 4.13. For the small-scale contactor the ratio of solution capacity/solute concentrations is the 31 whereas for the Shawnee contactor it is 6. It can be expected that the smaller droplets would saturate to a lesser extent leading to a greater measured N_g (as observed). This effect does not lead to a satisfying explanation for the observed N_g in case of the ammonia-water system. The discrepancies in the observed N_g for ammonia may be due to reported non-uniformities in fluidization of the packing. The calculated N_g for the

ammonia-water system could be somewhat inaccurate due to the extrapolation in gas velocities (at experimental conditions, $U_g = 2.2$ m/s; for calculation of N_g , $U_g = 3.8$ m/s).

Table 4.13: Comparison of the Solution Capacity for Absorption of Ammonia in Water (Douglas, 1964) with Solution Capacity for the Absorption of SO_2 in Na_2CO_3 Solution (Epstein et al., 1973; Dempsey, 1983).

	Shawnee [†]	EPA/RTP ^{††}	NH_3-H_2O [‡]
Solute/Solvent	SO_2 -Air/ Na_2CO_3	SO_2 -Flue Gas/ Na_2CO_3	NH_3 -Air/ Water
Gross Solubility (gmol/l)	0.027	0.54	0.23
L/G (l/gmol)	0.2	0.2	0.2
Solution Capacity (gmol - solute/ gmol gas)	0.0054	0.11	0.046
Solute Concentration (ppmv)	900	3600	4000
Solution Capacity (ppmv)	5×10^3	11×10^4	4.6×10^4
<u>Solution Capacity</u> <u>Solute Concentration</u>	6	31	11

[†] Epstein et al. (1973)

^{††} Dempsey (1983)

[‡] Douglas (1964)

4.8 NOTATION

a	= Area of packing (cm^2)
e_i	= Residual for the i^{th} experiment
f	= fractional absorption of SO_2
f_i	= Model responses
G	= Gas flow rate (gmol/s)

\mathbf{H}	= Hessian Matrix (dimensionless)
K_{CaCO_3}	= Limestone reactivity parameter (1/cm ²)
$\frac{k_L^o}{k_g}$	= Ratio of liquid to gas film mass transfer coefficient (atm-ml/gmol)
$(k_L^o/k_g)'$	= Normalized value of k_L^o/k_g
L	= Liquid flow rate (L/s)
$l(y \theta_i^*, \sigma^{ij})$	= Likelihood function
N_g	= Total number of gas film transfer units for scrubber (dimensionless)
n_g	= Number of gas film transfer units/stage (dimensionless)
N_g'	= Normalized value of N_g
$N_{g,z}$	= Total number of gas film mass transfer units for packed height Z (dimensionless)
N_L	= Total number of liquid phase mass transfer units in the scrubber (dimensionless)
P	= Pressure (atm)
p	= SO ₂ penetration (dimensionless)
$p(\theta, y)$	= Posterior probability density function (dimensionless)
$p(y)$	= Probability density function (dimensionless)
P_{SO_2}	= Partial pressure of SO ₂ in the bulk gas phase (atm.)
$P_{\text{SO}_2\text{-exit}}$	= Partial Pressure of SO ₂ at the scrubber exit (atm)
$P_{\text{SO}_2\text{-inlet}}$	= Partial Pressure of SO ₂ at the scrubber inlet (atm)
P_T	= Total pressure (atm)
\mathbf{V}	= Moment matrix of residuals
V_g	= Gas velocity (m/s)

V_L	= Liquid velocity (m/s)
y	= Measured response variable
Z	= Absorber height or packed height (cm)
$z_{0.025}$	= Value of Z-statistic at the 95% confidence level (dimensionless)

Greek Symbols

ε	= Random error
Φ	= Liquid phase enhancement factor
θ	= Parameter (to be estimated)
Σ^{-1}	= Co-variance matrix
$\Psi^2_{(m, \alpha)}$	= Chi-squared random variable of m degrees of freedom at α upper tail of the distribution

Subscripts and Superscripts

z	= Height of packing
-----	---------------------

CHAPTER 5

CONCLUSIONS AND RECOMMENDATIONS

5.1 CONCLUSIONS

The simultaneous estimation of model parameters along with confidence intervals has not been conducted prior to this work for limestone slurry scrubbing systems. The present study provides estimates for N_g , k_L°/k_g , N_L and limestone reactivity (scale2) for two different sizes of turbulent contact absorbers.

Based on this estimation study, the parameters for the EPA/RTP contactor are $N_g = 2.88 \pm 0.55$, $k_L^\circ/k_g = 292 \pm 169$ cc-atm/gmol, scale2 = 25.6 ± 76 and $N_L = 3.65 \pm 1.28$. In the case of the Shawnee contactor the estimated values of the parameters are $N_g = 2.97 \pm 0.54$, $k_L^\circ/k_g = 271 \pm 103$ cc-atm/gmol, scale2 = 4.3 ± 2.6 and $N_L = 4.04 \pm 0.94$.

The estimated values of N_g and k_L°/k_g are comparable for the data used in this study. This can be expected as the hydrodynamic conditions for the EPA/RTP and Shawnee contactors were similar in terms of liquid and gas velocities and packing heights. The estimated values of scale2 show that the particle size distribution for the large scale absorber was representative of a finer grind, than in the case of the small scale absorber.

For the data used in this study the estimated parameters have high negative co-variance. The effect of correlation between the parameters can be best understood on the basis of elliptical confidence regions. For limestone slurry scrubbing systems, least correlated estimates can be obtained using data at

extremes of gas and liquid film control. The parameter set N_g and N_L is less correlated than N_g and k_L°/k_g .

The solution pH must be accurately matched to predict observed SO_2 penetration. This is true in the case of large-scale as well as small-scale data. The model was not able to predict the pH for the small-scale data adequately. This could be due to poor measurements of limestone utilization or model inadequacies. The capabilities of the model should be further examined in this regard. For limestone slurry scrubbing systems, experimental results are often reported in terms of pH (at hold tank exit) rather than limestone utilization. Using pH as a means to determine limestone reactivity can prove to be a more useful procedure in modeling data for these systems.

The parameters were calculated using $-\ln p$ as well as p (SO_2 penetration) as dependent variables in the objective function. The former minimized the ratio between the measured and calculated penetration, whereas the latter minimized the absolute error in penetration. Using SO_2 penetration alone biased the regression towards data at higher values of penetration. $-\ln p$ was preferred as the dependent variable as it produced a better fit at lower SO_2 penetration. This resulted in more accurate estimates of N_g .

Based on empirical correlations it can be deduced that, in the absence of packing in the scrubber, the liquid rate plays an important role in determining the amount of SO_2 absorbed. However, in the presence of packing the superficial gas velocity is more important.

The model was used to study the effects of different variables on system chemistry and SO_2 absorption. The results of Chapter 3 show that hydrolysis

reactions are important in determining the absorption of SO_2 . The dissolved alkalinity in the form of HCO_3^- and SO_3^{2-} plays an important role only above pH 5. For most conditions, the equilibrium concentration of SO_2 in the bulk liquid is negligible. In the presence of high concentrations of dibasic acids, gas film control is reached at each stage of a three stage turbulent contact absorber. For a specified set of hydrodynamic conditions, operation under gas film control provides maximum capacity for absorption.

5.2 RECOMMENDATIONS

It is recommended that data from forced oxidation systems be included in the parameter estimation studies. There is a greater amount of published data for turbulent contact absorbers operating under this mode (versus natural oxidation). Although the hydrodynamic parameters for both these systems should be the same, this would enable estimation of parameters with smaller uncertainty.

Spray scrubbers are the most popular scrubbers for limestone slurry scrubbing applications. Renae Vandekemp (1993) incorporated calculations for spray scrubbing in FGDTX. The simulation of spray scrubbers using FGDTX would greatly enhance the utility of the model as a tool for troubleshooting and design.

APPENDIX A

MODEL EQUATIONS

A-1 INTRODUCTION

This appendix contains a statement of the equations used to simulate the limestone slurry scrubbing process. The stagewise mass balance equations for the scrubber and the hold tank are presented first (see section A-2 and A-3). Thereafter, the equations required to calculate the compositions in the bulk liquid, at the solid/liquid interface, and at the gas/liquid interface are shown (see section A-4). The equations used to determine concentrations, equilibrium constants, and diffusivities for the pseudo species and the equations required for the calculation of the limestone reactivity constant and film thickness are stated in section A-5. Finally, a short summary of the inputs required to calculate the variables present in the equations (in sections A-2 to A-5) is presented in section A-6.

A-1.2 Process Description

Limestone slurry scrubbing is modeled as a process consisting of two units: a scrubber and a hold tank. The scrubber is a staged contactor where each stage can comprise of spray headers or trays. The hold tank is usually a large, well-mixed tank. The calculations described in this appendix are suitable for modeling staged scrubbers consisting of dual-flow trays.

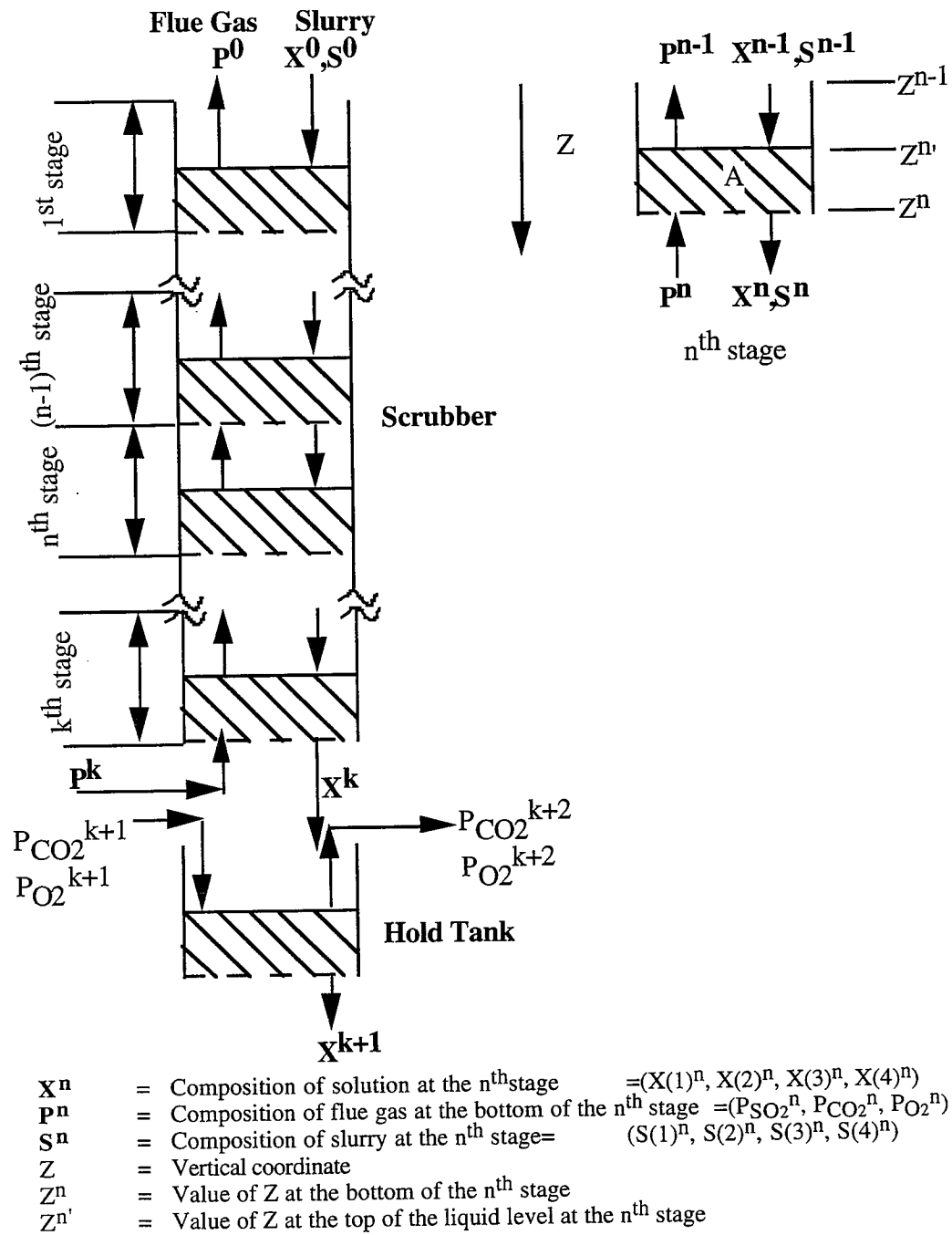


Figure A-1: Process Flow Diagram of the Limestone Slurry Scrubbing System.

In the scrubber, upward flowing flue gas is brought into counter-current contact with downward moving slurry (see Figure A-1). As a result of this contact, there is mass-transfer between the flue gas and the scrubbing solution. This results in the absorption or desorption of sulfur dioxide, carbon dioxide, and oxygen. Simultaneously, mass-transfer occurs between the solids suspended in the slurry and the scrubbing solution. This results in the dissolution or precipitation of solids: calcium sulfite hemihydrate, calcium sulfate hemihydrate, calcium carbonate, and calcium sulfate dihydrate (gypsum).

The slurry leaving the scrubber is taken into the hold tank where a fresh feed of limestone is added to it. Sufficient time is provided in the hold tank so that the solution in it is desupersaturated with respect to calcium sulfite and calcium sulfate. Thereafter, slurry from the hold tank is recirculated to the top of the scrubber.

A-1.3 Stagewise Calculations

A limestone slurry scrubbing system consisting of a staged scrubber having k stages and a hold tank ($k+1^{\text{th}}$ stage) is shown in Figure A-1. The stages are numbered in ascending order from the top (stage 1) to the bottom (stage k) of the scrubber. At each stage of the scrubber the slurry is well-mixed, whereas the gas is plug-flow. The slurry in the hold tank is also well-mixed and is modeled as in the scrubber stage. However, the gas phase mass-transfer calculations for the hold tank are different from those in the scrubber (see section A-4).

All the stages in the scrubber are modeled in the same manner. It is sufficient to define the streams associated with the n^{th} stage, and explain the mass balance calculations associated with it, to gain an understanding of the calculations applied to all the stages in the scrubber and most of the calculations in the hold tank.

Let Z denote the vertical coordinate, such that Z increases in value from the top stage (stage 1) to the bottom stage (stage k). Let Z^n and Z^{n-1} denote the values of Z at bottom of the n^{th} stage and the bottom of the $(n-1)^{\text{th}}$ stage respectively. The total height of the n^{th} stage is given by $Z^n - Z^{n-1}$. If $Z^{n'}$ indicates the level of liquid on the n^{th} stage, then $Z^n - Z^{n'}$ corresponds to the effective height of the n^{th} stage, i.e., the space where all the mass-transfer between gas and liquid occurs. The contribution of effective stage height on the mass transfer capacity is quantified in terms of the number of gas film mass transfer units (N_g). If N_g^n and N_g^{n-1} denote the number of mass transfer at the bottom of the n^{th} and $(n-1)^{\text{th}}$ stages respectively, then the number of mass transfer units available at the n^{th} stage is given as: $N_g^n - N_g^{n-1}$ (for the purposes of this discussion all k stages have the same actual and effective heights) .

$$N_g^n - N_g^{n-1} = \frac{k_g a (Z^n - Z^{n'})}{G}$$

where:

k_g = Gas film mass transfer coefficient (gmol/s)

a = Effective interfacial area for mass-transfer (cm^2/cc)

G = Gas flow rate (gmol/s)

At every point on the n^{th} stage, the solution composition can be specified in terms of the concentrations of four dissolved species: total sulfite ($X(1)^n$), total sulfate ($X(2)^n$), total carbonate ($X(3)^n$), and total calcium ($X(4)^n$). Similarly, the composition of solids suspended in the slurry at the n^{th} stage, can be stated in terms of four species: calcium sulfite hemihydrate ($S(1)^n$), calcium sulfate hemihydrate ($S(2)^n$), calcium carbonate ($S(3)^n$), and calcium sulfate dihydrate ($S(4)^n$).

At the n^{th} stage, the composition of the slurry is constant at every point on the stage, whereas the gas phase composition is dependent upon the vertical coordinate of a point on the stage and the liquid composition on the stage (the effects of changes in radial position are not modeled). At point A on the n^{th} stage (see Figure A-1), where the vertical coordinate is given as $Z^{n'} \leq Z^A \leq Z^n$, the gas phase composition is dependent upon both the liquid composition and the vertical coordinate or N_g^A ($N_g^{n-1} \leq N_g^A \leq N_g^n$). At other points on the n^{th} stage, the gas phase compositions are defined as shown below.

At $Z = Z^{n'}$; $N_g = N_g^{n-1}$; Gas composition: $P_{\text{SO}_2}^{n-1}$, $P_{\text{CO}_2}^{n-1}$, $P_{\text{O}_2}^{n-1}$

At $Z = Z^{n-1}$; $N_g = N_g^{n-1}$; Gas composition: $P_{\text{SO}_2}^{n-1}$, $P_{\text{CO}_2}^{n-1}$, $P_{\text{O}_2}^{n-1}$

At $Z = Z^n$; $N_g = N_g^n$; Gas composition: $P_{\text{SO}_2}^n$, $P_{\text{CO}_2}^n$, $P_{\text{O}_2}^n$

Let \mathbf{X}^n , \mathbf{P}^n and \mathbf{S}^n denote vectors such that: $\mathbf{X}^n = (X(1)^n, \dots, X(4)^n)$, $\mathbf{P}^n = (P_{\text{SO}_2}^n, P_{\text{CO}_2}^n, P_{\text{O}_2}^n)$, and $\mathbf{S}^n = (S(1)^n, \dots, S(4)^n)$. The vectors \mathbf{X}^{n-1} , \mathbf{P}^{n-1} , and \mathbf{S}^{n-1} can be defined similarly.

At the n^{th} stage, \mathbf{X}^{n-1} , \mathbf{S}^{n-1} , and \mathbf{P}^{n-1} are specified before the mass-balance calculations are begun. An iterative procedure is used to calculate \mathbf{X}^n . Once \mathbf{X}^n is specified \mathbf{S}^n and \mathbf{P}^n are completely determined.

The material balance calculations for the scrubber follow a sequential scheme, starting at the first stage (where \mathbf{X}^0 , \mathbf{P}^0 , and \mathbf{S}^0 are guessed) and proceeding downward. Using stagewise material balances, \mathbf{X}^n , \mathbf{P}^n , and \mathbf{S}^n are determined for each stage ($n=1, \dots, k$). The material balance calculations with respect to the scrubber are complete if $P_{\text{SO}_2}^k$ matches its specified value.

Hold tank calculations proceed in a similar manner as the stage calculations in the scrubber, i.e., \mathbf{X}^{k+1} is determined by an iterative procedure using specified values of \mathbf{X}^k , $P_{\text{CO}_2}^{k+1}$, $P_{\text{O}_2}^{k+1}$, and \mathbf{S}^k . Once the material balance calculations for the hold tank are completed, the composition of the inlet slurry to the scrubber is updated; $\mathbf{X}^0 = \mathbf{X}^{k+1}$, $S(1)^0 = S(1)^{k+1}$, $S(2)^0 = S(2)^{k+1}$, $S(3)^0 = S(3)^0$, and $S(4)^0 = S(4)^{k+1}$. Overall material balance calculations (for the scrubber and hold tank) are completed when \mathbf{X}^{k+1} is the same for two successive iterations through the scrubber and hold tank.

A-2 MATERIAL BALANCE EQUATIONS FOR THE N^{TH} STAGE

The material balance equations for the n^{th} stage can be stated as follows:

For each species ($i=1, 2, 3, 4$)

$$X(i)^n = X(i)^{n-1} + F(i)^n + G(i)^n$$

where:

$$X(1)^n = \text{Total concentration of the sulfite species in the liquid solution at the } n^{\text{th}} \text{ stage (gmol/L)}$$

$X(2)^n$ = Total concentration of sulfate species in the liquid solution at the n^{th} stage (gmol/L)

$X(3)^n$ = Total concentration of the carbonate species in the liquid solution at the n^{th} stage (gmol/L)

$X(4)^n$ = Total concentration of the calcium species in the liquid solution at the n^{th} stage (gmol/L)

$X(1)^{n-1}, \dots, X(4)^{n-1}$ are defined similarly for the $(n-1)^{\text{th}}$ stage

$F(i)^n$ = Change in the solution composition, in terms of $X(i)^n$, due to the absorption/desorption of gases at the n^{th} stage (gmol/L)

$G(i)^n$ = Change in the solution composition, in terms of $X(i)^n$, due to the dissolution/crystallization of solids at the n^{th} stage (gmol/L)

A-2.1 Calculation of $F(1)^n$ and $G(1)^n$

$$F(1)^n = f_{11}(C_{\text{SO}_3^=,b}^n, C_{\text{HSO}_3^-,b}^n, C_{\text{SO}_2,b}^n, C_{\text{SO}_3^=,i}^n, C_{\text{HSO}_3^-,i}^n, C_{\text{SO}_2,i}^n, \mathbf{p}_{11}) + f_{12}(C_{\text{O}_2,i}^n, \mathbf{p}_{12})$$

where:

$$f_{11}^n = f_{11}(C_{\text{SO}_3^=,b}^n, C_{\text{HSO}_3^-,b}^n, C_{\text{SO}_2,b}^n, C_{\text{SO}_3^=,i}^n, C_{\text{HSO}_3^-,i}^n, C_{\text{SO}_2,i}^n, \mathbf{p}_{11})$$

= Change in solution composition due to the absorption of sulfur dioxide at the n^{th} stage

$$\mathbf{p}_{11} = \text{Vector of parameters}$$

$$\begin{aligned}
 f_{12}^n &= f_{12}(\text{CO}_{2,i}^n, \mathbf{p}_{12}) \\
 &= \text{Change in solution composition due to the absorption of} \\
 &\quad \text{oxygen at the } n^{\text{th}} \text{ stage} \\
 \mathbf{p}_{12} &= \text{Vector of parameters}
 \end{aligned}$$

$$\begin{aligned}
 f_{11}^n &= \frac{G}{L} \frac{k_l^\circ}{k_g} \sqrt{\frac{1}{D_{\text{SO}_2}}} \int_{N_g^{n-1}}^{N_g^n} \sum_j \sqrt{D_j} \Delta C_j^n dN_g \\
 &= \frac{G}{L} (P_{\text{SO}_2}^n - P_{\text{SO}_2}^{n-1})
 \end{aligned}$$

where:

$$\begin{aligned}
 \mathbf{p}_{11} &= (G/L, k_l^\circ/k_g, N_g^n, N_g^{n-1}, D_{\text{SO}_3^-}, D_{\text{HSO}_3^-}, D_{\text{SO}_2}) \\
 \Delta C_j^n &= C_{j,i}^n - C_{j,b}^n \\
 C_{j,i}^n &= \text{Concentration of } j^{\text{th}} \text{ species at the gas liquid interface, at} \\
 &\quad \text{a location } Z \text{ on the } n^{\text{th}} \text{ stage } (Z^{n-1} \leq Z \leq Z^n, N_g^{n-1} \leq N_g \leq \\
 &\quad N_g^n) \\
 C_{j,b}^n &= \text{Concentration of the } j^{\text{th}} \text{ species in the bulk liquid at the} \\
 &\quad n^{\text{th}} \text{ stage} \\
 j &= \text{SO}_3^-, \text{SO}_2, \text{HSO}_3^-
 \end{aligned}$$

$$C_{j,i}^n = C_{j,i}(\mathbf{X}^n, \mathbf{P}^{n-1}, N_g, \mathbf{r}_1), \quad \text{where } N_g^{n-1} \leq N_g \leq N_g^n$$

$$C_{j,b}^n = C_{j,b}(\mathbf{X}^n, \mathbf{r}_2)$$

Concentration of the j^{th} species at the gas/liquid interface at a point on the n^{th} stage is dependent upon the bulk liquid composition (\mathbf{X}^n) and the position of

the point on the stage. At point A on the n^{th} stage ($Z^{n'} < Z^A < Z^n$), where $N_g = N_g^A$ and interfacial concentrations are given as $C_{j,i}^A$, the partial pressure of sulfur dioxide ($P_{\text{SO}_2}^A$) can be determined by integrating the equation shown below.

$$P_{\text{SO}_2}^A - P_{\text{SO}_2}^{n-1} = \frac{G}{L} \frac{k_1^o}{k_g} \sqrt{\frac{1}{D_{\text{SO}_2}}} \int_{N_g^{n-1}}^{N_g^A} \sum_j \sqrt{D_j} \Delta C_j^n dN_g$$

$$\Delta C_j^n = C_{j,i}^A - C_{j,b}^n$$

$$C_{j,i}^A = C_{j,i}(\mathbf{X}^n, \mathbf{P}^{n-1}, N_g^A, \mathbf{r}_1)$$

$$\begin{aligned} f_{12}^n &= -\frac{G}{L} \frac{k_1^o}{k_g} \sqrt{\frac{1}{D_{\text{SO}_2}}} \int_{N_g^{n-1}}^{N_g^n} (\sqrt{D_{\text{O}_2}} \Delta C_{\text{O}_2}^n) dN_g \\ &= -2 G/L (P_{\text{O}_2}^n - P_{\text{O}_2}^{n-1}) \end{aligned}$$

where:

$$\Delta C_{\text{O}_2}^n = C_{\text{O}_2,i}^n - C_{\text{O}_2,b}^n$$

$$C_{\text{O}_2,i}^n = \text{Concentration of oxygen at the gas liquid interface at a location } Z \text{ on the } n^{\text{th}} \text{ stage } (Z^{n'} \leq Z \leq Z^n, N_g^{n-1} \leq N_g \leq N_g^n)$$

$$C_{\text{O}_2,b}^n = \text{Concentration of oxygen in the bulk liquid solution at the } n^{\text{th}} \text{ stage}$$

$$\mathbf{p}_{12} = (G/L, k_1^o/k_g, N_g^n, N_g^{n-1}, D_{\text{O}_2}, D_{\text{SO}_2})$$

$$C_{\text{O}_2,i}^n = C_{\text{O}_2,i}(\mathbf{X}^n, \mathbf{P}^{n-1}, N_g, \mathbf{r}_1), \text{ where } N_g^{n-1} \leq N_g \leq N_g^n$$

$$C_{\text{O}_2,b}^n = 0$$

$$\begin{aligned}
G(1)^n &= \text{Change in solution composition, in terms of } X(1)^n, \text{ due} \\
&\quad \text{to the dissolution/crystallization of solids at the } n^{\text{th}} \text{ stage} \\
G(1)^n &= g_{11}(C_{\text{SO}_3^{=},b}^n, C_{\text{HSO}_3^-,b}^n, C_{\text{SO}_3^{=},s1}^n, C_{\text{HSO}_3^-,s1}^n, \mathbf{q}_{11}) \\
&\quad \tau_s S(1)^n + g_{12}(R_{\text{SCaSO}_3}^n, R_{\text{SCaSO}_4}^n, \mathbf{q}_{12}) \tau_s S(1)^n
\end{aligned}$$

where:

$$\begin{aligned}
g_{11}^n &= g_{11}(C_{\text{SO}_3^{=},s1}^n, C_{\text{HSO}_3^-,s1}^n, C_{\text{SO}_3^{=},b}^n, C_{\text{HSO}_3^-,b}^n, \mathbf{q}_{11}) \\
&= \text{Rate of change in solution composition due to the} \\
&\quad \text{dissolution/crystallization of } \text{CaSO}_3 \cdot 1/2\text{H}_2\text{O} \text{ at the} \\
&\quad n^{\text{th}} \text{ stage}
\end{aligned}$$

$$\mathbf{q}_{11} = \text{Vector of parameters}$$

$$\begin{aligned}
g_{12}^n &= g_{12}(R_{\text{SCaSO}_3}^n, R_{\text{SCaSO}_4}^n, \mathbf{q}_{12}) \\
&= \text{Rate of change in solution composition due to the} \\
&\quad \text{dissolution/crystallization of } \text{CaSO}_4 \cdot 1/2\text{H}_2\text{O} \text{ at the } n^{\text{th}} \\
&\quad \text{stage}
\end{aligned}$$

$$\mathbf{q}_{12} = \text{Vector of parameters}$$

$$\tau_s = \text{Slurry residence time/stage in the scrubber (s)}$$

$$\begin{aligned}
g_{11}^n &= K_{\text{CaSO}_3,d} \sum_j D_j \Delta C_j^n \\
&= 0 \text{ (if } R_{\text{SCaSO}_3}^n > 1)
\end{aligned}$$

where:

$$\mathbf{q}_{11} = (K_{\text{CaSO}_3,d}, D_j)$$

$$\Delta C_j^n = C_{j,s1}^n - C_{j,b}^n$$

$$K_{\text{CaSO}_3,d} = \text{Dissolution constant for calcium sulfite}$$

$C_{j,s1}^n$ = Concentration of j^{th} species at the surface of calcium sulfite at the n^{th} stage

$C_{j,b}^n$ = Concentration of j^{th} species in the bulk solution at the n^{th} stage

j = $\text{SO}_3^{=}$, HSO_3^-

$C_{j,s1}^n$ = $C_{j,s1}(\mathbf{X}^n, \mathbf{r}_3)$

$C_{j,b}^n$ = $C_{j,b}(\mathbf{X}^n, \mathbf{r}_2)$

g_{12}^n = $-K_{\text{CaSO}_3,c} \frac{(\text{RS}_{\text{CaSO}_3}^n - 1)}{\text{RS}_{\text{CaSO}_4}^n}$
 = 0 if $\text{RS}_{\text{CaSO}_3}^n \leq 1$

where:

\mathbf{q}_{12} = $(K_{\text{CaSO}_3,c}, K_{\text{sp}, \text{CaSO}_3}, K_{\text{sp}, \text{CaSO}_4})$

$\text{RS}_{\text{CaSO}_3}^n$ = Relative saturation calcium sulfite at the n^{th} stage

$\text{RS}_{\text{CaSO}_4}^n$ = Relative saturation of gypsum at the n^{th} stage

$K_{\text{CaSO}_3,c}$ = Crystallization constant for calcium sulfite hemihydrate

$K_{\text{sp}, \text{CaSO}_3}$ = Solubility product for calcium sulfite

$K_{\text{sp}, \text{CaSO}_4}$ = Solubility product for calcium sulfate

$\text{RS}_{\text{CaSO}_4}^n$ = $C_{\text{Ca}^{++},b}^n C_{\text{SO}_4^{=},b}^n / K_{\text{sp}, \text{CaSO}_4}$

$\text{RS}_{\text{CaSO}_3}^n$ = $C_{\text{Ca}^{++},b}^n C_{\text{SO}_3^{=},b}^n / K_{\text{sp}, \text{CaSO}_3}$

$C_{\text{Ca}^{++},b}^n$ = $C_{\text{Ca}^{++},b}(\mathbf{X}^n, \mathbf{r}_2)$

$C_{\text{SO}_3^{=},b}^n$ = $C_{\text{SO}_3^{=},b}(\mathbf{X}^n, \mathbf{r}_2)$

$$C_{SO_4^{2-},b}^n = C_{SO_4^{2-},b}(X^n, r_2)$$

The change in the concentration of solid calcium sulfite hemihydrate ($S(1)^n$) can be calculated on the basis of the rate of dissolution or crystallization of calcium sulfite hemihydrate.

$$S(1)^n = \frac{S(1)^{n-1}}{1 + g_{11}^n \tau_s}, \text{ if } RS_{CaSO_3}^n \leq 1$$

$$S(1)^n = S(1)^{n-1} (1 + g_{12}^n \tau_s), \text{ if } RS_{CaSO_3}^n > 1$$

When calcium sulfite hemihydrate dissolves/crystallizes, there is also simultaneous dissolution/crystallization of calcium sulfate hemihydrate ($S(2)^n$).

In the case of dissolution:

$$S(2)^n = \frac{S(2)^{n-1}}{1 + \sum_j D_j \Delta C_j K_{CaSO_4} / R_{SO_3SO_4} \tau_s}$$

where:

$$j = SO_4^{2-}, HSO_4^-$$

$$\Delta C_j = C_{j,s1}^n - C_{j,b}^n$$

$$R_{SO_3SO_4}^n = \text{Ratio of calcium sulfate hemihydrate to calcium sulfite hemihydrate in solid}$$

$$R_{SO_3SO_4}^n = \frac{S(2)^{n-1}}{S(1)^{n-1}} \text{ or } 0.17 \text{ if } n=1$$

In the case of crystallization:

$$S(2)^n = S(2)^{n-1} \left(1 + \frac{RS_{CaSO_3 \cdot 1/2H_2O}^n (S(1)^n - S(1)^{n-1}) / S(1)^n}{(1 - RS_{CaSO_3 \cdot 1/2H_2O}^n)} \right)$$

where:

$$RS_{CaSO_4 \cdot 1/2H_2O}^n$$

= Relative saturation of calcium sulfate hemihydrate in the liquid phase

$$= (0.41 - 0.25 RS_{CaSO_4}^n) RS_{CaSO_4}^n$$

$$= 0.17 \text{ (if } RS_{CaSO_4}^n > 0.82 \text{)}$$

A-2.2 Calculation of $F(2)^n$ and $G(2)^n$

$$F(2)^n = -f_{12}$$

$G(2)^n$ = Change of solution composition, in terms of $X(2)^n$, due to the dissolution/crystallization of solids at the n^{th} stage

$$= g_{21}(RS_{CaSO_4}^n, \mathbf{q}_{21}) \tau_s S(4)^{n-1} +$$

$$g_{22}(CHSO_4^-, {}_b^n, CSO_4^-, {}_b^n, CHSO_4^-, {}_{s1}^n, CSO_4^-, {}_{s1}^n,$$

$$RSO_3SO_4^n, \mathbf{q}_{22}) \tau_s S(2)^n +$$

$$g_{23}(RS_{CaSO_3 \cdot 1/2H_2O}, S(1)^n, S(2)^n, \mathbf{q}_{23}) \tau_s S(2)^{n-1}$$

$$g_{21}^n = g_{21}(RS_{CaSO_4}^n, \mathbf{q}_{21})$$

= Rate of change in solution composition due to the crystallization of gypsum at the n^{th} stage

$$\mathbf{q}_{21} = \text{Vector of parameters}$$

$$g_{22}^n = g_{22}(CHSO_4^-, {}_b^n, CSO_4^-, {}_b^n, CHSO_4^-, {}_{s1}^n, CSO_4^-, {}_{s1}^n, RSO_3SO_4^n, \mathbf{q}_{22})$$

= Rate of change in solution composition due to the dissolution of calcium sulfite hemihydrate at the n^{th} stage

q22 = Vector of parameters

g_{23}^n = $g_{23}(\text{RSCaSO}_3 \cdot 1/2\text{H}_2\text{O}, \text{S}(1)^n, \text{S}(2)^n, \mathbf{q}_{23})$

= Rate of change in solution composition due to the crystallization (precipitation) of calcium sulfate hemihydrate at the n^{th} stage

q23 = Vector of parameters

τ_s = Residence time for slurry on the n^{th} stage

g_{21}^n = $K_{\text{CaSO}_4} (\text{RSCaSO}_4^n - 1)$

g_{21}^n = 0 if $\text{RSCaSO}_4^n \leq 1$

where:

q21 = $(K_{\text{CaSO}_4}, K_{\text{sp,CaSO}_4})$

g_{22}^n = $(D_{\text{SO}_4^{2-}} \Delta C_{\text{SO}_4^{2-}} + D_{\text{HSO}_4^-} \Delta C_{\text{HSO}_4^-}) K_{\text{CaSO}_4} / \text{R}_{\text{SO}_3\text{SO}_4}$

= 0 if $\text{RSCaSO}_3^n > 1$

where:

ΔC_j = $C_{j,s1}^n - C_{j,b}^n$

j = $\text{SO}_4^{2-}, \text{HSO}_4^-$

q22 = $(D_{\text{SO}_4^{2-}}, D_{\text{HSO}_4^-}, K_{\text{CaSO}_4})$

g_{23}^n = $(\text{RSCaSO}_3 \cdot 1/2\text{H}_2\text{O} (\text{S}(1)^n - \text{S}(1)^{n-1}) / \text{S}(2)^n)$

$$= 0 \text{ if } R_{\text{CaSO}_3}^n \leq 1$$

where:

$$q_{23} = (K_{\text{sp}}, \text{CaSO}_3)$$

The concentration of solid gypsum (in the slurry) can be determined on the basis of the amount dissolved at a particular stage ($g_{21}^n \tau_s$).

$$S(4)^n = S(4)^{n-1} (1 + g_{21}^n \tau_s)$$

A-2.3 Calculation of $F(3)^n$ and $G(3)^n$

$$F(3)^n = f_{31} (C_{\text{CO}_3^{=},b}^n, C_{\text{HCO}_3^-,b}^n, C_{\text{CO}_2,b}^n, C_{\text{CO}_3^{=},i}^n, C_{\text{HCO}_3^-,i}^n, C_{\text{CO}_2,i}^n, \mathbf{p31})$$

f_{31}^n = Change in solution composition due to absorption of carbon dioxide at the n^{th} stage

$$= f_{31} (C_{\text{CO}_3^{=},b}^n, C_{\text{HCO}_3^-,b}^n, C_{\text{CO}_2,b}^n, C_{\text{CO}_3^{=},i}^n, C_{\text{HCO}_3^-,i}^n, C_{\text{CO}_2,i}^n, \mathbf{p31})$$

$$= \frac{G}{L} \frac{k_l}{k_g} \frac{1}{\sqrt{D_{\text{SO}_2}}} \int_{N_g^{n-1}}^{N_g^n} \sum_j \sqrt{D_j} \Delta C_j dN_g$$

$$= \frac{G}{L} (P_{\text{CO}_2}^n - P_{\text{CO}_2}^{n-1})$$

where:

$$\mathbf{p31} = (G/L, k_l/k_g, N_g^n, N_g^{n-1}, D_j, D_{\text{SO}_2})$$

$$\Delta C_j^n = C_{j,i}^n - C_{j,b}^n$$

$C_{j,i}^n$ = Concentration of j^{th} species at the gas liquid interface, at a location Z on the n^{th} stage ($Z^{n-1} \leq Z \leq Z^n, N_g^{n-1} \leq N_g \leq N_g^n$)

$C_{j,b}^n$ = Concentration of the j^{th} species in the bulk liquid at the n^{th} stage

j = $\text{CO}_3^{2-}, \text{HCO}_3^-, \text{CO}_2$

$C_{j,i}^n$ = $C_{j,i}(\mathbf{X}^n, \mathbf{P}^{n-1}, N_g, \mathbf{r}_1)$, where $N_g^{n-1} \leq N_g \leq N_g^n$

$C_{j,b}^n$ = $C_{j,b}(\mathbf{X}^n, \mathbf{r}_2)$

$G(3)^n$ = $g_{31}(C_{\text{Ca}^{++},s2}^n, C_{\text{Ca}^{++},b}^n, \mathbf{q31}) \tau_s S(3)^n$

g_{31}^n = $g_{31}(C_{\text{Ca}^{++},s2}^n, C_{\text{Ca}^{++},b}^n, \mathbf{q31})$

= Rate of change in solution composition due to the dissolution of limestone at the n^{th} stage

= $K_{\text{CaCO}_3,d} D_{\text{Ca}^{++}} \Delta C_{\text{Ca}^{++}}$

where:

$\mathbf{q31}$ = $(K_{\text{CaCO}_3,d}, D_{\text{Ca}^{++}})$

$\Delta C_{\text{Ca}^{++}}$ = $C_{\text{Ca}^{++},s2}^n - C_{\text{Ca}^{++},b}^n$

$C_{\text{Ca}^{++},s2}^n$ = Concentration of Ca^{++} , at the n^{th} stage, at the limestone surface

$C_{\text{Ca}^{++},b}^n$ = Concentration of Ca^{++} , at the n^{th} stage, in the bulk solution

$C_{\text{Ca}^{++},s2}^n$ = $C_{\text{Ca}^{++},s2}^n(\mathbf{X}^n, \mathbf{r}_4)$

$C_{\text{Ca}^{++},b}^n$ = $C_{\text{Ca}^{++},b}^n(\mathbf{X}^n, \mathbf{r}_2)$

The concentration of solid calcium carbonate at a stage can be determined using g_{31}^n as follows.

$$S(3)^n = \frac{S(3)^{n-1}}{1 + g_{31}^n \tau_s}$$

A-2.4 Calculation of $F(4)^n$ and $G(4)^n$

$F(4)^n$ = Change of solution composition, in terms of $X(4)^n$, due to the absorption/desorption of gases

$$= 0$$

$G(4)^n$ = Change of solution composition, in terms of $X(4)^n$, due to the dissolution/crystallization of solids

$$= G(1)^n + G(2)^n + G(3)^n$$

A-3 HOLD TANK CALCULATIONS

The material balance equations for the hold tank or $(k+1)^{\text{th}}$ stage can be stated as shown below.

For each species ($i=1, 2, 3, 4$)

$$X(i)^{k+1} = X(i)^k + H(i)^{k+1} + G(i)^{k+1}$$

where:

$X(1)^{k+1}$ = Total concentration of sulfite species in the liquid solution at the $(k+1)^{\text{th}}$ stage (gmol/L)

$X(2)^{k+1}$ = Total concentration of sulfate species in the liquid solution at the $(k+1)^{\text{th}}$ stage (gmol/L)

$X(3)^{k+1}$ = Total concentration of carbonate species in the liquid solution at the $(k+1)^{\text{th}}$ stage (gmol/L)

$X(4)^{k+1}$ = Total concentration of calcium species in the liquid solution at the $(k+1)^{\text{th}}$ stage (gmol/L)

$X(1)^k, \dots, X(4)^k$ are defined similarly for the k^{th} stage

$H(i)^{k+1}$ = Change in the solution composition in terms of $X(i)^{k+1}$ due to the absorption/desorption of gases at the $(k+1)^{\text{th}}$ stage

$G(i)^{k+1}$ = Change in the solution composition in terms of $X(i)^{k+1}$ due to the dissolution/crystallization of solids at the $(k+1)^{\text{th}}$ stage

In this section, the equations for the calculation of gas/ liquid absorption ($H(i)^{k+1}$) are shown. The solution equilibria (shown in section A-4.1 and A-4.3) are the same in the hold tank and the scrubber. Details of the calculations to determine the dissolution/ precipitation of solids ($G(i)^{k+1}$) are not shown as they are analogous to those in the scrubber.

A-3.1 Calculation of $H(1)^{k+1}$ and $G(1)^{k+1}$

$$H(1)^{k+1} = h_{11}(C_{O_2,b}^{k+1}, s_{11})$$

$$h_{11}^{k+1} = h_{11}(C_{O_2,b}^{k+1}, s_{11})$$

= Change in solution composition due to the absorption of oxygen at the $(k+1)^{\text{th}}$ stage

$$s_{11} = \text{Vector of parameters}$$

$$h_{11}^{k+1} = -2 G_2/L_2(P_{O_2}^{k+2} - P_{O_2}^{k+1})$$

where:

$$P_{O_2}^{k+2} = \frac{(P_{O_2}^{k+1} - C_{O_2,b}^{k+1} H_{O_2})}{\exp(-\frac{N_L L_2}{G_2 H_{O_2}})} + C_{O_2,b}^{k+1} H_{O_2}$$

Boundary condition:

$$C_{O_2,b}^{k+1} = \frac{P_{O_2}^{k+2}/H_{O_2}}{1 + k_{O_2} C_{SO_3^{2-},b}^{k+1}}$$

$$s_{11} = (k_{O_2}, N_L, L_2, G_2, H_{O_2}, P_{O_2}^{k+1})$$

$$\begin{aligned} k_{O_2} &= \text{Rate constant for sulfite oxidation} \\ &= 10^4 \text{ (L/gmol)} \end{aligned}$$

$$L_2 = \text{Liquid flow rate to the hold tank}$$

$$G_2 = \text{Gas flow rate to the hold tank}$$

$$H_{O_2} = \text{Henry's Law constant for oxygen}$$

$$N_L = \text{Number of liquid phase mass-transfer units in the hold tank}$$

$$\begin{aligned} P_{O_2}^{k+1} &= \text{Partial pressure of oxygen at the inlet to the hold tank} \\ &= \text{Partial pressure of oxygen in the ambient air} \end{aligned}$$

$$G(1)^{k+1} = g_{11}^{k+1} \tau_{ht} S(1)^{k+1} + g_{12}^{k+1} \tau_{ht} S(1)^{k+1}$$

where:

$$\tau_{ht} = \text{Slurry residence time in the hold tank (s)}$$

A-3.2 Calculation of $H(2)^{k+1}$ and $G(2)^{k+1}$

$$H(2)^{k+1} = -h_{11}(X^{k+1}, s_{11})$$

$$h_{11}^{k+1} = -h_{11}(X^{k+1}, s_{11})$$

$$\begin{aligned}
&= \text{Change in solution composition due to absorption of oxygen at the } (k+1)^{\text{th}} \text{ stage} \\
G(2)^{k+1} &= \text{Change of solution composition, in terms of } X(2)^{k+1}, \text{ due to the dissolution/crystallization of solids at the } (k+1)^{\text{th}} \text{ stage} \\
&= g_{21}^{k+1} \tau_{\text{ht}} S(4)^k + g_{22}^{k+1} \tau_{\text{ht}} S(2)^{k+1} + g_{23}^{k+1} \tau_{\text{ht}} S(2)^k
\end{aligned}$$

A-3.3 Calculation of $H(3)^{k+1}$ and $G(3)^{k+1}$

$$\begin{aligned}
H(3)^{k+1} &= \text{Change of solution composition, in terms of } X(3)^{k+1}, \text{ due to the absorption/desorption of gases at the } (k+1)^{\text{th}} \text{ stage} \\
&= h_{31}(C_{\text{CO}_2, \text{b}}^{k+1}, s_{31}) \\
h_{31}^{k+1} &= h_{31}(C_{\text{CO}_2, \text{b}}^{k+1}, s_{31}) \\
&= \text{Change in solution composition due to the absorption/desorption of carbon dioxide at the } (k+1)^{\text{th}} \text{ stage} \\
&= \frac{G_2/L_2 (P_{\text{CO}_2}^{k+2} - P_{\text{CO}_2}^{k+1})}{\exp(N_L L_2 / (G_2 H_{\text{CO}_2}))} + H_{\text{CO}_2} C_{\text{CO}_2, \text{b}}^{k+1} \\
P_{\text{CO}_2}^{k+2} &= \frac{P_{\text{CO}_2}^{k+1} - H_{\text{CO}_2} C_{\text{CO}_2, \text{b}}^{k+1}}{\exp(N_L L_2 / (G_2 H_{\text{CO}_2}))} + H_{\text{CO}_2} C_{\text{CO}_2, \text{b}}^{k+1}
\end{aligned}$$

where:

$$\begin{aligned}
s_{31} &= (P_{\text{CO}_2}^{k+1}, H_{\text{CO}_2}, N_L, L_2/G_2) \\
P_{\text{CO}_2}^{k+1} &= \text{Partial pressure of } \text{CO}_2 \text{ at the exit from the hold tank} \\
P_{\text{CO}_2}^{k+1} &= \text{Partial pressure of } \text{CO}_2 \text{ at the inlet to the hold tank} \\
&= \text{Partial pressure of } \text{CO}_2 \text{ in the ambient air} \\
H_{\text{CO}_2} &= \text{Henry's Law constant for carbon dioxide}
\end{aligned}$$

$C_{CO_2,b}^{k+1}$ = Concentration of undissociated carbon dioxide, in the bulk solution, in the $(k+1)^{th}$ stage

$G(3)^{k+1}$ = Change in solution composition, in terms of $X(3)^{k+1}$, due to the dissolution of limestone ($CaCO_3$)
 $= g_{31}^{k+1} \tau_{ht} S(3)^{k+1}$

A-3.4 Calculation of $H(4)^{k+1}$ and $G(4)^{k+1}$

$H(4)^{k+1}$ = Change of solution composition, in terms of $X(4)^{k+1}$, due to the absorption/desorption of gases
 $= 0$

$G(4)^{k+1}$ = Change of solution composition, in terms of $X(4)^{k+1}$, due to the dissolution/crystallization of solids
 $= G(1)^{k+1} + G(2)^{k+1} + G(3)^{k+1}$

A-4 CALCULATION OF COMPOSITION IN THE BULK SOLUTION, AT THE GAS/LIQUID INTERFACE AND AT THE SOLID SURFACE

The solution composition in the bulk liquid can be calculated once \mathbf{X}^n is specified. The composition of the liquid solution at the gas/liquid interface is dependent upon the bulk solution composition and the position ($Z^{n'} \leq Z \leq Z^n$) of the point on the stage, i.e., it is completely determined once \mathbf{X}^n , \mathbf{P}^{n-1} and N_g are

specified. The concentrations at the surface of the solids are completely specified once X^n is known.

A-4.1 Bulk Solution Composition ($C_{j,b}^n = C_{j,b}(X^n, r_2)$)

To determine bulk concentration of all species, hydrogen ion concentration ($C_{H^+,b}^n$) is iterated upon until the boundary condition of charge neutrality is satisfied in the bulk liquid. The concentrations shown below have not been expressed explicitly as functions of X^n . However, it is possible to convert each of them into non-linear functions of X^n by substituting the equilibria into the charge neutrality condition.

$$C_{CO_2,b}^n = \frac{X(3)^n}{1 + K_{H_2CO_3}/C_{H^+,b}^n + K_{HCO_3^-} K_{H_2CO_3}/(C_{H^+,b}^n)^2}$$

$$C_{SO_2,b}^n = \frac{X(1)^n}{1 + K_{SO_2}/C_{H^+,b}^n + K_{HSO_3^-} K_{SO_2}/(C_{H^+,b}^n)^2}$$

$$C_{SO_4^{=},b}^n = \frac{X(2)^n}{1 + C_{H^+,b}^n/K_{HSO_4^-}}$$

$$C_{Ca^{++},b}^n = X(4)^n$$

$$C_{HCO_3^-,b}^n = \frac{K_{H_2CO_3} C_{CO_2,b}^n}{C_{H^+,b}^n}$$

$$C_{OH^-,b}^n = \frac{K_{H_2O}}{C_{H^+,b}^n}$$

$$C_{HSO_3^-,b}^n = \frac{C_{SO_2,b}^n K_{SO_2}}{C_{H^+,b}^n}$$

$$C_{SO_3^{=},b}^n = \frac{C_{HSO_3^-,b}^n K_{HSO_3^-}}{C_{H^+,b}^n}$$

$$C_{CO_3^{=},b}^n = \frac{C_{HCO_3^-,b}^n K_{HCO_3^-}}{C_{H^+,b}^n}$$

$$\begin{aligned}
C_{\text{HSO}_4^-,b^n} &= \frac{C_{\text{SO}_4^{=},b^n} C_{\text{H}^+,b^n}}{K_{\text{HSO}_4^-}} \\
C_{\text{H}_2\text{A},b^n} &= \frac{C_{\text{H}_2\text{A},b^{n-1}} + C_{\text{HA}^-,b^{n-1}} + C_{\text{A}^=,b^{n-1}}}{1 + K_{\text{H}_2\text{A}}/C_{\text{H}^+,b^n} + K_{\text{H}_2\text{A}} K_{\text{HA}^-}/(C_{\text{H}^+,b^n})^2} \\
C_{\text{HA}^-,b^n} &= \frac{C_{\text{H}_2\text{A},b^n} K_{\text{H}_2\text{A}}}{C_{\text{H}^+,b^n}} \\
C_{\text{A}^=,b^n} &= \frac{C_{\text{HA}^-,b^n} K_{\text{HA}^-}}{C_{\text{H}^+,b^n}} \\
C_{\text{Mg}^{++},b^n} &= C_{\text{Mg}^{++},b^{n-1}} \\
C_{\text{Na}^+,b^n} &= C_{\text{Na}^+,b^{n-1}} \\
C_{\text{Cl}^-,b^n} &= C_{\text{Cl}^-,b^{n-1}} \\
C_{\text{O}_2,b^n} &= 0 \\
\text{Charge Neutrality} \\
\sum_j Q_j C_{j,b^n} &= 0 \\
j &= \text{H}^+, \text{Ca}^{++}, \text{Mg}^{++}, \text{Na}^+, \text{SO}_3^=, \text{CO}_3^=, \text{A}^=, \text{HA}^-, \\
&\quad \text{HSO}_3^-, \text{HSO}_4^-, \text{OH}^-, \text{HCO}_3^-, \text{and Cl}^- \\
Q_j &= \text{Charge of the } j^{\text{th}} \text{ species} \\
r_2 &= (K_{\text{H}_2\text{CO}_3}, K_{\text{HCO}_3^-}, K_{\text{SO}_2}, K_{\text{HSO}_3^-}, K_{\text{HSO}_4^-}, K_{\text{H}_2\text{A}}, \\
&\quad K_{\text{HA}^-})
\end{aligned}$$

A-4.2 Calculation of Concentrations at the gas/liquid interface

$$(C_{j,i}^n = C_{j,i}(\mathbf{X}^n, \mathbf{P}^{n-1}, N_g, \mathbf{r}_1))$$

The concentrations at the gas/liquid interface are dependent on the bulk liquid composition (\mathbf{X}^n) as well as the vertical position of a point on the stage. The

calculations shown here are suitable for determination of the interfacial concentrations at the bottom of the n^{th} stage, i.e., $N_g = N_g^n$.

The solution composition at the gas/liquid interface is determined by iteration on the hydrogen ion concentration at the interface to satisfy the boundary condition of zero charge flux.

$$C_{HA^-,i}^n = \frac{\sqrt{D_{H_2A}} C_{H_2A,b}^n + \sqrt{D_{HA^-}} C_{HA^-,b}^n + \sqrt{D_{A^-}} C_{A^-,b}^n}{\sqrt{D_{H_2A}} C_{H^+,i}^n / K_{H_2A} + \sqrt{D_{HA^-}} + \sqrt{D_{A^-}} K_{HA^-} / C_{H^+,i}^n}$$

$$C_{HSO_3^-,i}^n = \frac{\sqrt{D_{HSO_3^-}} C_{HSO_3^-,b}^n + \sqrt{D_{SO_3^{2-}}} C_{SO_3^{2-},b}^n + \sqrt{D_{SO_2}} C_{SO_2,b}^n}{\sqrt{D_{HSO_3^-}} + \sqrt{D_{SO_3^{2-}}} K_{HSO_3^-} / C_{H^+,i}^n + \sqrt{D_{SO_2}} \left(1 + H_{SO_2} / \left(\frac{k^o_l}{k_g} \right) \right) \frac{C_{H^+,i}^n}{K_{H_2SO_3}}}$$

$$C_{HSO_4^-,i}^n = \frac{\sqrt{D_{SO_2}} P_{O_2}^n / H_{O_2} + \sqrt{D_{HSO_4^-}} C_{HSO_4^-,b}^n + \sqrt{D_{SO_4^{2-}}} C_{SO_4^{2-},b}^n}{\sqrt{D_{HSO_4^-}} + \sqrt{D_{SO_4^{2-}}} K_{HSO_4^-} / C_{H^+,i}^n}$$

$$\begin{aligned} C_{CO_2,i}^n &= \frac{P_{CO_2}^n}{H_{CO_2}} \\ C_{OH,i}^n &= \frac{K_{H_2O}}{C_{H^+,i}^n} \\ C_{HCO_3^-,i}^n &= \frac{K_{H_2CO_3} C_{CO_2,i}^n}{C_{H^+,i}^n} \\ C_{CO_3^{2-},i}^n &= \frac{K_{HCO_3^-} C_{HCO_3^-,i}^n}{C_{H^+,i}^n} \\ C_{SO_3^{2-},i}^n &= \frac{K_{HSO_3^-} C_{HSO_3^-,i}^n}{C_{H^+,i}^n} \\ C_{SO_4^{2-},i}^n &= \frac{K_{HSO_4^-} C_{HSO_4^-,i}^n}{C_{H^+,i}^n} \\ C_{H_2A^-,i}^n &= \frac{C_{H^+,i}^n C_{HA^-,i}^n}{K_{H_2A}} \\ C_{A^-,i}^n &= \frac{K_{HA^-} C_{HA^-,i}^n}{C_{H^+,i}^n} \end{aligned}$$

$$C_{O_2,i}^n = \frac{P_{O_2}^n}{H_{CO_2}}$$

$$\text{if } \frac{P_{O_2}^n}{H_{CO_2}} > \frac{\sqrt{D_{HSO_3^-}}}{\sqrt{D_{SO_2}}} C_{HSO_3^-,b}^n + \frac{\sqrt{D_{SO_3^{=}}}}{\sqrt{D_{SO_2}}} C_{SO_3^{=},b}^n + \frac{P_{SO_2}^n}{2} \frac{k_g}{k_l} + C_{SO_2,b}^n$$

then

$$C_{O_2,i}^n = \frac{\sqrt{D_{HSO_3^-}}}{\sqrt{D_{SO_2}}} C_{HSO_3^-,b}^n + \frac{\sqrt{D_{SO_3^{=}}}}{\sqrt{D_{SO_2}}} C_{SO_3^{=},b}^n + \frac{P_{SO_2}^n}{2} \frac{k_g}{k_l} + C_{SO_2,b}^n$$

Boundary Condition

$$\sum_j Q_j D_j \Delta C_j^n = 0$$

where:

$$\Delta C_j^n = C_{j,i}^n - C_{j,b}^n$$

$$Q_j = \text{Numeric value of charge on the } j^{\text{th}} \text{ ionic species}$$

$$j = H^+, OH^-, HCO_3^-, CO_3^{=}, HSO_3^-, SO_3^{=}, HSO_4^-, SO_4^{=}, HA^-, \text{ and } A^=$$

$$\mathbf{r_1} = (K_{H_2CO_3}, K_{HCO_3^-}, K_{SO_2}, K_{HSO_3^-}, K_{HSO_4^-}, K_{H_2A}, K_{HA^-}, D_{HA^-}, D_{H_2A}, D_{A^=}, D_{SO_3^{=}}, D_{HSO_3^-}, D_{SO_2}, D_{HSO_4^-})$$

A-4.3 Calculation of the Compositions at the Surface of Limestone

($C_{j,s2}^n = C_{j,s2}(X^n, r_4)$) and Calcium Sulfite ($C_{j,s1}^n = C_{j,s1}(X^n, r_3)$)

Composition at the limestone surface is calculated by iteration on the surface concentration of hydrogen ($CH^+,s2^n$) to match the boundary condition at the limestone surface.

$$\begin{aligned}
 C_{SO_3^=,s2^n} &= \frac{DSO_3^= C_{SO_3^=,b^n} + D_{HSO_3^-} C_{HSO_3^-,b^n}}{DSO_3^= + D_{HSO_3^-} CH^+,s2^n / K_{HSO_3^-}} \\
 C_{A^=,s2^n} &= \frac{DH_2A C_{H_2A,b^n} + D_{HA^-} C_{HA^-,b^n} + D_{A^=} C_{A^=,b^n}}{DH_2A (CH^+,s2^n)^2 / K_{H_2A} K_{HA^-} + D_{HA^-} \frac{CH^+,s2^n}{K_{HA^-}} + D_{A^=}} \\
 C_{SO_4^=,s2^n} &= \frac{DSO_4^= C_{SO_4^=,b^n} + D_{HSO_4^-} C_{HSO_4^-,b^n}}{DSO_4^= + D_{HSO_4^-} CH^+,s2^n / K_{HSO_4^-}} \\
 C_{OH^-,s2^n} &= \frac{K_{H_2O}}{CH^+,s2^n} \\
 C_{HA^-,s2^n} &= \frac{CH^+,s2^n C_{A^=,s2^n}}{K_{HA^-}} \\
 C_{HSO_3^-,s2^n} &= \frac{CH^+,s2^n C_{SO_3^=,s2^n}}{K_{HSO_3^-}} \\
 C_{HSO_4^-,s2^n} &= \frac{CH^+,s2^n C_{SO_4^=,s2^n}}{K_{HSO_4^-}} \\
 C_{H_2A,s2^n} &= \frac{CH^+,s2^n C_{HA^-,s2^n}}{K_{H_2A}}
 \end{aligned}$$

The surface concentration of bicarbonate species and calcium are calculated as follows:

$$\begin{aligned}
 D_{HCO_3^-} C_{HCO_3^-,s2^n} &= D_{H^+} (CH^+,b^n - CH^+,s2^n) + D_{SO_3^=} (C_{SO_3^=,s2^n} - C_{SO_3^=,b^n}) + 2D_{A^=} (C_{A^=,s2^n} - C_{A^=,b^n}) + D_{SO_4^=} (C_{SO_4^=,s2^n} - 2C_{SO_4^=,b^n}) + D_{HA^-} (C_{HA^-,s2^n} - C_{HA^-,b^n}) + D_{OH^-} (C_{OH^-,s2^n} - C_{OH^-,b^n}) - D_{HSO_4^-} C_{HSO_4^-,b^n} - D_{HCO_3^-} C_{HCO_3^-,b^n} \\
 D_{Ca^{++}} C_{Ca^{++},s2^n} &= D_{HCO_3^-} (C_{HCO_3^-,s2^n} - C_{HCO_3^-,b^n}) + D_{CO_3^=} (C_{CO_3^=,s2^n} - C_{CO_3^=,b^n}) - D_{Ca^{++}} C_{Ca^{++},b^n}
 \end{aligned}$$

$$C_{\text{CO}_3^{=},s_2^n} = \frac{K_{\text{HCO}_3^-} C_{\text{HCO}_3^-,s_2^n}}{C_{\text{H}^+,s_2^n}}$$

The boundary conditions at the limestone surface are dependent upon the concentration of dissolved sulfite at the gas/liquid interface:

1) In the absence of dissolved sulfite ($\text{RSCaSO}_3 \leq 0.005$),

$$K_{\text{sp, CaCO}_3} = C_{\text{Ca}^{++},s_2^n} C_{\text{CO}_3^{=},s_2^n}$$

2) In the presence of dissolved sulfite,

$$\frac{D_{\text{Ca}^{++}} \Delta C_{\text{Ca}^{++}}}{\delta} = \frac{k_c (C_{\text{CaCO}_3, \text{eq}}^n - C_{\text{CaCO}_3, s_2^n})^{0.5}}{C_{\text{CaCO}_3, s_2^n} C_{\text{CaSO}_3, s_2^n}}$$

where:

$$C_{\text{CaCO}_3, s_2^n} = C_{\text{Ca}^{++}, s_2^n} C_{\text{CO}_3^{=}, s_2^n}$$

$$C_{\text{CaSO}_3, s_2^n} = C_{\text{Ca}^{++}, s_2^n} C_{\text{SO}_3^{=}, s_2^n}$$

$$C_{\text{CaCO}_3, \text{eq}}^n = K_{\text{sp, CaCO}_3}$$

$$\delta = \text{Average liquid film thickness around the limestone particle (see section A-5.3)}$$

$$\Delta C_{\text{Ca}^{++}} = C_{\text{Ca}^{++}, s_2^n} - C_{\text{Ca}^{++}, b^n}$$

$$k_c = \text{Surface rate constant for the dissolution of limestone}$$

$$\begin{aligned} \mathbf{r_4} = & D_{\text{SO}_3^{=}}, D_{\text{HSO}_3^-}, D_{\text{H}_2\text{A}}, D_{\text{HA}^-}, D_{\text{A}^{=}}, D_{\text{SO}_4^{=}}, D_{\text{HSO}_4^-}, \\ & D_{\text{H}^+}, D_{\text{OH}^-}, D_{\text{HSO}_4^-}, D_{\text{HCO}_3^-}, D_{\text{Ca}^{++}}, D_{\text{CO}_3^{=}}, K_{\text{H}_2\text{A}}, \\ & K_{\text{HA}^-}, K_{\text{HSO}_3^-}, K_{\text{HSO}_4^-}, K_{\text{H}_2\text{O}}, K_{\text{HCO}_3^-}, \delta, k_c, \\ & K_{\text{sp, CaCO}_3} \end{aligned}$$

Surface Concentrations for the Calcium Sulfite and Calcium Sulfate Hemihydrate

The calculation procedure involves iteration on the surface concentration of hydrogen, until the boundary condition is satisfied.

$$\begin{aligned}
 C_{OH^-,s1}^n &= \frac{K_{H_2O}}{C_{H^+,s1}^n} \\
 C_{CO_3^{2-},s1}^n &= \frac{D_{CO_3^{2-}} C_{CO_3^{2-},b}^n + D_{HCO_3^-} C_{HCO_3^-,b}^n}{D_{CO_3^{2-}} + D_{HCO_3^-} C_{H^+,s1}^n / K_{HCO_3^-}} \\
 C_{A^-,s1}^n &= \frac{D_{H_2A} C_{H_2A,b}^n + D_{HA^-} C_{HA^-,b}^n + D_{A^-} C_{A^-,b}^n}{D_{A^-} + C_{H^+,s1}^n \frac{D_{HA^-}}{K_{A^-}} + D_{H_2A} \frac{(C_{H^+,s1}^n)^2}{(K_{A^-} K_{HA^-})}} \\
 C_{HA^-,s1}^n &= \frac{C_{A^-,s1}^n C_{H^+,s1}^n}{K_{HA^-}} \\
 C_{HCO_3^-,s1}^n &= \frac{C_{H^+,s1}^n C_{CO_3^{2-},s1}^n}{K_{HCO_3^-}} \\
 C_{H_2A,s1}^n &= \frac{C_{H^+,s1}^n C_{HA^-,s1}^n}{K_{HA^-}}
 \end{aligned}$$

The formation of calcium sulfite hemihydrate and calcium sulfate hemihydrate occurs as a single solid solution. The calculations take this effect into account in determination of the surface concentrations of the sulfite, sulfate, and calcium ions. For the sake of convenience the following ratios can be defined.

$$R_{SO_3SO_4}^n = \text{Ratio of calcium sulfate hemihydrate to calcium sulfite hemihydrate in the solid phase}$$

$$\begin{aligned}
 &= \frac{S(2)^{n-1}}{S(1)^{n-1}} \\
 R_{SO_3,s1}^n &= \frac{D_{SO_3^{2-}} C_{SO_3^{2-},s1}^n + D_{HSO_3^-} C_{HSO_3^-,s1}^n}{D_{HSO_3^-} C_{HSO_3^-,s1}^n} \\
 &= 1 + \frac{D_{SO_3^{2-}} K_{HSO_3^-}}{C_{H^+,s1} D_{HSO_3^-}}
 \end{aligned}$$

so that

$$R1^n = \frac{1}{R_{SO_3,s1}^n} (D_{SO_3^{2-}} C_{SO_3^{2-},b}^n + D_{HSO_3^-} C_{HSO_3^-,b}^n)$$

$$= \frac{D_{SO_3^=C_{SO_3^=,b^n}} + D_{HSO_3^-} C_{HSO_3^-,b^n}}{D_{SO_3^=C_{SO_3^=,s1^n}} + D_{HSO_3^-} C_{HSO_3^-,s1^n}} D_{HSO_3^-} C_{HSO_3^-,s1^n}$$

$$\begin{aligned} R_{SO_4,s1^n} &= \frac{D_{SO_4^=C_{SO_4^=,s1^n}} + D_{HSO_4^-} C_{HSO_4^-,s1^n}}{D_{HSO_4^-} C_{HSO_4^-,s1^n}} \\ &= 1 + \frac{D_{SO_4^=} K_{HSO_4^-}}{C_{H^+,s1} D_{HSO_4^-}} \end{aligned}$$

Similarly

$$\begin{aligned} R_{2^n} &= \frac{1}{R_{SO_3,s1}} (D_{SO_4^=C_{SO_4^=,b^n}} + D_{HSO_4^-} C_{HSO_4^-,b^n}) \\ &= \frac{D_{SO_4^=C_{SO_4^=,b^n}} + D_{HSO_4^-} C_{HSO_4^-,b^n}}{D_{SO_4^=C_{SO_4^=,s1^n}} + D_{HSO_4^-} C_{HSO_4^-,s1^n}} D_{HSO_4^-} C_{HSO_4^-,s1^n} \end{aligned}$$

$$\begin{aligned} &D_{OH^-} (C_{OH^-,s1^n} - C_{OH^-,b^n}) - D_{H^+} (C_{H^+,s1^n} - C_{H^+,b^n}) + \\ &2 D_A = (C_{A^=,s1^n} - C_{A^=,b^n}) + 2 D_{CO_3^=} (C_{CO_3^=,s1^n} - C_{CO_3^=,b^n}) + D_{HA^-} (C_{HA^-,s1^n} - C_{HA^-,b^n}) + D_{HCO_3^-} (C_{HCO_3^-,s1^n} - C_{HCO_3^-,b^n}) - \\ &(R_1 - D_{HSO_3^-} C_{HSO_3^-,b^n}) - (R_2 - D_{SO_4^=C_{HSO_4^-,b^n}} - D_{HSO_4^-} C_{HSO_4^-,b^n}) \end{aligned}$$

$$\sum_j D_j \Delta C_j^n = \frac{2 R_{SO_3SO_4} / R_{SO_4} + 1 / R_{SO_3}}$$

$$j = SO_3^=, HSO_3^-$$

$$\Delta C_j^n = C_{j,s2^n} - C_{j,b^n}$$

$$C_{SO_3^=,s1^n} = \frac{\sum_j D_j \Delta C_j^n R_{SO_3SO_4} + D_{HSO_3^-} C_{HSO_3^-,b^n} + D_{SO_3^=C_{SO_3^=,b^n}}}{(D_{HSO_3^-} + C_{H^+,s1^n} / K_{HSO_3^-})}$$

$$\sum_k D_k \Delta C_k^n = R_{SO_3SO_4} \sum_j D_j \Delta C_j^n$$

$$j = SO_3^=, HSO_3^-, k = SO_4^=, HSO_4^-$$

$$\Delta C_j^n = C_{j,s2^n} - C_{j,b^n}$$

$$C_{SO_4^{=},s1^n} = \frac{\sum_k D_k \Delta C_k^n + D_{HSO_4^-} C_{HSO_3^-,b^n} + D_{SO_4^{=}} C_{SO_3^{=},b^n}}{(D_{HSO_4^-} + C_{H^+,s1^n} / K_{HSO_4^-})}$$

$$C_{HSO_3^-,s1^n} = \frac{C_{H^+,s1^n} C_{SO_3^{=},s1^n}}{K_{HSO_3^-}}$$

$$C_{HSO_4^-,s1^n} = \frac{C_{H^+,s1^n} C_{SO_4^{=},s1^n}}{K_{HSO_4^-}}$$

$$C_{Ca^{++},s1^n} = \frac{\sum_j D_j \Delta C_j^n (1 + R_{SO_3SO_4})}{D_{Ca^{++}}} + C_{Ca^{++},b^n}$$

Boundary Condition:

$$K_{sp,CaSO_3} = C_{Ca^{++},s1^n} C_{SO_3^{=},s1^n}$$

$$r_3 = K_{H_2O}, K_{HSO_4^-}, K_{HSO_3^-}, K_{HCO_3^-}, K_A^=, K_{HA^-}, D_{H_2A}, \\ D_{CO_3^{=}}, D_{HCO_3^-}, D_A^=, D_{HA^-}, D_{SO_3^{=}}, D_{HSO_3^-}, D_{SO_4^{=}}, \\ D_{HSO_4^-}, D_{OH^-}, D_{H^+}, S(2)^{n-1}, S(1)^{n-1}, K_{sp,CaSO_3}$$

A-5 INITIAL CALCULATIONS

Before the stagewise material balance calculation are begun, the calculation of the following is necessary:

Pseudo-equilibrium concentrations, diffusivities, and equilibrium constants

Composition of liquid and solid at the top stage

Limestone dissolution constant and average film thickness around limestone particle

Besides \mathbf{X}^0 , none of the above mentioned variables are updated during subsequent calculations for stagewise mass balances.

A-5.1 Pseudo-Equilibrium Calculations

The Bechtel-Modified Radian Equilibrium Program (BMREP) contains a database of constants for the calculation of concentrations, diffusion coefficients, activity coefficients, and temperature dependent equilibrium constants for forty-one 'true' species. The reader is referred to Lowell et al. (1970) for a comprehensive discussion of the procedure used for these calculations. This report (Lowell et al., 1970) also contains a list of values for the following:

- 1) Parameters used for the calculation of temperature dependent equilibrium constants for thirty equilibria.
- 2) The constants in the modified Debye-Huckel theory that determine the effect of temperature and ionic strength on activity coefficients for forty-one species.

The BMREP calculations are based on an initial guess of the inlet concentrations at the top stage of the scrubber. Subsequently, for all calculations, the number of species is reduced from forty-one to seventeen by defining a new set of 'pseudo-species'. The equations used to define pseudo-species are shown below. The concentrations on the right hand side of each equation represent 'true' species concentrations (as determined by BMREP), whereas concentrations on the left hand side denote pseudo-concentrations.

$$C_{Ca^{++},b}^0 = C_{Ca^{++},b}^0 + C_{CaOH^+,b}^0 + C_{CaHCO_3^+,b}^0 + C_{CaCO_3,b}^0 + C_{CaSO_3,b}^0 + C_{CaSO_4,b}^0 + C_{CaA,b}^0 + C_{CaNO_3^+,b}^0 + C_{CaHSO_3^-,b}^0$$

$$\begin{aligned}
C_{HCO_3^-,b}^0 &= C_{HCO_3^-,b}^0 + C_{CaHCO_3^+,b}^0 + C_{MgHCO_3^+,b}^0 + \\
&\quad C_{NaHCO_3,b}^0 \\
C_{CO_3^=,b}^0 &= C_{CO_3^=,b}^0 + C_{CaCO_3,b}^0 + C_{MgCO_3,b}^0 + C_{NaCO_3^-,b}^0 \\
C_{SO_3^=,b}^0 &= C_{SO_3^=,b}^0 + C_{CaSO_3,b}^0 + C_{MgSO_3,b}^0 \\
C_{SO_4^=,b}^0 &= C_{SO_4^=,b}^0 + C_{CaSO_4,b}^0 + C_{MgSO_4,b}^0 + C_{NaSO_4^-,b}^0 \\
C_{A^=,b}^0 &= C_{A^=,b}^0 + C_{CaA,b}^0 \\
C_{OH^-,b}^0 &= C_{OH^-,b}^0 + C_{CaOH^+,b}^0 + C_{MgOH^+,b}^0 + C_{NaOH,b}^0 \\
C_{H^+,b}^0 &= C_{H^+,b}^0 \\
C_{H_2A,b}^0 &= C_{H_2A,b}^0 \\
C_{HA^-,b}^0 &= C_{HA^-,b}^0 \\
C_{HSO_4^-,b}^0 &= C_{HSO_4^-,b}^0 \\
C_{Na^+,b}^0 &= C_{Na^+,b}^0 + C_{NaNO_3,b}^0 + C_{NaOH^+,b}^0 + C_{NaHCO_3,b}^0 + \\
&\quad C_{NaCO_3^-,b}^0 + C_{NaSO_4^-,b}^0 \\
C_{Mg^{++},b}^0 &= C_{Mg^{++},b}^0 + C_{MgOH^+,b}^0 + C_{MgHCO_3^+,b}^0 + \\
&\quad C_{MgCO_3,b}^0 + C_{MgSO_3,b}^0 + C_{MgSO_4,b}^0 \\
C_{SO_2,b}^0 &= C_{H_2SO_3,b,b}^0 \\
C_{CO_2,b}^0 &= C_{H_2CO_3,b}^0 \\
C_{HSO_3^-,b}^0 &= C_{HSO_3^-,b}^0 + C_{CaHSO_3^+,b}^0 + C_{MgHSO_3^+,b}^0 + \\
&\quad C_{NaHSO_3,b}^0 \\
C_{Cl^-,b}^0 &= C_{Cl^-,b}^0
\end{aligned}$$

Calculation of X^0

The mass balance equations, at each stage, are based on the total concentration of sulfite, sulfate, carbonate, and calcium present in the liquid phase.

The concentrations of these species are determined on the basis of the concentrations of pseudo-species as follows:

$$X(1)^0 = C_{SO_3^=,b}^0 + C_{HSO_3^-,b}^0 + C_{SO_2,b}^0$$

$$X(2)^0 = C_{SO_4^=,b}^0 + C_{HSO_4^-,b}^0$$

$$X(3)^0 = C_{CO_3^=,b}^0 + C_{HCO_3^-,b}^0 + C_{CO_2,b}^0$$

$$X(4)^0 = C_{Ca^{++},b}^0$$

Calculation of S^0

The composition of solids entering the first stage can be determined on the basis of the specified input values of limestone utilization (U), fractional oxidation (OX), and total solid loading (TS).

For systems of interest to this study the concentration of gypsum is known to be low, $S(4)^0 = 0.001$ gmol/L

$$S(1)^0 = \frac{TS - m_4 S(4)^0 - m_3 U S(4)^0}{m_1 + OX m_2 + U OX m_3 + U m_3}$$

$$S(2)^0 = S(1)^0 OX$$

$$S(3)^0 = U (S(1)^0 + S(2)^0 + S(4)^0)$$

$$\begin{aligned} m_1 &= \text{Molecular weight of calcium sulfite hemihydrate} \\ &= 129.15 \text{ g/gmol} \end{aligned}$$

$$\begin{aligned} m_2 &= \text{Molecular weight of calcium sulfate hemihydrate} \\ &= 145.15 \text{ g/gmol} \end{aligned}$$

$$\begin{aligned} m_3 &= \text{Molecular weight of calcium carbonate} \\ &= 100.09 \text{ g/gmol} \end{aligned}$$

$$\begin{aligned} m_4 &= \text{Molecular weight of gypsum} \\ &= 172.17 \text{ g/gmol} \end{aligned}$$

TS = total solids concentration (g of solids/L of solution)

U = Limestone utilization (dimensionless)

Pseudo-equilibrium constants

The pseudo-equilibrium constants are defined on the basis of concentrations of the pseudo-species as follows:

$$K_{\text{HCO}_3^-} = \frac{C_{\text{H}^+,b}^0 C_{\text{CO}_3^{2-},b}^0}{C_{\text{HCO}_3^-,b}^0}$$

$$K_{\text{HSO}_3^-} = \frac{C_{\text{H}^+,b}^0 C_{\text{SO}_3^{2-},b}^0}{C_{\text{HSO}_3^-,b}^0}$$

$$K_{\text{HSO}_4^-} = \frac{C_{\text{H}^+,b}^0 C_{\text{SO}_4^{2-},b}^0}{C_{\text{HSO}_4^-,b}^0}$$

$$K_{\text{H}_2\text{O}} = \frac{C_{\text{H}^+,b}^0 C_{\text{OH}^-,b}^0}{C_{\text{H}_2\text{O},b}^0}$$

$$K_{\text{HA}^-} = \frac{C_{\text{H}^+,b}^0 C_{\text{A}^-,b}^0}{C_{\text{HA},b}^0}$$

$$K_{\text{H}_2\text{A}} = \frac{C_{\text{H}^+,b}^0 C_{\text{HA}^-,b}^0}{C_{\text{H}_2\text{A},b}^0}$$

$$K_{\text{SO}_2} = \frac{C_{\text{H}^+,b}^0 C_{\text{HSO}_3^-,b}^0}{C_{\text{SO}_2,b}^0}$$

$$K_{\text{H}_2\text{CO}_3} = \frac{C_{\text{H}^+,b}^0 C_{\text{HCO}_3^-,b}^0}{C_{\text{CO}_2,b}^0}$$

Pseudo Solubility Product values are defined on the basis of pseudo concentrations, true concentrations, and true solubility product values (as determined by BMREP).

$$K_{\text{sp}, \text{CaCO}_3} = \frac{C_{\text{Ca}^{++},b}^0 C_{\text{CO}_3^{2-},b}^0}{C_{\text{Ca}^{++},b}^0 C_{\text{CO}_3^{2-},b}^0} K_{\text{sp}, \text{CaCO}_3}$$

$$K_{\text{sp}, \text{CaSO}_4} = \frac{C_{\text{Ca}^{++},b}^0 C_{\text{SO}_4^{2-},b}^0}{C_{\text{Ca}^{++},b}^0 C_{\text{SO}_4^{2-},b}^0} K_{\text{sp}, \text{CaSO}_4}$$

$$K_{\text{sp}, \text{CaSO}_3} = \frac{C_{\text{Ca}^{++},b}^0 C_{\text{SO}_3^{2-},b}^0}{C_{\text{Ca}^{++},b}^0 C_{\text{SO}_3^{2-},b}^0} K_{\text{sp}, \text{CaSO}_3}$$

In the above equations, $K_{\text{sp}, \text{CaCO}_3}$, $K_{\text{sp}, \text{CaSO}_4}$, and $K_{\text{sp}, \text{CaSO}_3}$ represent the pseudo-solubility product values for calcium carbonate, calcium sulfate, and

calcium sulfite respectively. The constants $K_{sp, CaCO_3}$, $K_{sp, CaSO_4}$, and $K_{sp, CaSO_3}$ represent the true values of the solubility products of calcium carbonate, calcium sulfate, and calcium sulfite as determined by BMREP.

The diffusivity values for the seventeen pseudo-species are defined on the basis of the diffusivity values and the concentrations of forty-one 'true' species.

Values of 'true' liquid phase diffusivities at 25°C have been compiled by Mehta and Rochelle (1982), Chan and Rochelle (1982) and Tseng and Rochelle (1986). These are listed in Table A-2.

Table A-2: Diffusivity Values at 25°C†.

Species (i)	$D_i \times 10^5$ (cm ² /s)	Species (i)	$D_i \times 10^5$ (cm ² /s)
H ⁺	9.31	Mg ⁺⁺	0.70
OH ⁻	5.24	MgOH ⁺	0.70
H ₂ CO ₃	2.0	MgHCO ₃ ⁺	0.72
HCO ₃ ⁻	1.18	MgHSO ₃ ⁺	0.73
CO ₃ ⁼	0.96	MgCO ₃	0.53
H ₂ SO ₃ ⁰	2.0	MgSO ₄	0.58
HSO ₃ ⁻	1.33	Na ⁺	1.35
SO ₃ ⁼	0.96	NaOH	1.35
HSO ₄ ⁻	1.33	NaHCO ₃	1.18
SO ₄ ⁼	1.06	NaCO ₃ ⁻	0.96
Ca ⁺⁺	0.79	NaSO ₄ ⁻	1.06
CaOH ⁺	0.79	Cl ⁻	2.03
CaHCO ₃ ⁺	0.73	H ₂ A	0.736
CaCO ₃	0.53	HA ⁻	0.72
CaSO ₃	0.53	A ⁼	0.705
CaSO ₄	0.58	CaA	0.39

The liquid phase diffusivity, at the temperature of the slurry is calculated using the Stokes-Einstein relationship.

$$D_{T,i} = D_{25,i} \left(\frac{T}{298} \right)^{\left(\frac{\mu_{25}}{\mu_T} \right)}$$

where

T	=	Temperature of slurry (° K)
$D_{T,i}$	=	Diffusivity of i^{th} species at temperature T °K
$D_{25,i}$	=	Diffusivity of i^{th} species at 25 °C
μ_T	=	Viscosity of solution at T (cp)
	=	$1.7695 \times 10^{-3} \exp (1853.88/T)$
μ_{25}	=	Viscosity of solution at 25 °C (cp)
i	=	$H^+, OH^-, H_2CO_3, HCO_3^-, CO_3^{=}, H_2SO_3^0, HSO_3^-,$ $SO_3^{=}, HSO_4^-, SO_4^{=}, Ca^{++}, CaOH^+, CaHCO_3^+,$ $CaCO_3, CaSO_3, CaSO_4, Mg^{++}, MgOH^+, MgHCO_3^+,$ $MgHSO_3^+, MgCO_3, MgSO_4, Na^+, NaOH, NaHCO_3,$ $NaCO_3^-, NaSO_4^-, Cl^-, H_2A, HA^-, A^=, CaA.$

The pseudo-diffusivities are defined on the basis of diffusivities and concentrations of the component species. An example for the calculation of diffusivity of the sulfite ion is shown below. The pseudo-diffusivity values for the remaining species are defined in a similar manner.

The pseudo-concentration of sulfite species is defined as follows:

$$C_{SO_3^{=},b}^0 = C_{SO_3^{=},b}^0 + C_{CaSO_3,b}^0 + C_{MgSO_3,b}^0$$

For absorption/ desorption the pseudo diffusion coefficient of sulfite is defined as follows:

$$\sqrt{D_{SO_3^{2-}}} = \frac{\sqrt{D_{SO_3^{2-}} C_{SO_3^{2-},b}^0} + \sqrt{D_{CaSO_3} C_{CaSO_3,b}^0}}{C_{SO_3^{2-},b}^0} + \frac{\sqrt{D_{MgSO_3} C_{MgSO_3,b}^0}}{C_{SO_3^{2-},b}^0}$$

For solid dissolution:

$$D_{SO_3^{2-}} = \frac{D_{SO_3^{2-}} C_{SO_3^{2-},b}^0 + D_{CaSO_3} C_{CaSO_3,b}^0}{C_{SO_3^{2-},b}^0} + \frac{D_{MgSO_3} C_{MgSO_3,b}^0}{C_{SO_3^{2-},b}^0}$$

The Henry's Law constant for the absorption of oxygen is calculated as shown below. The values of Henry's law constant for SO₂ and CO₂ are calculated by BMREP.

$$H_{O_2} = 3475.7 \log_{10} T - 19009.5$$

$$H_{O_2} = \text{Henry's law constant for oxygen}$$

$$T = \text{Absolute temperature of slurry } ^\circ K$$

A-5.2 Calculation of Limestone Reactivity ($K_{CaCO_3,d}$)

The limestone reactivity is used for the calculation of total dissolution of limestone. Limestone reactivity parameter is calculated on the basis of $k_m \tau$ and limestone utilization as shown below.

$$K_{CaCO_3,d} = \frac{6^{1/3} \pi^{2/3} 2}{\rho_m} \frac{U}{k_m \tau (1-U)}$$

where:

$$U = \text{Limestone Utilization}$$

$$\rho_m = \text{Molar density of limestone}$$

$$= 0.027 \text{ gmol/cc}$$

$k_m\tau$ = Limestone reactivity parameter for a well-mixed stage

The calculation of $k_m\tau$ is done using an iterative procedure to match the specified limestone utilization.

$$U = 1 - \sum_p \Phi_p \frac{1}{k_m\tau} \int_1^0 \frac{f_p \exp\left(-\frac{(k_m\tau)_p}{k_m\tau}\right)}{\frac{df_p}{d(k_m\tau)_p}} df_p$$

$$(k_m\tau)_p = \frac{3}{B^2} \left[(BV_{o,p})^{1/3} (1-f_p^{1/3}) + \ln \frac{1 + BV_{o,p}^{1/3} f_p^{1/3}}{1 + BV_{o,p}^{1/3}} \right]$$

$$\frac{df_p}{d(k_m\tau)_p} = \frac{f_p^{1/3}}{V_{o,p}^{2/3}} - \frac{Bf_p^{2/3}}{V_{o,p}^{1/3}}$$

where:

Φ_p = Weight fraction of particles having diameter between $d_{o,p}$ and $d_{o,p-1}$ in feed (dimensionless)

f_p = Fraction of undissolved particles having diameter d_p (dimensionless)

B = Enhancement factor due to liquid phase agitation, 765 (cm^{-1})

$V_{o,p}$ = Initial size of particle in p^{th} size fraction (cc)
 $= \frac{\pi d_{o,p}^3}{6}$

$d_{o,p}$ = Initial diameter of particle in p^{th} size fraction (cm)

A-5.3 Calculation of Average Film Thickness

In order to match the surface flux condition for limestone, the average film thickness at the surface of the limestone particle is determined as follows:

$$\frac{1}{\delta} = \frac{2 \sum_p \Phi_p \int_0^1 \frac{e^{-(k_m t)_p / k_m \tau}}{-1 - B V_{o,p}^{1/3} f_p^{1/3}} df_p}{\sum_p \Phi_p d_{o,p} \int_1^0 \frac{f_p^{1/3} e^{-(k_m t)_p / k_m \tau}}{-1 - B V_{o,p}^{1/3} f_p^{1/3}} df_p} + 1.612 B$$

A-6 SUMMARY

The equations shown in section A-2 through section A-5 involve relationships between several constants and variables. A short summary of the inputs required for the calculation of each variable is provided in Table A-3. A list of typical values of the constants required for the simulation of the limestone slurry scrubbing process is provided in Tables A-4 and A-5.

Table A-3: Calculated Variables

Variables	Inputs required for calculation	Location of Equation
$C_{i,b}^0$	BMREP parameters, temperature of slurry, guess for concentrations of $C_{Ca^{++},b}^0$, $C_{Mg^{++},b}^0$, $C_{Na^+,b}^0$, $C_{K^+,b}^0$, $C_{SO_3^=,b}^0$, $C_{Cl^-,b}^0$, $C_{H_2Ad,b}^0$, $C_{H^+,b}^0$	BMREP
$C_{j,b}^0$	$C_{i,b}^0$	Section A-5.1
$C_{i,b}^n$	X^n , $K_{H_2CO_3}$, $K_{HCO_3^-}$, K_{SO_2} , $K_{HSO_3^-}$, $K_{HSO_4^-}$, K_{H_2A} , K_{HA^-}	Section A-4.1
$C_{i,i}^n$	X^n , P^{n-1} , N_g , $K_{H_2CO_3}$, $K_{HCO_3^-}$, K_{SO_2} , $K_{HSO_3^-}$, $K_{HSO_4^-}$, K_{H_2A} , K_{HA^-} , D_{HA^-} , D_{H_2A} , $D_{A^=}$, $D_{SO_3^=}$, $D_{HSO_3^-}$, D_{SO_2} , $D_{HSO_4^-}$	Section A-4.2
$C_{i,s1}^n$	X^n , K_{H_2O} , $K_{HSO_4^-}$, $K_{HSO_3^-}$, $K_{HCO_3^-}$, $K_{A^=}$, K_{HA^-} , D_{H_2A} , $D_{CO_3^=}$, $D_{HCO_3^-}$, $D_{A^=}$, D_{HA^-} , $D_{SO_3^=}$, $D_{HSO_3^-}$, $D_{SO_4^=}$, $D_{HSO_4^-}$, D_{OH^-} , D_{H^+} , $S(2)^{n-1}$, $S(1)^{n-1}$, $K_{sp,CaSO_3}$	Section A-4.3
$C_{i,s2}^n$	X^n , $D_{SO_3^=}$, $D_{HSO_3^-}$, D_{H_2A} , D_{HA^-} , $D_{A^=}$, $D_{SO_4^=}$, $D_{HSO_4^-}$, D_{H^+} , D_{OH^-} , $D_{HSO_4^-}$, $D_{HCO_3^-}$, $D_{Ca^{++}}$, $D_{CO_3^=}$, K_{H_2A} , K_{HA^-} , $K_{HSO_3^-}$, $K_{HSO_4^-}$, K_{H_2O} , $K_{HCO_3^-}$, δ , k_c , $K_{sp,CaCO_3}$	Section A-4.3
δ	Φ_p , $k_m\tau$, $(k_{mt})_p$, f_p , B , $V_{o,p}$	Section A-5.3
D_i	BMREP parameters	BMREP
D_j	D_i , $C_{i,b}^0$	A-5.1

Table A-3, continued

Variables	Inputs required for calculation	Location of Equation
$F(1)^n$	f_{11}^n, f_{12}^n	Section A-2.1
$F(2)^n$	$-f_{12}^n$	Section A-2.2
$F(3)^n$	f_{31}^n	Section A-2.3
$F(4)^n$	0	Section A-2.4
f_{11}^n	$CSO_3^-, b^n, CHSO_3^-, b^n, CSO_2, b^n, CSO_3^-, i^n, CHSO_3^-, i^n, CSO_2, i^n, G, k_l^o, k_g, L, N_g^n, N_g^{n-1}, DSO_3^-, DSO_2, DHSO_3^-$	Section A-2.1
f_{12}^n	$CO_2, i^n, G, k_l^o, k_g, L, N_g^n, N_g^{n-1}, DO_2, DSO_2$	Section A-2.1
f_{31}^n	$CCO_3^-, b^n, CHCO_3^-, b^n, CCO_2, b^n, CCO_3^-, i^n, CHCO_3^-, i^n, CCO_2, i^n, G, k_l^o, k_g, L, N_g^n, N_g^{n-1}, DHCO_3^-, DCO_2, DCO_3^-, DSO_2$	Section A-3.1
$G(1)^n$	$g_{11}^n, g_{12}^n, S(1)^n, \tau_s$	Section A-2.1
$G(2)^n$	$g_{21}^n, g_{22}^n, g_{23}^n, S(4)^{n-1}, S(2)^n, S(2)^{n-1}, \tau_s$	Section A-2.2
$G(3)^n$	$g_{31}^n, S(3)^{n-1}, \tau_s$	Section A-2.3
$G(4)^n$	$G(1)^n, G(2)^n, G(3)^n$	Section A-2.4
g_{11}^n	$CSO_3^-, s_1^n, CHSO_3^-, s_1^n, CSO_3^-, b^n, CHSO_3^-, b^n, K_{CaSO_3, d}, DSO_3^-, DHSO_3^-$	Section A-2.1
g_{12}^n	$RS_{CaSO_3}^n, RS_{CaSO_4}^n, K_{CaSO_3, c}$	Section A-2.1
g_{21}^n	$RS_{CaSO_4}^n, K_{CaSO_4}, K_{sp, CaSO_4}$	Section A-2.2
g_{22}^n	$CHSO_4^-, b^n, CSO_4^-, b^n, CHSO_4^-, s_1^n, CSO_4^-, s_1^n, RSO_3SO_4^n, DSO_4^-, DSO_4^-, K_{CaSO_4}$	Section A-2.2
g_{23}^n	$RS_{CaSO_3 \cdot 1/2H_2O}, S(1)^n, S(2)^n, K_{sp}, CaSO_3$	Section A-2.2
g_{31}^n	$CCa^{++}, s_2^n, CCa^{++}, b^n, K_{CaCO_3, d}, D_{Ca^{++}}$	Section A-2.3
$H(1)^{k+1}$	h_{11}^{k+1}	Section A-3.1
$H(2)^{k+1}$	h_{11}^{k+1}	Section A-3.2
$H(3)^{k+1}$	h_{31}^{k+1}	Section A-3.3

Table A-3, continued

Variables	Inputs required for calculation	Location of Equation
h_{11}^{k+1}	$CO_{2,b}^{k+1}, k_{O_2}, N_L, L_2, G_2, H_{O_2}, PO_2^{k+1}$	Section A-3.1
h_{31}^{k+1}	$CCO_{2,b}^{k+1}, PCO_2^{k+1}, HCO_2, N_L, L_2/G_2$	Section A-3.3
H_{CO_2}	BMREP parameters	BMREP
H_{O_2}	Temperature	A-5.1
H_{SO_2}	BMREP parameters	BMREP
$K_{CaCO_3,d}$	$U, \rho_m, k_m\tau$	Section A-5.2
K_{H_2A}	$CH^+, b^0, CHA^-, b^0, CH_2A, b^0$	Section A-5.1
$K_{H_2CO_3}$	$CH^+, b^0, CHCO_3^-, b^0, CCO_2, b^0$	Section A-5.1
K_{H_2O}	CH^+, b^0, COH^-, b^0	Section A-5.1
K_{HA^-}	$CH^+, b^0, CA^=, b^0, CHA^-, b^0$	Section A-5.1
$K_{HCO_3^-}$	$CH^+, b^0, CCO_3^=, b^0, CHCO_3^-, b^0$	Section A-5.1
$K_{HSO_3^-}$	$CH^+, b^0, CSO_3^=, b^0, CHSO_3^-, b^0$	Section A-5.1
$K_{HSO_4^-}$	$CH^+, b^0, CSO_4^=, b^0, CHSO_4^-, b^0$	Section A-5.1
$k_m\tau$	$(k_{mt})_p, \Phi_p, B, V_{o,p}, U$	Section A-5.2
$K_{sp, CaCO_3}$	BMREP parameters	BMREP
$K_{sp, CaCO_3}$	$CCa^{++}, b^0, CCO_3^=, b^0, CCa^{++}, b^0, CCO_3^=, b^0, K_{sp, CaCO_3}$	Section A-5.1
$K_{sp, CaSO_3}$	BMREP parameters	BMREP
$K_{sp, CaSO_3}$	$CCa^{++}, b^0, CSO_3^=, b^0, CCa^{++}, b^0, CSO_3^=, b^0, K_{sp, CaSO_3}$	Section A-5.1
$K_{sp, CaSO_4}$	BMREP parameters	BMREP
$K_{sp, CaSO_4}$	$CCa^{++}, b^0, CSO_4^=, b^0, CCa^{++}, b^0, CSO_4^=, b^0, K_{sp, CaSO_4}$	Section A-5.1
PCO_2^{k+2}	$CCO_{2,b}^{k+1}, HCO_2, N_L, L_2/G_2,$	Section A-3.3
PCO_2^n	$G, k_l^o, k_g, L, N_g^n, N_g^{n-1}, DCO_3^=, DCO_2, DHCO_3^-, PSO_2^{n-1}, CCO_3^=, i^n, CHCO_3^-, i^n, CCO_2, i^n, CCO_3^=, b^n, CHCO_3^-, b^n, CCO_2, b^n$	Section A-2.3
PO_2^{k+2}	$k_{O_2}, N_L, L_2/G_2, H_{O_2}, PO_2^{k+1}, CSO_3^=, b^{k+1}$	Section A-3.1

Table A-3, continued

Variables	Inputs required for calculation	Location of Equation
PO_2^n	$G, k^o_l, k_g, L, N_g^n, N_g^{n-1}, DO_2, CO_{2,i}^n, D_{SO_2}$	Section A-2.1
PSO_2^n	$G, k^o_l, k_g, L, N_g^n, N_g^{n-1}, D_{SO_3^=}, D_{SO_2}, D_{HSO_3^-}, PSO_2^{n-1}, CSO_3^=,i^n, CSO_3^=,b^n, CHSO_3^-,i^n, CHSO_3^-,b^n, CSO_{2,i}^n, CSO_{2,b}^n$	Section A-2.1
PO_2^{k+1}	$CO_{2,b}^{k+1}, CSO_3^=, k_{O_2}, N_L, L_2, G_2, H_{O_2}, PO_2^{k+1}$	Section A-4.1
PCO_2^{k+1}	$CCO_{2,b}^{k+1}, PCO_2^{k+1}, HCO_2, N_L, L_2/G_2$	Section A-4.3
$RS_{CaSO_3}^n$	$CCa^{++},b^n, CSO_3^=,b^n, K_{sp}, CaSO_3$	Section C-2.1
$RS_{CaSO_4}^n$	$CCa^{++},b^n, CSO_4^=,b^n, K_{sp}, CaSO_4$	Section C-2.1
$S(3)^n$	$S(3)^n, g_{31}^n, \tau_s$	Section A-2.3
$S(4)^n$	$S(4)^n, g_{21}^n, \tau_s$	Section A-2.2
$V_{o,p}$	$d_{o,p}$	Section A-5.2
$X(1)^0$	$CSO_3^=,b^0, CHSO_3^-,b^0, CSO_{2,b}^0$	Section A-5.1
$X(2)^0$	$CSO_4^=,b^0, CHSO_4^-,b^0$	Section A-5.1
$X(3)^0$	$CCO_3^=,b^0, CHCO_3^-,b^0, CCO_{2,b}^0$	Section A-5.1
$X(4)^0$	CCa^{++},b^0	Section A-5.1
$X(1)^n$	$X(1)^{n-1}, F(1)^n, G(1)^n$	Section A-2.1
$X(2)^n$	$X(2)^{n-1}, F(2)^n, G(2)^n$	Section A-2.2
$X(3)^n$	$X(3)^{n-1}, F(3)^n, G(3)^n$	Section A-2.3
$X(3)^n$	$X(4)^{n-1}, F(4)^n, G(4)^n$	Section A-2.4

Table A-4: Typical values of constants

Symbol	Value	Units
B	765	cm ⁻¹
E	1	dimensionless
k	3	dimensionless
k _c	10 ^{-11.25}	(gmol/L) ^{5/2}
		cm/s
K _{CaSO₃,c}	0.9	1/s
K _{CaSO₃,d}	3 × 10 ⁵	L/cm ² -gmol
K _{CaSO₄,c}	0.8	1/s
K _{CaSO₄,d}	3 × 10 ⁵	L/cm ² -gmol
k _{O₂}	10 ⁴	L/gmol
k ^o _l /k _g	0.20	L-atm/gmol
L/G	0.20	gmol/l
L ₂ /G ₂	45	L/gmol
N _g ⁿ - N _g ⁿ⁻¹	2.3	dimensionless
N _L	3	dimensionless
OX	0.15	dimensionless
P _{CO₂} ⁰	0.07	atm
P _{CO₂} ^{k+1}	3.3 × 10 ⁻⁴	atm
P _{O₂} ⁰	0.058	atm
P _{O₂} ^{k+1}	0.21	atm
P _{SO₂} ⁰	5.4 × 10 ⁻⁴	atm
P _{SO₂} ^k	2.9 × 10 ⁻³	atm
TS	100	g/L
T	333	°K
τ _{ht}	540	s
τ _s	3	s
U	0.80	dimensionless

Table A-5: Typical values for the limestone particle size distribution. The tabulated values show the initial diameter of particles ($d_{o,p}$) versus the weight fraction of total particles present in size between $d_{o,p}$ and $d_{o,p-1}$ (Φ_p) for Fredonia Coarse (Toprac, 1981).

$d_{o,p} \times 10^6$ (cm)	$\Phi_p \times 100$
0.794	0.4
1.0	1.1
1.26	2.0
1.59	3.1
2.0	4.2
2.52	5.3
3.17	5.1
4.0	3.7
5.04	2.8
6.35	2.4
8.0	2.2
10.08	2.2
12.7	2.5
16.0	2.9
20.2	3.3
25.4	4.1
32.0	4.7
40.3	5.8
50.8	7.2
64.0	7.4
80.6	8.8
101.6	8.5
128.0	4.9
161.0	3.2
210.	1.7
297.0	0.6
420.	0.2

A-7 NOTATION

A^-	=	Adipate ion, $^-OOC(CH_2)_6COO^-$
B	=	Agitation enhancement factor, cm^{-1}
$C_{j,b}^0$	=	Concentration of pseudo-species j in the bulk solution at the inlet to the first stage, $gmol/L$
$C_{i,b}^0$	=	Concentration of true species i in the bulk solution at the inlet to the first stage, $gmol/L$
$C_{j,b}^n$	=	Concentration of the j^{th} species in the bulk liquid solution at the n^{th} stage, $gmol/L$
$C_{j,i}^n$	=	Concentration of the j^{th} species at the gas liquid interface at a point on the n^{th} stage, $gmol/L$
$C_{j,s1}^n$	=	Concentration of species j at the surface of calcium sulfite hemihydrate at the n^{th} stage, $gmol/L$
$C_{j,s2}^n$	=	Concentration of species j at the surface of calcium carbonate at the n^{th} stage, $gmol/L$
δ	=	Average film thickness around the limestone particle, cm
D_i	=	Diffusivity of species i (true species), cm^2/s
D_j	=	Diffusivity of pseudo-species j , cm^2/s
$d_{o,p}$	=	Initial diameter of particle in p^{th} size fraction, cm
E	=	Oxidation enhancement factor, dimensionless
$F(i)^n$	=	Change in composition of solution, in terms of $X(i)^n$, due to the absorption/desorption of gases, $gmol/L$
Φ_p	=	Weight fraction of particles of size between $d_{o,p}$ and $d_{o,p-1}$, dimensionless
f_p	=	Fraction of undissolved particles in p^{th} size fraction, dimensionless
G	=	Gas flow rate, $gmol/min$
$G(i)^n$	=	Change in composition of solution, in terms of $X(i)^n$, due to the dissolution/crystallization of solids, $gmol/L$

G/L	=	Ratio of gas to liquid flow rate in the scrubber, gmol/l
$H(i)^{k+1}$	=	Change in solution composition, in terms of $X(i)^{k+1}$, due to the absorption of gases, gmol/L
H_{CO_2}	=	Henry's Law constant for carbon dioxide, L-atm/gmol
H_{O_2}	=	Henry's Law constant for oxygen, L-atm/gmol
H_{SO_2}	=	Henry's Law constant for sulfur dioxide, L-atm/gmol
H_2A	=	Adipic Acid, $HOOC(CH_2)_6COOH$
k_c	=	Surface rate constant, $M^{5/2}$ cm/s
k_{mt}	=	Limestone reactivity parameter for a batch system, cm^2 -L/gmol
$k_{m\tau}$	=	Limestone reactivity parameter for a well-mixed stage, cm^2 -L/gmol
$K_{CaCO_3,d}$	=	Dissolution constant for limestone (limestone reactivity parameter), L/ cm^2 -gmol
$K_{CaSO_3,d}$	=	Dissolution constant of calcium sulfite, L/ cm^2 -gmol
$K_{CaSO_4,d}$	=	Dissolution constant for gypsum, L/ cm^2 -gmol
$K_{CaSO_3,c}$	=	Crystallization constant of calcium sulfite, 1/s
$K_{CaSO_4,c}$	=	Crystallization constant for gypsum, 1/s
K_{H_2A}	=	Pseudo-equilibrium constant for H_2A , gmol/L
$K_{H_2CO_3}$	=	Pseudo-equilibrium constant for H_2CO_3 , gmol/L
K_{H_2O}	=	Pseudo-equilibrium constant for H_2O , gmol/L
K_{HA^-}	=	Pseudo-equilibrium constant for HA^- , gmol/L
$K_{HCO_3^-}$	=	Pseudo-equilibrium constant for HCO_3^- , gmol/L
$K_{HSO_3^-}$	=	Pseudo-equilibrium constant for HSO_3^- , gmol/L
$K_{HSO_4^-}$	=	Pseudo-equilibrium constant for HSO_4^- , gmol/L
k_{O_2}	=	Rate constant of reaction between oxygen and sulfite in the bulk liquid solution, L/gmol
K_{SO_2}	=	Pseudo-equilibrium constant for SO_2 , gmol/L
$K_{sp, CaCO_3}$	=	Solubility product of calcium carbonate, (gmol/L) ²
$K_{sp, CaCO_3}$	=	Pseudo-solubility product of calcium carbonate, (gmol/L) ²
$K_{sp, CaSO_3}$	=	Pseudo-solubility product of calcium sulfite, (gmol/L) ²
$K_{sp, CaSO_3}$	=	Solubility product for calcium sulfite, (gmol/L) ²

$K_{sp, CaSO_4}$	=	Pseudo-solubility product of calcium sulfate, (gmol/L) ²
$K_{sp, CaSO_4}$	=	Solubility product for gypsum, (gmol/L) ²
k^o_l/k_g	=	Ratio of liquid film to gas film mass-transfer coefficient, L-atm/gmol
L_2/G_2	=	Ratio of liquid to gas flow rate in the hold tank, L/gmol
N_g	=	Number of gas film mass transfer units, dimensionless
N_g^n	=	Value of N_g at the bottom of the n^{th} stage, dimensionless
N_L	=	Number of liquid phase transfer units in the hold tank, dimensionless
$P_{CO_2}^{k+1}$	=	Partial pressure of carbon dioxide in the bulk gas phase at the inlet to the hold tank (atm)
$P_{CO_2}^{k+2}$	=	Partial pressure of carbon dioxide at the exit from the hold tank (atm)
\mathbf{P}^n	=	Vector of partial pressures at the inlet of the n^{th} stage
	=	($P_{SO_2}^n, P_{CO_2}^n, P_{O_2}^n$), atm
$P_{O_2}^{k+1}$	=	Partial pressure of oxygen in the bulk gas phase at the inlet to the hold tank, atm
$P_{O_2}^{k+2}$	=	Partial pressure of oxygen at the exit from the hold tank, atm
Q_j	=	Charge on j^{th} ionic species, dimensionless
$RS_{CaSO_3}^n$	=	Relative Saturation of calcium sulfite at the n^{th} stage, dimensionless
$RS_{CaSO_4}^n$	=	Relative saturation of gypsum at the n^{th} stage, dimensionless
$RS_{CaSO_4 \cdot 1/2H_2O}^n$	=	Relative saturation of calcium sulfate hemihydrate at the n^{th} stage, dimensionless
τ_{ht}	=	Residence time of slurry in the hold tank, s
τ_s	=	Residence time of slurry at each stage of the scrubber, s
$V_{o,p}$	=	Initial volume of particle in p^{th} size fraction, cc
\mathbf{X}^n	=	Vector of concentrations at the n^{th} stage
	=	($X(1)^n, X(2)^n, X(3)^n, X(4)^n$), gmol/L
\mathbf{X}^0	=	Vector of concentrations at inlet to the first stage
	=	($X(1)^0, X(2)^0, X(3)^0, X(4)^0$), gmol/L

Z	=	Vertical coordinate, dimensionless
Z^n	=	Value of Z at the bottom of the n^{th} stage, dimensionless
$Z^{n'}$	=	Value of Z at top of the liquid level on the n^{th} stage, dimensionless

APPENDIX B
CALCULATED RESULTS SHOWING THE EFFECTS OF SOLUTION
CHEMISTRY

Table B-1: Data showing calculated values of bulk, interfacial solution compositions, SO₂ partial pressure, and driving force for absorption of SO₂ at each stage for the three stage EPA/RTP absorber.

Species	Top Stage		Middle Stage		Bottom Stage	
	Bulk	Interface	Bulk	Interface	Bulk	Interface
2900 ppm						
H ⁺	7.01E-05	4.86E-04	2.66E-04	5.35E-04	5.17E-05	5.58E-04
HSO ₃ ⁻	5.48E-03	8.25E-03	1.08E-02	1.27E-02	1.67E-02	1.85E-02
SO ₃ ⁼	9.06E-04	1.96E-05	4.70E-04	2.76E-05	3.74E-04	3.83E-05
SO ₂	3.59E-06	3.23E-04	2.60E-05	6.25E-04	8.05E-05	9.39E-04
HCO ₃ ⁻	3.33E-04	2.04E-06	6.50E-05	1.84E-06	3.05E-05	1.76E-06
CO ₃ ⁼	1.41E-07	1.26E-11	7.40E-09	1.04E-11	1.78E-09	9.53E-12
HSO ₄ ⁻	2.18E-06	1.50E-04	8.70E-06	1.74E-04	1.79E-05	1.91E-04
SO ₄ ⁼	7.78E-03	7.80E-03	8.30E-03	8.24E-03	8.77E-03	8.70E-03
d.f. (atm)	4.27E-04		4.06E-04		4.45E-04	
P _{SO2} (atm)	1.26E-03		2.02E-03		2.87E-03	
1900 ppm						
H ⁺	3.80E-06	2.49E-04	1.40E-05	4.46E-04	3.20E-05	4.81E-04
HSO ₃ ⁻	3.35E-03	5.70E-03	7.20E-03	9.20E-03	1.10E-02	1.36E-02
SO ₃ ⁼	1.00E-03	2.65E-05	5.90E-04	2.40E-05	4.20E-04	3.28E-05
SO ₂	1.22E-06	1.20E-04	9.40E-6	3.30E-04	3.50E-05	5.84E-04
HCO ₃ ⁻	4.70E-04	4.00E-06	1.08E-04	2.20E-06	4.50E-05	2.00E-06
CO ₃ ⁼	3.70E-07	4.80E-11	2.30E-08	1.50E-11	4.20E-09	1.29E-11
HSO ₄ ⁻	1.60E-06	1.90E-04	6.30E-06	1.97E-04	1.48E-05	2.20E-04
SO ₄ ⁼	1.10E-02	1.09E-02	1.13E-02	1.10E-02	1.17E-02	1.16E-02
d.f. (atm)	9.99E-06		1.14E-05		1.22E-05	
P _{SO2} (atm)	6.20E-04		1.20E-03		1.88E-03	
5000 ppm						
H ⁺	1.73E-05	7.60E-04	6.63E-05	7.24E-04	9.70E-05	7.02E-04
HSO ₃ ⁻	9.10E-03	1.21E-02	1.70E-02	1.92E-02	2.50E-02	2.70E-02
SO ₃ ⁼	6.12E-04	1.85E-05	2.90E-04	3.00E-05	3.00E-04	4.50E-05
SO ₂	1.50E-05	1.04E-03	1.05E-04	1.03E-03	2.29E-04	1.45E-03
HCO ₃ ⁻	1.78E-04	1.30E-06	3.10E-05	1.35E-06	1.83E-05	1.38E-06
CO ₃ ⁼	1.50E-05	5.10E-12	1.40E-09	5.60E-12	5.70E-10	5.98E-12
HSO ₄ ⁻	4.50E-06	1.95E-04	1.88E-05	2.00E-04	3.00E-05	2.15E-04
SO ₄ ⁼	6.60E-03	6.53E-03	7.20E-03	7.15E-03	7.80E-03	7.78E-03
d.f. (atm)	1.99E-05		1.86E-05		2.01E-05	
P _{SO2} (atm)	2.70E-03		3.78E-03		5.00E-03	

Table B-2: Data showing calculated values of bulk, interfacial solution compositions, SO₂ partial pressure, and driving force for absorption of SO₂ at each stage for the three stage EPA/RTP absorber (U = 65%, U = 95%; U = 65%, t_{res} = 100s).

Species	Top Stage		Middle Stage Concentrations (M)		Bottom Stage	
	Bulk	Interface	Bulk	Interface	Bulk	Interface
	U = 65 %, t _{res} = 540s					
H ⁺	4.69E-06	4.20E-04	1.50E-05	5.69E-04	3.04E-05	5.94E-04
HSO ₃ ⁻	4.68E-03	7.70E-03	9.51E-03	1.20E-02	1.50E-02	1.73E-02
SO ₃ ⁼	1.15E-03	2.10E-05	7.33E-04	2.46E-05	5.72E-04	3.40E-05
SO ₂	2.00E-06	2.74E-04	1.33E-05	5.81E-04	4.30E-05	9.36E-04
HCO ₃ ⁻	4.90E-04	2.30E-06	1.20E-04	1.73E-06	5.90E-05	1.65E-06
CO ₃ ⁼	3.10E-07	1.69E-11	2.50E-08	9.20E-12	5.90E-09	8.40E-12
HSO ₄ ⁻	1.36E-06	1.21E-04	4.54E-06	1.70E-04	9.62E-06	1.85E-04
SO ₄ ⁼	7.35E-03	7.35E-03	7.65E-03	7.60E-03	7.99E-03	7.92E-03
d.f. (atm)	1.42E-05		1.53E-05		1.65E-05	
P _{SO2} (atm)	1.14E-03		1.97E-03		2.92E-03	
Species			U=95 %, t _{res} = 540s			
	Bulk	Interface	Bulk	Interface	Bulk	Interface
	U = 95 %, t _{res} = 540s					
H ⁺	2.71E-05	4.43E-04	6.20E-05	4.46E-04	8.79E-05	4.62E-04
HSO ₃ ⁻	1.08E-02	1.26E-02	1.64E-02	1.78E-02	2.26E-02	2.38E-02
SO ₃ ⁼	4.63E-04	3.28E-05	3.08E-04	4.63E-05	2.97E-04	5.98E-05
SO ₂	2.70E-05	4.77E-04	9.55E-05	7.32E-04	1.85E-04	9.75E-04
HCO ₃ ⁻	7.75E-05	2.24E-06	2.26E-05	2.22E-06	1.35E-05	2.14E-06
CO ₃ ⁼	8.60E-09	1.52E-11	1.11E-09	1.50E-11	4.66E-10	1.40E-11
HSO ₄ ⁻	9.50E-06	1.53E-04	2.40E-05	1.65E-04	3.48E-05	1.82E-04
SO ₄ ⁼	8.82E-03	8.79E-03	9.41E-03	9.38E-03	1.01E-02	1.00E-02
d.f. (atm)	1.11E-05		1.08E-05		1.19E-05	
P _{SO2} (atm)	1.57E-03		2.22E-03		2.88E-03	
Species			U = 65%, Residence time = 100 s			
	Bulk	Interface	Bulk	Interface	Bulk	Interface
	U = 65%, Residence time = 100 s					
H ⁺	6.82E-06	4.00E-04	1.68E-05	5.14E-04	3.08E-05	5.71E-04
HSO ₃ ⁻	5.80E-03	8.25E-03	1.03E-02	1.26E-02	1.56E-02	1.79E-02
SO ₃ ⁼	9.80E-04	2.40E-05	7.15E-04	2.86E-05	5.89E-04	3.63E-05
SO ₂	3.70E-05	2.97E-04	1.60E-05	5.86E-04	4.50E-05	9.26E-04
HCO ₃ ⁻	3.20E-04	2.44E-06	1.08E-04	1.92E-06	5.85E-05	1.72E-06
CO ₃ ⁼	1.42E-07	1.82E-11	1.96E-08	1.11E-11	5.75E-09	9.11E-12
HSO ₄ ⁻	2.07E-06	1.23E-04	5.30E-06	1.61E-04	1.01E-05	1.86E-04
SO ₄ ⁼	7.72E-03	7.70E-03	8.02E-03	7.97E-03	8.35E-03	8.28E-03
d.f. (atm)	1.26E-05		1.40E-05		1.61E-05	
P _{SO2} (atm)	1.15E-03		1.94E-03		2.88E-03	

Table B-3: Data showing calculated values of bulk, interfacial solution compositions, SO₂ partial pressure, and driving force for absorption of SO₂ at each stage for the three stage EPA/RTP absorber. Effect of changes in L/G ratio are studied at L/G = 0.16 l/gmol and 0.24 l/gmol respectively, effect of N_g (= 1.84) at low L/G is also calculated.

Species	Top Stage		Middle Stage		Bottom Stage	
	Bulk	Interface	Bulk	Interface	Bulk	Interface
Concentrations (M)						
L/G = 0.16 l/gmol						
H ⁺	9.99E-06	4.67E-04	4.00E-04	5.11E-04	6.77E-05	4.96E-04
HSO ₃ ⁻	6.76E-03	9.22E-03	1.30E-02	1.47E-02	1.96E-02	2.11E-02
SO ₃ ⁼	7.87E-04	2.28E-05	3.75E-04	3.34E-05	3.36E-04	4.94E-05
SO ₂	6.30E-06	3.89E-04	4.90E-05	6.66E-04	1.24E-04	9.60E-04
HCO ₃ ⁻	2.41E-04	2.12E-06	4.14E-05	1.93E-06	2.21E-05	1.98E-06
CO ₃ ⁼	7.30E-08	1.37E-11	3.10E-09	1.14E-11	2.21E-05	1.21E-11
HSO ₄ ⁻	2.99E-06	1.40E-04	1.29E-05	1.63E-04	2.33E-05	1.70E-04
SO ₄ ⁼	7.63E-03	7.61E-03	8.10E-03	8.12E-03	8.73E-03	8.70E-03
d.f. (atm)	1.30E-05		1.25E-05		1.29E-05	
P _{SO2} (atm)	1.40E-03		2.10E-03		2.87E-03	
L/G = 0.24 l/gmol						
H ⁺	5.45E-06	4.69E-04	1.91E-05	6.08E-04	4.05E-05	6.09E-04
HSO ₃ ⁻	4.57E-03	7.48E-03	9.14E-03	1.15E-02	1.45E-02	1.65E-02
SO ₃ ⁼	9.73E-04	1.84E-05	5.54E-04	2.20E-05	4.14E-04	3.15E-05
SO ₂	2.39E-06	2.79E-04	1.63E-05	5.75E-04	5.47E-05	9.24E-04
HCO ₃ ⁻	4.15E-04	2.11E-06	9.30E-05	1.62E-06	4.01E-05	1.61E-06
CO ₃ ⁼	2.38E-07	1.36E-11	1.47E-08	8.06E-12	3.01E-09	8.00E-12
HSO ₄ ⁻	1.80E-06	1.54E-04	6.56E-06	2.06E-04	1.45E-05	2.16E-04
SO ₄ ⁼	8.37E-03	8.33E-03	8.70E-03	8.60E-03	9.10E-03	8.99E-03
d.f. (atm)	1.42E-05		1.53E-05		1.59E-05	
P _{SO2} (atm)	1.15E-03		1.95E-03		2.87E-03	
L/G = 0.16, N_g = 1.84/stage						
H ⁺	8.65E-06	5.44E-04	3.19E-05	5.44E-04	5.42E-05	5.49E-04
HSO ₃ ⁻	6.27E-03	9.10E-03	1.20E-02	1.38E-02	1.78E-02	1.95E-02
SO ₃ ⁼	8.42E-04	1.93E-05	4.34E-04	2.96E-05	3.81E-04	4.13E-05
SO ₂	5.07E-06	4.20E-04	3.56E-05	6.89E-04	9.01E-04	9.40E-04
HCO ₃ ⁻	2.91E-04	1.83E-06	5.65E-05	1.82E-06	2.96E-05	1.79E-06
CO ₃ ⁼	1.02E-07	1.01E-11	5.36E-09	1.01E-11	1.65E-09	9.98E-12
HSO ₄ ⁻	2.56E-06	1.60E-04	9.99E-06	1.69E-04	1.80E-05	1.81E-04
SO ₄ ⁼	7.51E-03	7.47E-03	7.94E-03	7.89E-03	8.43E-03	8.36E-03
d.f. (atm)	1.50E-05		1.35E-05		1.45E-05	
P _{SO2} (atm)	1.54E-03		2.19E-03		2.87E-03	

Table B-4: Data showing calculated values of bulk, interfacial solution compositions, SO₂ partial pressure, and driving force for absorption of SO₂ at each stage for the three stage EPA/RTP absorber. The effect of DBA is studied over a range of concentration values as well as N_g = 1 and N_g = 2.3.

	Top Stage		Middle Stage		Bottom Stage	
Species	Bulk	Interface	Concentrations (M)		Bulk	Interface
			Bulk	Interface		
DBA = 200 ppm						
H ⁺	6.30E-06	2.38E-04	1.99E-05	3.94E-04	3.95E-04	4.89E-04
HSO ₃ ⁻	6.15E-03	9.96E-03	1.23E-02	1.51E-02	1.91E-02	2.16E-02
SO ₃ ⁼	1.15E-03	4.92E-05	7.29E-04	4.54E-05	5.70E-04	5.21E-05
HCO ₃ ⁻	5.11E-04	4.15E-06	1.03E-04	2.50E-06	4.35E-05	2.00E-06
CO ₃ ⁼	2.48E-07	5.33E-11	1.59E-08	1.94E-11	3.37E-09	1.25E-11
SO ₂	3.60E-06	2.21E-04	2.27E-05	5.56E-04	7.01E-05	9.89E-04
HSO ₄ ⁻	1.11E-06	4.24E-05	3.76E-06	7.54E-05	8.32E-06	1.03E-04
SO ₄ ⁼	4.54E-03	4.57E-03	4.86E-03	4.93E-03	5.42E-03	5.45E-03
H ₂ A	5.82E-05	1.02E-03	2.42E-04	1.15E-03	4.67E-04	1.19E-03
HA ⁻	4.99E-04	2.62E-04	7.41E-04	1.77E-04	7.16E-04	1.48E-04
A ⁼	8.91E-04	1.13E-05	3.85E-04	4.65E-06	1.87E-04	3.13E-06
d.f. (atm)	1.75E-05		1.64E-05		1.78E-05	
P _{SO2}	9.67E-04		1.90E-03		2.92E-03	
DBA = 400 ppm						
H ⁺	3.70E-06	4.28E-05	1.54E-05	3.21E-04	3.49E-05	4.29E-04
HSO ₃ ⁻	4.30E-03	8.46E-03	1.11E-02	1.52E-02	1.90E-02	2.23E-02
SO ₃ ⁼	1.39E-03	2.37E-04	8.71E-04	5.67E-05	6.56E-04	6.25E-05
HCO ₃ ⁻	8.39E-04	2.33E-05	1.36E-04	3.08E-06	5.08E-05	2.30E-06
CO ₃ ⁼	7.04E-07	1.68E-09	2.75E-08	2.97E-11	4.51E-09	1.66E-11
SO ₂	1.47E-06	3.36E-05	1.58E-05	4.53E-04	6.15E-05	8.88E-04
HSO ₄ ⁻	6.07E-07	7.28E-06	2.74E-06	5.84E-05	6.87E-06	8.54E-05
SO ₄ ⁼	4.28E-03	4.43E-03	4.65E-03	4.73E-03	5.14E-03	5.19E-03
H ₂ A	4.27E-05	9.46E-04	3.57E-04	2.22E-03	8.37E-04	2.35E-03
HA ⁻	7.04E-04	1.34E-03	1.41E-03	4.20E-04	1.46E-03	3.33E-04
A ⁼	1.99E-03	3.28E-04	9.65E-04	1.36E-05	4.38E-04	8.14E-06
d.f. (atm)	1.78E-05		2.12E-05		2.07E-05	
P _{SO2} (atm)	5.69E-04		1.67E-03		2.88E-03	

Table B-4. Continued

Species	Top Stage		Middle Stage Concentrations (M)		Bottom Stage	
	Bulk	Interface	Bulk	Interface	Bulk	Interface
DBA = 1000[†] ppm, N_g = 2.3/stage						
H ⁺	1.85E-06	2.35E-06	7.03E-06	6.60E-05	3.07E-05	3.72E-04
HSO ₃ ⁻	2.10E-03	2.91E-03	6.77E-03	1.31E-02	1.55E-02	2.12E-02
SO ₃ ⁼	1.42E-03	1.55E-03	1.21E-03	2.49E-04	6.33E-04	7.13E-05
HCO ₃ ⁻	1.53E-03	4.42E-04	2.90E-04	1.55E-05	6.21E-05	2.72E-06
CO ₃ ⁼	2.64E-05	6.01E-07	1.32E-07	7.50E-10	6.46E-09	2.34E-11
SO ₂	3.56E-07	6.27E-07	4.35E-06	7.91E-05	4.36E-05	7.20E-04
HSO ₄ ⁻	3.62E-07	4.73E-07	1.43E-06	1.37E-05	6.51E-06	7.97E-05
SO ₄ ⁼	5.30E-03	5.45E-03	5.52E-03	5.66E-03	5.74E-03	5.80E-03
H ₂ A	2.99E-05	4.63E-05	2.94E-04	3.14E-03	1.84E-03	5.73E-03
HA ⁻	9.99E-04	1.22E-03	2.58E-03	2.94E-03	3.70E-03	9.51E-04
A ⁼	5.82E-03	5.57E-03	3.96E-03	4.81E-04	1.30E-03	2.75E-05
d.f. (atm)	5.18E-06		2.96E-05		3.14E-05	
P _{SO2} (atm)	1.59E-04		1.10E-03		2.79E-03	
DBA = 3600 ppm, N_g = 2.3/stage						
H ⁺	2.09E-06	1.81E-06	2.80E-06	4.78E-06	1.21E-05	6.57E-05
HSO ₃ ⁻	1.86E-03	1.86E-03	2.72E-03	4.98E-03	1.28E-02	2.81E-02
SO ₃ ⁼	1.30E-03	1.49E-03	1.42E-03	1.51E-03	1.55E-03	6.23E-04
HCO ₃ ⁻	1.53E-03	6.14E-04	6.74E-04	2.28E-04	1.46E-04	1.65E-05
CO ₃ ⁼	2.62E-06	1.21E-06	8.60E-07	1.71E-07	4.32E-08	8.96E-10
SO ₂	3.41E-07	2.95E-07	6.68E-07	2.09E-06	1.36E-05	1.62E-04
HSO ₄ ⁻	3.46E-07	3.10E-07	4.80E-07	8.44E-07	2.10E-06	1.18E-05
SO ₄ ⁼	5.18E-03	5.33E-03	5.34E-03	5.50E-03	2.11E-06	5.59E-03
H ₂ A	1.17E-04	9.03E-05	2.00E-04	5.08E-04	2.11E-03	1.15E-02
HA ⁻	3.63E-03	3.22E-03	4.63E-03	6.86E-03	1.13E-02	1.08E-02
A ⁼	2.09E-02	2.14E-02	1.98E-02	1.71E-02	1.13E-02	1.98E-03
d.f. (atm)	1.30E-06		1.23E-05		7.44E-05	
P _{SO2} (atm)	4.03E-05		3.80E-04		2.68E-03	

[†]1000 ppm DBA = 16.8 mM of Adipic Acid

Table B-4. continued

DBA = 1000 ppm, N_g = 1/stage						
H⁺	3.44E-06	1.52E-05	9.44E-06	1.19E-04	1.98E-05	3.08E-04
HSO₃⁻	3.95E-03	8.42E-03	8.96E-03	1.60E-02	1.57E-02	2.26E-02
SO₃⁼	1.44E-03	6.96E-04	1.19E-03	1.68E-04	1.00E-03	9.21E-05
HCO₃⁻	1.20E-03	6.73E-05	3.22E-04	8.51E-06	1.28E-04	3.27E-06
CO₃⁼	1.12E-06	1.41E-08	1.09E-07	2.28E-10	2.07E-08	3.40E-11
SO₂	1.25E-06	1.17E-05	7.73E-06	1.75E-04	2.86E-05	6.38E-04
HSO₄⁻	3.52E-07	1.64E-06	1.01E-06	1.34E-05	2.30E-06	3.70E-05
SO₄⁼	2.77E-03	2.93E-03	2.90E-03	3.04E-03	3.15E-03	3.26E-03
H₂A	9.13E-05	8.35E-04	4.56E-04	4.21E-03	3.67E-03	5.52E-03
HA⁻	1.64E-03	3.40E-03	2.98E-03	2.17E-03	3.67E-03	1.10E-03
A⁼	5.12E-03	2.41E-03	3.41E-03	1.96E-04	2.00E-03	3.86E-05
d.f. (atm)	2.06E-05		3.39E-05		3.59E-05	
P_{SO2} (atm)	7.49E-04		1.71E-03		2.89E-03	

Table B-5: Sample calculations for flux and enhancement factors
(DBA = 200 ppm).

B	C	D	E	F	G	H	I	J
4		Top Stage		Middle Stage		Bottom Stage		
5	Species	C_b (M)	C_i (M)	C_b (M)	C_i (M)	C_b (M)	C_i (M)	Diffusivity (cm^2/s)
6	H^+	6.30E-06	2.38E-04	1.99E-05	3.94E-04	3.95E-04	4.89E-04	1.41E-02
7	HSO_3^-	6.15E-03	9.96E-03	1.23E-02	1.51E-02	1.91E-02	2.16E-02	4.96E-03
8	$\text{SO}_3^{=}$	1.15E-03	4.92E-05	7.29E-04	4.54E-05	5.70E-04	5.21E-05	3.47E-03
9	HCO_3^-	5.11E-04	4.15E-06	1.03E-04	2.50E-06	4.35E-05	2.00E-06	4.81E-03
10	$\text{CO}_3^{=}$	2.48E-07	5.33E-11	1.59E-08	1.94E-11	3.37E-09	1.25E-11	3.44E-03
11	H_2SO_3	3.60E-06	2.21E-04	2.27E-05	5.56E-04	7.01E-05	9.89E-04	6.56E-03
12	HSO_4^-	1.11E-06	4.24E-05	3.76E-06	7.54E-05	8.32E-06	1.03E-04	5.35E-03
13	$\text{SO}_4^{=}$	4.54E-03	4.57E-03	4.86E-03	4.93E-03	5.42E-03	5.45E-03	4.06E-03
14	H_2A	5.82E-05	1.02E-03	2.42E-04	1.15E-03	4.67E-04	1.19E-03	3.94E-03
15	HA^-	4.99E-04	2.62E-04	7.41E-04	1.77E-04	7.16E-04	1.48E-04	3.98E-03
16	$\text{A}^{=}$	8.91E-04	1.13E-05	3.85E-04	4.65E-06	1.87E-04	3.13E-06	3.68E-03
17	flux SO_2 (gmol/l)	1.75E-05		1.64E-05		1.78E-05		
18	PSO_2 (atm)	9.67E-04		1.90E-03		2.92E-03		
19	flux SO_2 (atm)	=D17*30.48		=F17*30.48		=H17*30.48		
20	CSO_2	=D11	=(D18-D19)/D21	=F11	=(F18-F19)/F21	=H11	=(H18-H19)/H21	
21	HSO_2	2.58	2.58	2.58		2.58		

Table B-5 continued

Concentration Driving Force (gmol/l)						
24	H^+	=E6-D6	=J6*D24	=G6-F6	=J6*F24	=I6-H6
25	HSO_3^-	=E7-D7	=J7*D25	=G7-F7	=J7*F25	=I7-H7
26	SO_3^{2-}	=E8-D8	=J8*D26	=G8-F8	=J8*F26	=I8-H8
27	HCO_3^-	=E9-D9	=J9*D27	=G9-F9	=J9*F27	=I9-H9
28	CO_3^{2-}	=E10-D10	=J10*D28	=G10-F10	=J10*F28	=I10-H10
29	H_2SO_3	=E11-D11	=J11*D29	=G11-F11	=J11*F29	=I11-H11
30	HSO_4^-	=E12-D12	=J12*D30	=G12-F12	=J12*F30	=I12-H12
31	SO_4^{2-}	=E13-D13	=J13*D31	=G13-F13	=J13*F31	=I13-H13
32	H_2A	=E14-D14	=J14*D32	=G14-F14	=J14*F32	=I14-H14
33	HA^-	=E15-D15	=J15*D33	=G15-F15	=J15*F33	=I15-H15
34	A^{2-}	=E16-D16	=J16*D34	=G16-F16	=J16*F34	=I16-H16
35	Flux		E29+E25+E26+E30+E31		G29+G25+G26+G30+G31	I29+I25+I26+I30+I31
37	E_{total}	=E35/E29		=G35/G29		=I35/I29
38			Enhancement Factors			
41	H^+	=E24/E\$29		=G24/G\$29		=I24/I\$29
42	SO_3^{2-}	=E26/E\$29		=G26/G\$29		=I26/I\$29
43	HCO_3^-	=E27/E\$29		=G27/G\$29		=I27/I\$29
44	CO_3^{2-}	=E28/E\$29		=G28/G\$29		=I28/I\$29
45	HSO_4^-	=E30/E\$29		=G30/G\$29		=I30/I\$29
46	SO_4^{2-}	=E31/E\$29		=G31/G\$29		=I31/I\$29
47	HA^-	=E33/E\$29		=G33/G\$29		=I33/I\$29
48	A^{2-}	=E34/E\$29		=G34/G\$29		=I34/I\$29
50	K_g/k_g	=(D18-E11*D21)/D18		=(F18-F21*G11)/F18		=(H18-H21*I11)/H18

Table B-6: Particle Size Distribution for Fredonia Coarse Limestone (54% < 325 mesh, 69.6% < 200 mesh or 74 microns, 97.1 % < 70 mesh or 200 micron; Toprac, 1981).

Diameter, d(i) (microns)	% volume (< size d(i))
0.794	0.4
1	1.1
1.26	2
1.59	3.1
2	4.2
2.52	5.3
3.17	5.1
4	3.7
5.04	2.8
6.35	2.4
8	2.2
10.08	2.2
12.7	2.5
16	2.9
20.2	3.3
25.4	4.1
32	4.7
40.3	5.8
50.8	7.2
64	7.4
80.6	8.8
101.6	8.5
128	4.9
161	3.2
210	1.7
297	0.6
420	0.2

APPENDIX C

SAMPLE CALCULATIONS - DESIGN EXAMPLE

This appendix contains input and output files from a sample calculation using the model FGDTX. The purpose of this calculation was to determine the number of gas film mass transfer units (N_g) required to reach SO_2 penetration ($p = 1 - \text{fractional removal}$) of 0.10. Some of the important design specifications are summarized in Table C-1. Values of constants for the dissolution of CaSO_3 and crystallization of gypsum can be found in the input file mdiva.dat. The particle size distribution of Fredonia Coarse limestone is also shown in mdiva.dat (as well as Table B-5).

Table C-1: Design specifications for achieving SO_2 penetration of 0.10.

Contactor	Three stage turbulent contact absorber
Liquid flow rate	1200 gpm
Gas flow rate	30000 acfm (60 °C)
Inlet Concentration of SO_2	3000 ppmv
Slurry Temperature	60 °C
Slurry residence time (scrubber)	9† s
Slurry residence time (hold tank)	540 s
Dibasic acid concentration	0 ppm
k_L/k_g	275 (cc-atm/gmol)
Limestone utilization	80 %
Percent oxidation of $\text{CaSO}_{3(s)}$	15 %
Limestone type	Fredonia Coarse
Solid loading in slurry	10 %
N_1 (hold tank)	0.6
L/G (hold tank)	45 L/gmol

† The slurry residence time is based on a liquid hold-up of nine inches of water

A trial and error procedure was used to match the specified SO_2 penetration by varying N_g . At $N_g = 4.5$, calculated SO_2 penetration was 0.101. The details of solution speciation, driving force for absorption, limestone dissolution and SO_2 absorption at each stage are shown in the attached output file. Under similar gas and liquid flow rates, $N_g = 3.9$ has been measured under experimental conditions (Head, 1977) for a three stage turbulent contact absorber. For this contactor, fifteen inches of packing were required (five inches/stage) to achieve $N_g = 3.9$. For small-scale contactors (Douglas, 1964) the following correlation has been derived from experimental data.

$$N_g = 1.74 U_g^{-1.2} U_l^{0.22} h_s^{0.48}$$

where,

U_g = Gas velocity (m/s)

U_l = Liquid velocity (m/s)

h_s = Height of stagnant Packing height (m)

Using the above correlation, the effect of packing height was extrapolated from $N_g = 3.9$ and $h_s = 15$ inches, to $N_g = 4.5$. A packing height of 16.1 inches was predicted.

It must be noted that lower values of N_g would have been calculated if the solution contained high concentrations of dibasic acid or if limestone utilization was specified at a lower value.

C-1 INPUT FILE : MDIVA.DAT

The input file mdiva.dat is used to specify inputs to the Bechtel Modified Radian Equilibrium Program (BMREP) as well as to the program FGDTX. The calculations for the equilibrium concentrations in the solution are done by BMREP. A line by line description of inputs provided in mdiva.dat is given below.

Line 1:

IDENT = An identifier for the case study (maximum 80 alpha numeric characters)

Line 2:

INFLAG = A flag indicating whether to use default values for some of the inputs (see Line 3).

= 1 = use defaults

= 2 = specify BMREP defaults

NDIFF = A flag indicating choice of differential equation solver

= 1 = Use LSODE

= 2 = Use other (DGEAR)

If INFLAG = 1

Line 3:

XK1 = A flag indicating the concentration units for the input species

= 1 = Input concentrations in ppm

= 2 = Input concentrations in gmol/L

TK = Slurry temperature, °K

pH = Scrubber inlet solution pH

If INFLAG = 2

Line 3:

XPR = A flag indicating the amount of output from BMREP which is to be printed

= 0 = No printout

= 1 = Full printout

= 2 = Short printout

XK1 = A flag indicating the concentration units for the input species

= 1 = Input concentrations in ppm

= 2 = Input concentrations in gmol/L

SJ = A flag indicating whether solids are present (default = 0)

= 0 = no solids present (default)

= 1 = solids may be present (specify partial pressure of CO₂)

TK = Slurry temperature, °K

PP(1) = Equilibrium partial pressure of SO₂, atm (default = 0)

PP(2) = Equilibrium partial pressure of CO₂, atm

SS(1)	= Relative saturation of CaSO_3 at which crystallization occurs (default = 0.55)
SS(2)	= Relative saturation of CaCO_3 at which crystallization occurs (default = 1.0)
SS(3)	= Relative saturation of CaSO_4 at which crystallization occurs (default = 1.0)
XIPH	= A flag indicating whether pH is specified = 0 = pH not specified = 1 = pH specified (default)
pH	= Scrubber inlet pH (if XIPH = 0, pH = 0)
Line 4:	
CCM	= The initial guess for the concentrations of Ca, Mg, Na, K, SO_3^- , SO_4^- , CO_3^- , Cl^- and H_2Ad respectively (if no buffer additive is present, set $\text{H}_2\text{Ad} = 0.0015$ ppm or 1×10^{-8} gmol/l)
Line 5:	
BPP	= The initial guess for the outlet partial pressures of SO_2 , CO_2 , and O_2 respectively (atm.)
RKLKG	= The ratio of liquid to gas film mass transfer coefficients (cc-atm/gmol)
Line 6:	
RLG	= The ratio of liquid to gas flow rates (L/gmol). The gas flow rate is calculated on a dry basis at inlet.
Line 7:	
XKSP(1,1)	= Dissolution rate parameter for CaSO_3 in the scrubber (cm^{-2})
XKSP(2,1)	= Dissolution rate parameter for gypsum in the scrubber (cm^{-2})
Line 8:	
FSP	= Specified value for the inlet partial pressure of SO_2 (atm.)
NTUSP	= Number of gas film mass transfer units per stage
NFLAG	= A flag indicating single or multistage scrubbing = 9 = Single stage = 11 = Multistage
NFLAG2	= A flag indicating co-current or counter-current flow = 10 = Counter-current flow of gas and liquid = 12 = Co-current flow of gas and liquid
Line 9:	
NMIX	= Number of stages
CKCAAD	= Equilibrium constant at the scrubber temperature for the calcium anion pair formed by the addition of acid buffer (gmol/L)
Line 10:	
LA	= A flag indicating whether the particle size distribution (PSD) for limestone is to be calculated = 0 = PSD is to be calculated from sieve data = 1 = PSD is specified as input

U = Limestone utilization (percent)

Line 11:

S = Percent solids in slurry

O = Percent oxidation

Line 12:

TAUSC = Slurry residence time in the scrubber, sec./stage

TAUHT = Slurry residence time in hold tank (s)

B = Enhancement factor for limestone dissolution

Line 13:

RLG2 = Ratio of liquid to gas flow rate in the hold tank (L/gmol)

CXKSP(1,2) = Crystallization constant for CaSO_3

CXKSP(2,2) = Crystallization constant for gypsum

Line 14:

RATEK = Limestone surface rate constant (to account for the effect of limestone type)

RD = Factor to reduce limestone reactivity

Line 15:

E = Oxidation enhancement factor in the hold tank (dimensionless)

N_1 = Number of liquid film mass transfer units in the hold tank (dimensionless)

Line 16:

If LA = 0, sieve data are required

P1 = The weight fraction of limestone which is less than size D1 (percent)

D1 = A sieve mesh diameter (μm)

P2 = The weight fraction of limestone which is less than size D2 (percent)

D2 = A sieve mesh diameter (μm)

If LA = 1 complete particle size distribution is required

Line 16:

N = Number of size fractions in particle size distribution

Line 17 to (17 + N)

D(i) = Diameter (μm)

PHI(i) = Weight fraction of particles between sizes D(i) and D(i-1)

Mdiva.dat

FRED.COARSE-4

1,1
1,333.,5.5
383.,283.,248.,0.,2260.,1320.,292.,462.,0.0015
5.4E-4,0.07,0.058,200.
0.20,1.0
3.0E5,3.0E5
3.00E-3,1.5,11,10
3,1.0E-2
1,80
10,15
3.0,540.0,765.
45.0,0.80,0.90
11.2500,1.0
1.0,0.60
27
0.794,0.4
1.0,1.1
1.26,2.0
1.59,3.1
2.0,4.2
2.52,5.3
3.17,5.1
4.0,3.7
5.04,2.8
6.35,2.4
8.0,2.2
10.08,2.2
12.7,2.5
16.0,2.9
20.2,3.3
25.4,4.1
32.0,4.7
40.3,5.8
50.8,7.2
64.0,7.4
80.6,8.8
101.6,8.5
128.0,4.9
161.0,3.2
210.,1.7
297.0,0.6
420.,0.2

C-2 INPUT FILE: P_EST.DAT

This file is used to specify some of the inputs for the parameter estimation routine, Generalized REGression (GREG). The values specified in this file supersede the values specified in the file mdiva.dat when calculations for parameter estimation are done. The inputs common to p_est.dat and mdiva.dat are NTUSP, RKLKG, CC(I, J), UU(I), SS(I), OX(I), POUT(I), PIN(I).

Line 1:

IEST = Flag for estimation
 = 1 = Estimate parameters
 = 1 = Calculate performance for one experiment and stop

Line 2:

NTUSP = Number of gas film mass transfer units

Line 3:

RKLKG = Ratio of liquid to gas film mass transfer units (cc-atm/gmol)

Line 4:

DBA = DBA concentration, ppm (to prevent a zero input)

Line 5:

SCALE = Factor used to reduce the calculated limestone reactivity

Line 6:

ITEST = Flag used to test parameter estimation routine (redundant)

Line 7:

BNDLW(1), BNDUP (1) = Lower and upper bounds on the parameter NTUSP

Line 8:

BNDLW(2), BNDUP (2) = Lower and upper bounds on the parameter RKLKG

Line 9:

BNDLW(3), BNDUP (3) = Lower and upper bounds on the parameter SCALE

Line 10:

CC(I, J) = Solution composition for the ith experiment (ppm)

Line 11:

UU(I) = Limestone utilization for the ith experiment (percent)

pH (I) = Solution pH for the ith experiment

Line 12:

SS(i) = Solids' concentration for the ith experiment (fraction)

OX(i) = Oxidation level of solid CaSO₃ (percent)

Line 13:

POUT (i) = Initial guess for outlet partial pressure of SO₂ (atm.)

PIN(i) = Specified value of inlet partial pressure of SO₂ (atm.)

Note:

The inputs specified in line 10 -13 are repeated for each experimental data point.

P_est.dat

```

1
1.5
275
0.0015
1.0
0
4,0.1
3,0.1
10,0.1
383.,283.,248.,0.,2260.,1320.,292.,462.,0.0015
80.00,5.50
15,10
0.3e-3,3.00e-3
383.,283.,248.,0.,2260.,1320.,292.,462.,0.0015
45.3,5.80
15,10
3.4e-4,2.9e-3
383.,283.,248.,0.,2260.,1320.,292.,462.,0.0015
82,5.00
15,10
6e-4,2.9e-3
383.,283.,248.,0.,2260.,1320.,292.,462.,1620
91,5.00
15,10
1e-3,2.9e-3
383.,283.,248.,0.,2260.,1320.,292.,462.,2200
95.0,5.00
15,10
1.0e-3,2.90e-3
383.,283.,248.,0.,2260.,1320.,292.,462.,1000
91.3,5.00
15,10
4e-4,2.9e-3
383.,283.,248.,0.,2260.,1320.,292.,462.,1000
91,4.80
15,10
5e-4,2.9e-3
383.,283.,248.,0.,2260.,1320.,292.,462.,1000
68,5.80
15,10
14e-4,2.9e-3
383.,283.,248.,0.,2260.,1320.,292.,462.,1000
73,5.60
15,10
5e-4,2.9e-3

```

C-3 OUTPUT FILE : SAMPLE CALCULATION

filename : mdiva.out

FRED-COARSE - 4

BECHTEL MODIFIED RADIAN EQUILIBRIUM PROGRAM**INPUT DATA**

K1	JS	TK	PPSO2	PPCO	SSO3	SCO3	SSO4	IPH	PH
				2					
1	0	333.	.00	.00	.55	1.00	1.00	1	5.50

CONCENTRATIONS, GMOL/LITER AND PPM(WT)

CA	MG	NA	K	SO3	SO4	CO3	CL	H2AD
.02036	.01164	.01079	.000	.02823	.01374	.00487	.01303	.00
816.	283.	248.	0.	2260.	1320.	292.	462.	0.

CALCULATED RESULTS

COMPONENT	GMOL/LITER	ACTIVITY COEFFICIENT
H+	.3819E-05	.8280
OH-	.3887E-07	.7772
H2CO3	.3945E-02	1.0149
HCO3-	.8216E-03	.7748
CO3--	.4047E-07	.3603
H2SO3	.8497E-05	1.0149
HSO3-	.2307E-01	.7748
SO3--	.5846E-03	.3603
HSO4-	.2607E-05	.7772
SO4--	.7062E-02	.3209
CA++	.1292E-01	.3761
CAOH+	.5577E-08	.7772
CAHCO3	.6737E-04	.7772
CACO3	.3096E-06	1.0149
CASO3	.3792E-02	1.0149
CASO4	.3582E-02	1.0149
MG++	.7897E-02	.4013
MGOH+	.7200E-07	.7772
MGHCO3	.2853E-04	.7772
MGCO3	.1712E-06	1.0149
MGSO3	.7777E-03	1.0149
MGSO4	.2938E-02	1.0149

Calculated Results, Continued

Component	Concentration	Activity Coefficient
NA+	.1063E-01	.7897
NAOH	.6724E-10	1.0149
NAHCO ₃	.2960E-05	1.0149
NACO ₃ -	.3727E-08	.7772
NASO ₄ -	.1563E-03	.7772
CL-	.1303E-01	.7679
H ₂ AD	.1969E-09	1.0149
HAD-	.3012E-08	.7772
AD--	.6025E-08	.3209
CAAD	.1040E-08	1.0149

PH = 5.500 PPSO₂ = .2146E-04 ATM PPCO₂ = 0.2657ATM

THE IONIC STRENGTH OF THE SOLUTION = 0.0845

PERCENT ERROR IN IONIC BALANCE = .0

PERCENT SULFATE SATURATION = 54.8 (KSP = .2011E-04)

TOTAL DISSOLVED SOLIDS = 5681. PPM

ANALYSIS OF SLURRY	LIQUID		SOLID	
	GMOL/LITER	PPM	GMOL/LITER	PPM
CA	.2036E-01	816.	.0000E+00	0.
MG	.1164E-01	283.	.0000E+00	0.
NA	.1079E-01	248.	.0000E+00	0.
SO ₃	.2823E-01	2260.	.0000E+00	0.
SO ₄	.1374E-01	1320.	.0000E+00	0.
CO ₃	.4866E-02	292.	.0000E+00	0.
CL	.1303E-01	462.	.0000E+00	0.
H ₂ AD	.1027E-07	0.	.0000E+00	0.

FOR LIMESTONE UTILIZATION OF .800 AND KTAU =1123.403
LIMESTONE REACTIVITY EQUALS .30805E+06 IN THE SCRUBBER
AND

.55449E+08 IN THE HOLD TANK
THE AVERAGE FILM THICKNESS IS .39075E-03 CM
RELATIVE SATURATION

RSCASO₃= 4.1382
RSCASO₄= .54753
RSCACO₃= .40530E-01

YOU ARE USING THE LSODE DIFFERENTIAL EQUATION SOLVER

STAGE #	1	2	3
TOTAL OUTLET CONCENTRATION (GMOL/L)			
SO ₂ T	.1206E-01	.1728E-01	.2323E-01
CO ₂ T	.4517E-02	.2584E-02	.2047E-02
SO ₄ T	.1198E-01	.1227E-01	.1261E-01
CAT	.9168E-02	.1118E-01	.1408E-01
BULK COMPOSITION (GMOL/L)			
H+	.2289E-05	.5388E-05	.1059E-04
OH	.1944E-06	.8259E-07	.4201E-07
H ₂ CO ₃	.3250E-02	.2218E-02	.1888E-02
HCO ₃ -	.1266E-02	.3668E-03	.1589E-03
CO ₃ =	.1205E-05	.1483E-06	.3267E-07
H ₂ SO ₃	.1983E-05	.7839E-05	.2208E-04
HSO ₃ -	.8981E-02	.1508E-01	.2161E-01
SO ₃ =	.3073E-02	.2192E-02	.1598E-02
HSO ₄ -	.1361E-05	.3283E-05	.6633E-05
SO ₄ =	.1198E-01	.1227E-01	.1261E-01
H ₂ A	.8125E-10	.3440E-09	.9190E-09
HA-	.2074E-08	.3729E-08	.5068E-08
A=	.8119E-08	.6201E-08	.4287E-08
CA++	.9168E-02	.1118E-01	.1408E-01
CL-	.1303E-01	.1303E-01	.1303E-01
PH	5.722	5.351	5.057
% Removal	73.30	44.41	32.07

OVERALL % REMOVAL 89.92

STAGE #	1	2	3
GAS INLET CONCENTRATION (ATM.)			
PSO ₂	.1155E-02	.2078E-02	.3060E-02
PCO ₂	.6872E-01	.6811E-01	.6770E-01
PO ₂	.5802E-01	.5804E-01	.5806E-01
DEL.FLUX	.4941E-08	.1274E-07	.1759E-07
CACO ₃			
DEL.FLUX	.2668E-08	.4090E-08	-.9589E-09
CASO ₃			
FLUXSO ₂	.1905E-04	.1822E-04	.1893E-04
FLUXCO ₂	-.2084E-04	-.9725E-05	-.6578E-05
FLUXO ₂	.3236E-06	.3237E-06	.3238E-06

DIFFERENCE BETWEEN OUTLET AND INLET TOTAL CONC.(GMOL/L)			
SO2T	.4007E-02	.5227E-02	.5950E-02
CO2T	-.5964E-02	-.1932E-02	-.5374E-03
SO4T	.2011E-03	.2937E-03	.3419E-03
CAT	.4033E-03	.2011E-02	.2904E-02
Make Per	.4234E-02	.4616E-02	.4905E-02
Pass			
Scrubber	.8147E-03	.1247E-02	-.2489E-04
CASO3			
Scrubber	.4304E-03	.1106E-02	.1518E-02
CACO3			

CACO3 BOUNDARY CONDITION

	.4941E-08	.1274E-07	.1759E-07
CA++	.9492E-02	.1202E-01	.1524E-01
CO3=	.1607E-05	.5382E-06	.3407E-06
SO3=	.3463E-02	.3180E-02	.2919E-02
PH	5.783	5.525	5.331

SOLID CONCENTRATION(GMOL/L.SOLN)

CASO3(S)	1.019	1.018	1.017
MIXCRY	.1132	.1131	.1129
CACO3(S)	.2828	.2817	.2801
CASO4(S)	.1000E-02	.1000E-02	.1000E-02

RELATIVE SATURATION

RSCASO3	1.033	.8986	.8251
RSCASO4	.1999	.2496	.3232

HOLD TANK OUTLET TOTAL CONC. (GMOL/L)	
SO2T	.7904E-02
CO2T	.1005E-01
SO4T	.1171E-01
CAT	.8621E-02
BULK COMPOSITION (GMOL/L)	
H+	.1066E-05
OH	.4173E-06
H2CO3	.5469E-02
HCO3-	.4571E-02
CO3=	.9338E-05
H2SO3	.4687E-06
HSO3-	.4557E-02
SO3=	.3346E-02
HSO4-	.6200E-06
SO4=	.1171E-01
H2A	.1991E-10
HA-	.1091E-08
A=	.9163E-08
CA++	.8621E-02
CL-	.1303E-01
PH	6.054

AT THE SURFACE OF THE LIMESTONE

PH	6.064
CA++	0.8668E-02
CO3=	0.9611E-05
SO3=	0.3403E-02
CACO3 BC	0.7168E-09
DEL.FLUXCACO3	0.7168E-09
DEL.FLUXCASO3	-0.1723E-08
DEL.FLUXCASO4	-0.1905E-09

AIR STREAM INLET AND OUTLET COMPOSITION (ATM.)

	INLET	OUTLET
PCO2	.3300E-03	.1219
PO2	.2100	.2054

REL. SAT. CASO3 1.0580
REL. SAT. CASO4 .1837

INLET		OUTLET	
CASO3(S)	1.031	CASO3(S)	1.019
MIXCRY	.1140	MIXCRY	.1132
CACO3(S)	.2694	CACO3(S)	.2832
CASO4(S)	.1000E-02	CASO4(S)	.1000E-02

RUN CONCLUDED

APPENDIX D

SAMPLE FILES FOR PARAMETER ESTIMATION

D-1 DRIVER ROUTINE FOR CALLING GREG (P_EST.F)

```
C*****
C  AUTHOR:    Rajesh Agarwal
C  FILE:      p_est.f (subroutine model and main program)
C  PURPOSE:   To call subroutine GREG for calculation of model parameters
C*****
C  implicit real*8 (a-h, o-z)
C  implicit integer*4 (i-n)
C  real*8 NL, K(50), NTUSP, NTUSP1
C  parameter (npars=3,nobs=11)
C  EXTERNAL MODEL

C  dimension obs(nobs), par(npars), bndlwn(npars), bndup(npars),
C  $ chmax(npars)
C  dimension dsc(119), isc(28), iobs(nobs), idet(1), del(npars)

c  data from EPA/RTP for -lnp
c  data obs/1.27,
c  $ 1.89,
c  $ 0.79,
c  $ 1.56,
c  $ 1.71,
c  $ 1.20,
c  $ 1.04,
c  $ 2.99,
c  $ 2.40,
c  $ 2.07,
c  $ 2.52/

c  data from EPA/RTP for p
c  data obs/0.28,
c  $ 0.15,
c  $ 0.45,
c  $ 0.21,
c  $ 0.18,
c  $ 0.30,
c  $ 0.35,
c  $ 0.05,
```

```

c      $      0.09,
c      $      0.12,
c      $      0.08/

common/parameters/ntusp1,rklkg1,react1,scale

c
c      open input files p_est.dat and mdiva.dat
c
c      open(unit=5,file='p_est.dat',status='unknown')

c      open(unit=17,file='mdiva.dat',status='old')
c      open(unit=11,file='mdiva1.out',status='new')

c*****
C      checks if estimation is to be done
c      GREG is called if iest .eq. 1
c*****

c      read(5,*)iest

c      initialize the parameter values
c      read(5,*)ntusp1
c      read(5,*)rklkg1

c
c      Change the variable rklkg1 to store the value of the product
c      b/w rklkg1 and ntusp1.
c      also make change in subroutine model
c
c      rklkg1 = rklkg1 * ntusp1

c
c      normalize all the parameters
c
c      par(1) = 1
c      par(2) = 1
c      par(3) = 1

c*****
c variables
C      NOB = TOTAL # OBSERVATIONS
C      NPAR = # PARAMETERS TO BE ESTIMATED
C      BNDLW = LOWER BOUNDS ON PARAMETERS
C      BNDUP = UPPER BOUNDS ON PARAMETERS
C      CHMAX = TRUST REGION OF QUADRATIC APPROXIMATION

```

```

C  MDSC = DIMENSION OF ARRAY DSC
C  MISC = DIMENSION OF ARRAY ISC
C*****

      npar=3
      do 10 i=1, npar
        read(5,*)bndup(i),bndlwl(i)
        chmax(i) = -1.0
        del(i) = -10.0d-2
10    continue

c      call mdiva(rklkg1,ntusp1,dba1,scale,u1,iest)
        if(iest.ne.1)stop

      nob=11
      mdsc = 119
      misc = 28

C*****
C  RPTOL = TOLERANCE FOR ACCURACY OF PARAMETER VALUES
C  RSTOL = TOLERANCE OF PARAMETER VALUES
CC  VPIV = SMALLEST ACCEPTABLE RATIO OF A PIVOT ELEMENT
TO ORIGINAL IN THE MOMENT MATRIX OF RESIDUALS
C  APIV = SMALLEST ACCEPTABLE RATIO OF A PIVOT ELEMENT
FOR NORMAL EQUATIONS
C*****

      rptol = 1d-2
      rstol = 1.0d-2
      vpiv = 1d-2
      apiv = 1.0d-2

c
C  INITIALIZE THE ISC ARRAY
c
C*****
C  ISC(1) = SEQUENCE # OF PROBLEM BEING SOLVED
C  ISC(2) = TYPE OF REGRESSION
C  ISC(3) = DEFAULT FLAG FOR
BNDLW,BNDUP,CHMAX,DEL,APIV,VPIV,RPTOL
C          RSTOL,LISTS,ITMAX,IDIF{C  ISC(NOBS) = MAXIMUM #
ITERATIONS
C  ISC(5) = PRINTOUT FLAG
C  ISC(6) = TOTAL # OF EXPERIMENTS
C  ISC(7) = NUMBER OF UNCORRELATED GROUPS OF RESPONSES
C  ISC(8) = ORDER OF THE VARIANCE-COVARIANCE MATRIX
C  ISC(9) = PROCEDURE OF FINITE DIFFERENCE CALCULATIONS

```



```

c*****

isc(1) = 1
isc(2) = 20
      write(6,*)isc(2)
isc(3) = 1

isc(4) = 25
isc(5) = 5
isc(6) = 11
isc(7) = 1      !2 for 2 response fit
isc(8) = 1
isc(9) = 1
      emod = 1d-2
c
C   INPUT THE DATA STRUCTURE
c

      idet(1) = 1
      do 35 i=1, nobs
        iobs(i) = 1
35    continue
c
C   CALL THE REGRESSION ROUTINE
c
      call greg (nob, obs, npar,par,bndlwbndup,chmax,del,mdsc,dsc,
&    misc, isc, iobs, idet, emod, vpiv, apiv, rptol, rstol,
& model)
      stop
      end

      subroutine model(par, f, nob, npar, ider, deriv, minfo)

c
c   this program computes the predicted responses
c

c*****
C   PAR = CURRENT VALUE OF PARAMETER VECTOR
C   F = PREDICTED VALUES OF RESPONSES
C   IDER = USED TO SPECIFY TASKS FOR MODEL
C   DERIV = CONTAINS THE FIRST DERIVATIVES OF PREDICTED
RESPONSESD
C   MINFO = USED TO INDICATE IF SOMETHING WENT WRONG
c*****

```

```

implicit double precision(a-h, o-z)
dimension par(1), f(1,11), deriv(3, 12, 1), t(12), rpar(3)
real*8 ntusp, ntusp1, nmix,nl, k(50)
parameter (nexp=11)
dimension ovreme(nexp), dba(nexp),u(nexp)
dimension cc(9,nexp),uu(nexp),ph(nexp),ss(nexp),ox(nexp),
$  pout(nexp),pin(nexp)

C  COMMON BLOCK ADDED FOR PARAMETER ESTIMATION
common/removal/ovrem
common/phvalue1/ph
common/phvalue2/inexp
C*****
C
C  these common blocks ; INPUT2 and RTIME are added for passing
C  paramters to and from the paramter estimation routine
C
C*****
COMMON /INPUT2/RLG,XKSP(3,2),EF,NMIX

COMMON /RTIME/TAUSC,TAUHT,DELAVE
common/inputsp/ so2in, fsp, ntusp

C*****
C  The common block ph1 passes the value of ph calculated by the
C  model ( at the hold tank exit)
C*****
common/ph1/htph
common/parameters/ntusp1,rklkg1,react1,scale
common/model1/rntusp
common/casedata/u2,ph1,s1,ox1,pin1,pout1,cs1(9)

iter = iter + 1
if(iter.eq.1)then
  do 5 i=1, nexp

    read(5,*)(cc(j,i),j=1,9)
    write(*,*)(cc(j,i),j=1,9)
    read(5,*)uu(i),ph(i)
    write(*,*)uu(i),ph(i)
    read(5,*)ss(i),ox(i)
    write(*,*)ss(i),ox(i)
    read(5,*)pout(i),pin(i)
    write(*,*)pout(i),pin(i)
5  continue

```

```

else
endif

do 10 i=1, nexp
  iobs1 = 1
  inexp=i
  write(10,*)'inexp=',inexp

c*****
c
c The paramters are scaled appropriately and passed to the model.
c In addition to the parameters NTUSP1, RKLKG1,XKSP(3,2),XKSP(3,1)
c The dba conc. is also passed as DBA1

c*****

  rntusp = par(1)*ntusp1
c
c Change the value of rklkg to divide out the effect of Ng
c also make change in main program
c   rklkg = par(2)*rklkg1 !
c

  rklkg = par(2) * rklkg1/rntusp

  dba1 = dba(i)
  u1 = u(i)
c   xscale = par(3) *scale

  xscale = 1.0 ! for matching pH
c*****
c assign data values to the appropriate variables
c
  u2 = uu(i)
  ph1 = ph(i)
  s1 = ss(i)
  ox1 = ox(i)
  pin1 = pin(i)
  pout1 = pout(i)
  do 15 j = 1,9
    cs1(j) = cc(j,i)
15  continue
  iest = 1
  write(10,*)' from model ntusp=',ntusp
  write(10,*)'rklkg=',rklkg,'u1=',u2
  call mdiva(rklkg,rntusp,dba1,xscale,u1,iest)
  f(1,i) = -dlog(1- ovrem/100)

```

```
c      modify for penetration instead of lnp
c      f(1,i) = 1 - ovrem/100

c      f(2,i) = htph
      write(10,*)'f(1,*)=',f(1,i),'ovrem=',ovrem
      write(10,*)'f(2,*)=',f(2,i),'htph=',htph

10 continue

      return
      end
```

D-2 INPUT FILE FOR PARAMETER ESTIMATION (EPA/RTP DATA).

filename: p_est.dat

```

1      !flag for estimation (y=1,n=0)
.964   !ng
291.9  !rklkg
.0015  !dba
1.0    !scale
0      !flag for tester (y=1,n=0)
4,0.1  ! upper and lower bounds on the 3 parameters respectively
3,0.1
1,1.0
383.,283.,248.,0.,2260.,1320.,292.,462.,0.0015      !solution composition
65.3,5.50      ! utilization, pH
15,10      ! solids(%),oxidation(%)
1.3e-3,2.9e-3 ! so2 out (ppm), so2 in (ppm)
383.,283.,248.,0.,2260.,1320.,292.,462.,0.0015
45.3,5.80
15,10
3.4e-4,2.9e-3
383.,283.,248.,0.,2260.,1320.,292.,462.,0.0015
82,5.00
15,10
6e-4,2.9e-3
383.,283.,248.,0.,2260.,1320.,292.,462.,1620
91,5.00
15,10
1e-3,2.9e-3
383.,283.,248.,0.,2260.,1320.,292.,462.,2200
95.0,5.00
15,10
1.0e-3,2.90e-3
383.,283.,248.,0.,2260.,1320.,292.,462.,1000
91.3,5.00
15,10
4e-4,2.9e-3
383.,283.,248.,0.,2260.,1320.,292.,462.,1000
91,4.80
15,10
5e-4,2.9e-3
383.,283.,248.,0.,2260.,1320.,292.,462.,1000
68,5.80
15,10
14e-4,2.9e-3

```

383.,283.,248.,0.,2260.,1320.,292.,462.,1000
73,5.60
15,10
5e-4,2.9e-3
383.,283.,248.,0.,2260.,1320.,292.,462.,1000
84,5.40
15,10
14e-4,2.9e-3
383.,283.,248.,0.,2260.,1320.,292.,462.,3600
88,5.00
15,10
14e-4,2.9e-3

D-3 INPUT FILE FOR PARAMETER ESTIMATION (SHAWNEE DATA).

```

1      !flag for estimation (y=1,n=0)
1.00   !ng
200    !rklkg
.0015  !dba
1      !scale
0      !flag for tester (y=1,n=0)
4,0.1  ! upper and lower bounds on 3 parameters respectively
4,0.1
10,0.1
1060.,215.,35.,45.,295.,1565.,292.,1010.,.0015      !926-2a
80,5.65      ! utilization, pH
15.1,12.0    ! solids(%),oxidation(%)
7e-4,2.75e-3 ! so2 out (ppm), so2 in (ppm)
1515.,655.,55.,110.,450.,2290.,292.,2445.,350      !927-2a
84,5.3
14.6,19
5.75e-4,2.3e-3
1940.,755.,70.,110.,300.,1940.,292.,3225.,1600      !928-2a
85,5.40
14.9,14
1.8e-4,2.6e-3
1985.,765.,70.,100.,255.,2100.,292.,3565.,885      !929-2a
80,5.5
15,10
1.8e-4,2.3e-3
1960.,825.,75.,100.,190.,1560.,292.,4005.,700      !930-2a
75,5.6
15,13
1.8e-4,2.55e-3
2105.,875.,75.,125.,1025.,2160.,292.,4030.,840      !931-2a
93,4.95
13.9,24
5.3e-4,2.3e-3
2180.,625.,55.,80.,245.,1850.,292.,3875.,.0015      !933-2a
83,5.45
13.8,24
4.7e-4,1.95e-3

```

Input file with description of operating parameters for the turbulent contact absorber and particle size distribution of limestone (same for EPA/RTP and Shawnee).

filename: mdiva.dat

FRED.COARSE-4

1,1

1,333.0,6.1

1120.,283.,0.0,0.0,170.,672.,284.,6300.,0.0015

5.4E-4,0.07,0.058,200.0

0.23,1.0

3.0E5,3.0E5

2.9E-3,2.3,11,10

3,1.0E-2

1,77

8.4,12.2 ! (percent solid and oxidation respectively)

1.0,540.0,765. ! changed from .05 to 3 (change tres)

0.33d-3,0.21

45.0,0.80,0.90 !

11.2500,1.0

1.0,.60

27

0.794,0.4

1.0,1.1

1.26,2.0

1.59,3.1

2.0,4.2

2.52,5.3

3.17,5.1

4.0,3.7

5.04,2.8

6.35,2.4

8.0,2.2

10.08,2.2

12.7,2.5

16.0,2.9

20.2,3.3

25.4,4.1

32.0,4.7

40.3,5.8

50.8,7.2

64.0,7.4

80.6,8.8

101.6,8.5

128.0,4.9

161.0,3.2

210.,1.7

297.0,0.6
420.,0.2

D-4 OUTPUT FILE SHOWING RESULTS OF REGRESSION (EPA/RTP DATA).

```

***** G R E G *****
***** General Regression Software Package *****
***** for Nonlinear Parameter Estimation. *****
***** Version of August, 1990 *****
*****

```

```

***** Level = 20 *****
***** modified Box-Draper objective *****
***** with optional numerical derivatives. *****
*****

```

```

***** Data structure *****

```

```

1
1
1
1
1
1
1
1
1
1
1
1

```

Start of problem no. 1 with 11 observations and 3 parameters

```

BNDUP(I)= 4.000000D+00 3.000000D+00 1.000000D+00
PAR(I) = 1.000000D+00 1.000000D+00 1.000000D+00
BNDLW(I)= 1.000000D-01 1.000000D-01 1.000000D+00

```

```

DEL(I) = -2.500000D-02 -2.500000D-02 -2.500000D-02
CHMAX(I)= -1.000000D+00 -1.000000D+00 0.000000D+00

```

```

VPIV = 1.0000D-02 RSTOL = 1.0000D-02 ITMAX = 25 LISTS = 5
APIV = 1.0000D-02 RPTOL = 1.0000D-02 IDIF = 1
EMOD = 1.0000D-02

```

All derivatives are obtained by finite differences

***** Iteration no. 1 no. of function calls 0 *****
 PAR(I) = 1.000000D+00 1.000000D+00 1.000000D+00
 ***** Moment matrix of the residuals *****
 8.8571D-01

Normalized diagonal of factored residual moment matrix; RANK = 1
 Elements near VPIV (= 1.0000D-02) or less indicate linear dependence.

1.0000D+00

**** Current value of the objective function = -1.33497D+00 ****

***** Matrix of normal equations *****

1.9915D+02
 9.8519D+01 8.8185D+01
 0.0000D+00 0.0000D+00 0.0000D+00
 -5.6528D+00 3.7923D-02 0.0000D+00 -1.3350D+00

The pivotal element is : 1
 The pivotal increment is : -2.8385D-02
 Solution arrays after 1 transformations:

LBAS(I) = 1 0 0
 LBOX(I) = 0 0 -3
 PAR(I) = 9.716151D-01 1.000000D+00 1.000000D+00
 Transformed matrix a including basis inverse
 5.0214D-03 4.9470D-01 0.0000D+00 0.0000D+00
 -4.9470D-01 3.9448D+01 0.0000D+00 2.8344D+00
 0.0000D+00 0.0000D+00 0.0000D+00 0.0000D+00
 0.0000D+00 2.8344D+00 0.0000D+00 -1.6045D-01

The pivotal element is : 2
 The pivotal increment is : 7.1850D-02
 Solution arrays after 2 transformations:

LBAS(I) = 1 2 0
 LBOX(I) = 0 0 -3
 PAR(I) = 9.360708D-01 1.071850D+00 1.000000D+00
 Transformed matrix a including basis inverse
 1.1225D-02 -1.2540D-02 0.0000D+00 0.0000D+00
 -1.2540D-02 2.5350D-02 0.0000D+00 0.0000D+00
 0.0000D+00 0.0000D+00 0.0000D+00 0.0000D+00
 0.0000D+00 0.0000D+00 0.0000D+00 -3.6411D-01

Quadratic minimization has been completed in 2 steps
 Determinant is 7.856*10** 3 with 2 normal equations solved,

1 active constraints and 1 indeterminate parameters

The basic parameters are:

1 2 0

The constrained parameters are:

0 0 -3

Matrix solution predicts $S = -1.69907D+00$ at $H = 1.$,
with the following parameter values:

PAR(I) = 9.360708D-01 1.071850D+00 1.000000D+00

Summary of search:	grid points	factor RHO:=
HT	ST	(ST-S0)/(PRED S1-S0)
1.00000D+00	-1.97415D+00	1.75548D+00

The grid point at $H = 1.00000D+00$ is selected.

***** Iteration no. 2 no. of function calls 4 *****

***** Moment matrix of the residuals *****

8.3571D-01

Normalized diagonal of factored residual moment matrix; RANK = 1
Elements near VPIV (= 1.0000D-02) or less indicate linear dependence.

1.0000D+00

**** Current value of the objective function = -1.97415D+00 ****

***** Matrix of normal equations *****

5.4347D+02			
-1.8447D+02	3.6715D+02		
0.0000D+00	0.0000D+00	0.0000D+00	
1.2615D+01	-2.2872D+01	0.0000D+00	-1.9741D+00

The pivotal element is : 1

The pivotal increment is : 2.3211D-02

Solution arrays after 1 transformations:

LBAS(I) = 1 0 0

LBOX(I) = 0 0 -3

PAR(I) = 9.592821D-01 1.071850D+00 1.000000D+00

Transformed matrix a including basis inverse

1.8400D-03	-3.3942D-01	0.0000D+00	0.0000D+00
3.3942D-01	3.0454D+02	0.0000D+00	-1.8590D+01
0.0000D+00	0.0000D+00	0.0000D+00	0.0000D+00

0.0000D+00 -1.8590D+01 0.0000D+00 -2.9280D-01

The pivotal element is : 2

The pivotal increment is : -6.1043D-02

Solution arrays after 2 transformations:

LBAS(I) = 1 2 0

LBOX(I) = 0 0 -3

PAR(I) = 9.385626D-01 1.010807D+00 1.000000D+00

Transformed matrix a including basis inverse

2.2183D-03	1.1146D-03	0.0000D+00	0.0000D+00
1.1146D-03	3.2837D-03	0.0000D+00	0.0000D+00
0.0000D+00	0.0000D+00	0.0000D+00	0.0000D+00
0.0000D+00	0.0000D+00	0.0000D+00	-1.4276D+00

Quadratic minimization has been completed in 2 steps

Determinant is 1.655*10** 5 with 2 normal equations solved,

1 active constraints and 1 indeterminate parameters

The basic parameters are:

1 2 0

The constrained parameters are:

0 0 -3

Matrix solution predicts S = -3.40174D+00 at H = 1.,

with the following parameter values:

PAR(I) = 9.385626D-01 1.010807D+00 1.000000D+00

***** Moment matrix of the residuals *****

7.9951D-01

Normalized diagonal of factored residual moment matrix; RANK = 1

Elements near VPIV (= 1.0000D-02) or less indicate linear dependence.

1.0000D+00

**** Current value of the objective function = -2.46130D+00 ****

***** Matrix of normal equations *****

7.4562D+02			
1.7075D+03	6.4969D+03		
0.0000D+00	0.0000D+00	0.0000D+00	
-1.4432D+01	-8.1708D+01	0.0000D+00	-2.4613D+00

The pivotal element is : 1

The pivotal increment is : -1.9356D-02

Solution arrays after 1 transformations:

LBAS(I) = 1 0 0

LBOX(I) = 0 0 -3

PAR(I) = 9.167152D-01 1.071850D+00 1.000000D+00

Transformed matrix a including basis inverse

1.3412D-03	2.2901D+00	0.0000D+00	0.0000D+00
-2.2901D+00	2.5866D+03	0.0000D+00	-4.8658D+01
0.0000D+00	0.0000D+00	0.0000D+00	0.0000D+00
0.0000D+00	-4.8658D+01	0.0000D+00	-2.7934D-01

The pivotal element is : 2

The pivotal increment is : -1.8812D-02

Solution arrays after 2 transformations:

LBAS(I) = 1 2 0

LBOX(I) = 0 0 -3

PAR(I) = 9.597960D-01 1.053038D+00 1.000000D+00

Transformed matrix a including basis inverse

3.3687D-03	-8.8537D-04	0.0000D+00	0.0000D+00
-8.8537D-04	3.8661D-04	0.0000D+00	0.0000D+00
0.0000D+00	0.0000D+00	0.0000D+00	0.0000D+00
0.0000D+00	0.0000D+00	0.0000D+00	-1.1947D+00

Quadratic minimization has been completed in 2 steps

Determinant is 1.929*10** 6 with 2 normal equations solved,

1 active constraints and 1 indeterminate parameters

The basic parameters are:

1 2 0

The constrained parameters are:

0 0 -3

Matrix solution predicts S = -3.65600D+00 at H = 1.,

with the following parameter values:

PAR(I) = 9.597960D-01 1.053038D+00 1.000000D+00

***** S cannot be reduced further for the model and derivatives as calculated.

***** Final value of objective function = -2.46130D+00 *****

***** 95% HPD intervals PAR(I)+-DIF(I) for parameters in basis; *****

**** last value and bounds for any parameters that are not in basis ****

UPR(I) = 1.049831D+00 1.110389D+00 1.000000D+00
 PAR(I) = 9.360708D-01 1.071850D+00 1.000000D+00
 LWR(I) = 8.223107D-01 1.033312D+00 1.000000D+00
 DIF(I) = 1.137601D-01 3.853848D-02 1.000000D+30

Normalized test divisors for final basis selection.
 values near .010000(=APIV) or less indicate indeterminate parameters.

.398121 .398121 .000000

The model parameter estimate consists of the particular vector PAR just given,
 plus an arbitrary linear combination of the null-space basis vectors which follow.
 Vector I is the derivative of this solution
 with respect to parameter I.

Vector 3:
 .000 .000 -1.000

Normalized covariances of parameter estimates

1.00000
 -.77581 1.00000
 .00000 .00000 .00000

observed values	predicted values	residuals
1.27000D+00	1.06943D+00	2.00567D-01
1.89000D+00	1.53695D+00	3.53054D-01
7.90000D-01	6.49272D-01	1.40728D-01
1.56000D+00	1.89782D+00	-3.37821D-01
1.71000D+00	2.05772D+00	-3.47719D-01
1.20000D+00	1.57742D+00	-3.77421D-01
1.04000D+00	1.22555D+00	-1.85553D-01
2.99000D+00	2.53285D+00	4.57149D-01
2.40000D+00	2.41096D+00	-1.09620D-02
2.07000D+00	2.19181D+00	-1.21814D-01
2.52000D+00	2.31867D+00	2.01335D-01

MIN = -3.77421D-01 MAX = 4.57149D-01

End of problem no. 1 no. of function calls = 28
 no. of iterations = 3

ng=0.96
 klkg=291.9
 scale=52.6, 21.3, 11.8, 76.9, 11.0, 4.3, 71.4, 8.5, 9.5, 10.0, 5.0

D-5 CALCULATED VALUES OF THE H MATRIX (EPA/RTP DATA).

$$N_g=2.88, k_L k_g = 292$$

$$\mathbf{H} = \begin{bmatrix} 516.38 & 154.75 \\ 154.75 & 57.9 \end{bmatrix}$$

$$N_g=2.88, N_L = 3.65$$

$$\mathbf{H} = \begin{bmatrix} 230.15 & 78.58 \\ 78.58 & 57.9 \end{bmatrix}$$

REFERENCES CITED

- Acurex Corporation, "Pilot Plant Tests of Chloride Ion Effects on Wet FGD System Performance," Draft Final Report, EPA Contract No. 68-02-3648, (June, 1983).
- Agarwal, R. S., and G. T. Rochelle, "Chemistry of Limestone Slurry Scrubbing," presented at the SO₂ Control Symposium, Boston (August, 1993).
- Bard Y., *Non Linear Parameter Estimation*, Academic Press, New York (1977).
- Box, G. E. P., and N. R. Draper, "Bayesian Estimation of Common Parameters from Several Responses," *Biometrika*, **52**, 355 (1965).
- Box, G. E. P., and N. R. Draper, "Estimation and Design Criteria for Multi-response Non-Linear Models with Non-Homogenous Variance," *Appl. Statistics*, **21**, 13 (1972).
- Burbank, D. A., and S. C. Wang, "Adipic Acid-Enhanced Lime and Limestone Testing at the EPA Alkali Scrubbing Test Facility," EPA 68-02-3114 (1981).
- Caracotsios, M. L., "Model Parametric Sensitivity Analysis and Nonlinear Parameter Estimation, Theory and Applications," Ph.D. Dissertation, University of Wisconsin-Madison (1986).
- Chan, P. K., and G. T. Rochelle, "Limestone Dissolution - Effects of pH, CO₂, and Buffers Modeled by Mass Transfer," *ACS Symp. Ser.*, **188**, 75 (1982).
- Chan, P. K., and G. T. Rochelle, "Modeling of SO₂ Removal by Limestone Slurry Scrubbing: Effects of Chlorides," presented at EPA/EPRI Symposium on Flue Gas Desulfurization, New Orleans (1983).
- Chan, P. K., and G. T. Rochelle, "Modeling of SO₂ Removal by Limestone Slurry Scrubbing: Effects of Chlorides," Proceedings: 8th Symposium on Flue Gas Desulfurization EPA-600/9-84-017a, 7:57-78 (1984).
- Chang, J. C. S., and D. Laslo, "Chloride Ion Effects on Limestone FGD System Performance", presented at the EPA/EPRI FGD Symposium, Hollywood, Florida (1982).
- Chang, J. C. S., and G. T. Rochelle, "Effect of Organic Acid Additives on SO₂ Absorption into CaO/CaCO₃ slurries," *AIChE J*, **28** (2), 261 (1982).

- Chang, J. C. S., and G. T. Rochelle, "SO₂ absorption into NaOH and Na₂SO₃ Aqueous Solutions", *Ind. Eng. Chem. Fundam.*, **24**, 7 (1985).
- Chang, J. C. S., and G. T. Rochelle, "Surface Renewal Theory for Simultaneous Mass Transfer and Chemical Reaction," presented at AIChE National Meeting, Philadelphia (June, 1980).
- Chang, J. C. S., and J. H. Dempsey, "Limestone Slurry Scrubbing of SO₂ at EPA/RTP Pilot Plant," EPA contract no. 68-02-3648, project no. 7676, progress reports 51-53 (1981).
- Chang, J. C. S., and J. H. Dempsey, "Pilot Plant Evaluation of By-Product Dibasic Acids as Buffer Additives for Limestone Flue Gas Desulfurization Systems," presented at the EPA/EPRI FGD Symposium, Hollywood, Florida (1982).
- Chen, B. H., and W. J. M. Douglas, "Liquid Hold-up and Minimum Fluidization Velocity in a Turbulent Contactor," *Can. J. Chem. Eng.*, **46**, 1245 (1968).
- Chen, B. H., and W. J. M. Douglas, "Axial Mixing of Liquid in a Turbulent Bed Contactor," *Can. J. Chem. Eng.*, **47**, 133 (1969).
- Davies, C.W., *Ion Association*, Washington, D.C., Butterworths (1962).
- Dempsey, J. H., J. C. S. Chang, and J. A. Mulholland, "Operation of EPA Owned Pilot SO₂ Scrubber and High Temperature Baghouse," Acurex-RTP Progress Report-39: EPA Contract No. 68-02-3648 (March, 1979).
- Dempsey, J. H., J. C. S. Chang, and J. A. Mulholland, "Operation of EPA Owned Pilot SO₂ Scrubber and High Temperature Baghouse," EPA Contract No. 68-02-3648, Progress Report No. 7676-33 (August, 1983).
- Donaldson, J. R., and R. B. Schnabel, "Computational Experience with Confidence Regions and Confidence Intervals for Non Linear Least Squares," *Technometrics*, **29** (1), 67 (1987).
- Douglas, W. J. M., "Heat and Mass Transfer in a Turbulent Bed Contactor, " *Chem. Eng. Progr.*, **60** (7), 66 (1964).
- Epstein, M., "EPA Alkali Scrubbing Test Facility : Summary of Testing through October 1974", EPA-650/2-75-047, NTIS No. PB-244 901 (1975).
- Epstein, M., L. Siebert, and I. A. Raben, "EPA Alkali Scrubbing Test Facility: Sodium Carbonate and Limestone Test Results," EPA Contract No. 650/2-73-013 (August, 1973).

- Gage, C. L., "Limestone Dissolution in Modeling of Slurry Scrubbing for Flue Gas Desulfurization," Ph.D. Dissertation, University of Texas, Austin (1989).
- Gage, C. L., "Modeling of SO₂ Removal in Slurry Scrubbing as a Function of Limestone Type and Grind," Proceedings: 1990 SO₂ Control Symposium, EPRI GS-6963, 3, 143 (September, 1990).
- Gage, C. L., and G. T. Rochelle, "Limestone Dissolution in Flue Gas Scrubbing: Effect of Sulfite," *J. Air Waste Manage. Assoc.*, **42** (7), 926 (1992).
- Garrels, R. M., and C. L. Christ, *Solutions, Minerals and Equilibria*, Harper and Row, New York (1965).
- Harned, H. S., and B. B. Owen, *The Physical Chemistry of Electrolytic Solutions*, Third Edition, Reinhold, New York (1958).
- Head, H. N., "EPA Alkali Scrubbing Test: Advanced Program, Third Progress Report," EPA-600/7-77-105 (September, 1977).
- Jarvis, J., D. A. Stewart, and T. Trofe, "Effects of High Dissolved Chloride on Bence Scale FGD Performance," presented at the EPA/EPRI Symposium on Flue Gas Desulfurization, New Orleans (1983).
- Klotz, I. M., *Chemical Thermodynamics*, Benjamin, New York (1964).
- Lasdon, L. S., and A. D. Warren, "GRG2 User's Guide," available from, Department of General Business, School of Business Administration, University of Texas, Austin, Texas 78712 (1986).
- Laslo, D., J. C. S. Chang, and J. D. Mobley, "Pilot Plant Tests on the Effects of Dissolved Salts on Lime/Limestone FGD Chemistry," presented at the EPA/EPRI Symposium on Flue Gas Desulfurization, New Orleans (November, 1983).
- Lowell, P. S., D. M. Ottmers, K. Schwitzgebel, T. I. Strange, and D. W. Deberry, "A Theoretical Description of the Limestone Injection-Wet Scrubbing Process," USEPA, APID 1287, PB 1931-029 (1970).
- Mehta, R. R., "Modeling of SO₂ Removal and Limestone Utilization in Slurry Scrubbing Systems with Forced Oxidation," M.S. Thesis, University of Texas, Austin (1982).
- Miller, S. M., "Modeling and Quality Control Strategies for Batch Cooling Crystallizers," Ph. D. Dissertation, University of Texas, Austin (1993).

- Mobley, J. D., and J. C. S. Chang, "The Adipic Acid Enhanced Limestone Flue Gas Desulfurization Process- An Assessment," *JAPCA*, **31**, 1249 (1981).
- Neeter J., W. Wasserman, and M. J. Kutner, *Applied Linear Statistical Methods*, Third edition, IRWIN, Boston (1990).
- Noblett, J. G. , D. P. DeKraker, and R. E. Moser, "FGDPRISM, EPRI's FGD Process Model - Recent Applications," presented at the EPA/EPRI Symposium on Flue Gas Desulfurization, Washington (1990).
- Noblett, J. G. , M. J. Hebets, and R. E. Moser, "EPRI's FGD Process Model (FGDPRISM)," presented at the EPA/EPRI Symposium on Flue Gas Desulfurization, New Orleans (1991).
- Noblett, J. G., T. M. Shires, and R. E. Moser, "Update on Electric Power Research Institute's FGDPRISM Process Simulation Model (Version 2.0)," presented at the EPA/EPRI Symposium on Flue Gas Desulfurization, Boston (1993).
- Pepe, F., "Limestone Slurry Scrubbing - Modeling of Forced Oxidation", Report, Department of Chemical Engineering, University of Texas at Austin (1993).
- Plummer, L.N., and E. Busenberg, "The Solubilities of Calcite, Aragonite, and Vaterite in CO₂-H₂O Solutions between 0 and 90° C, and the Evaluation of the Aqueous Model for the System CaCO₃-CO₂-H₂O", *Geochim. Cosmochim. Acta.*, **46**, 1011 (1982).
- Rochelle, G. T., "Buffer Additives for Limestone Scrubbing: A Review of R & D Results", presented at the EPA/EPRI Symposium, Florida (1982).
- Rochelle, G. T., W. T. Weems, R. J. Smith, and M. W. Hsiang, "Buffer Additives for Lime/ Limestone Slurry Scrubbing," *ACS Symp. Ser.* , **188**, 243 (1982).
- Sharma, M. M., and L. K. Doraiswamy, *Heterogeneous Reactions: Analysis, Examples, and Reactor Design*, **2**, 323, John Wiley & Sons (1983).
- Sharma, M. M., and R. K. Gupta, "Mass Transfer Characteristics of Plate Columns Without Downcomers," *Trans. Instn. Chem. Engrs.*, **45**, T169 (1967).
- Smith, J. M., *Chemical Engineering Kinetics*, McGraw Hill (1981).
- Stewart, W. E. , and J. P. Sorenson, "Bayesian Estimation of Common Parameters from Multiresponse Data with Missing Observations," *Technometrics*, **23** (2), (1981).

- Stewart, W. E., "Multi-response Parameter Estimation with a New and Non Informative prior," *Biometrika*, **74**, 557 (1987).
- Stewart, W. E., M. Caracotsios, and J. P. Sorenson, "Parameter Estimation from Multi-response Data," *AIChE J*, **38** (5), 641 (1992).
- Toprac, A. J. , and G. T. Rochelle, "Limestone Dissolution in Stack Gas Desulfurization Processes - Effects of Type and Grind," *Env. Prog.*, **1**(1), 52 (1982).
- Toprac, A. J., "Limestone Dissolution in Stack Gas Desulfurization Processes," M.S. Thesis, University of Texas, Austin (1981).
- Tseng, P. C., "Calcium Sulfitte Hemihydrate Dissolution and Crystallization," Ph.D. Dissertation, University of Texas, Austin (1984).
- Tseng, P. C., and G.T. Rochelle, "Dissolution Rate of Calcium Sulfitte Hemihydrate in Flue Gas Desulfurization Processes," *Envir. Prog.*, **5**, 34 (1986).
- Vandekemp, R. M., "Modeling of Limestone Slurry Scrubbing in Plug-Flow and Well-Mixed Contactors," M.S. Thesis, University of Texas, Austin (1993).

Vita

Rajesh Satish Agarwal was born in Lucknow, Uttar Pradesh, India on April 14, 1968, the son of Satish Kumar and Rajyashri Agarwal. After graduation from Mithibai College in 1985, he entered the Department of Chemical Technology at the University of Bombay (U.D.C.T.). He earned a Bachelor of Chemical Engineering (B. Chem. Engg.) degree in July, 1989. In August, 1989 he joined the graduate program in Chemical Engineering at The University of Texas at Austin. He received a M.S. degree in December, 1992.

Permanent address: 501 Sea Castle
Seven Bungalows Road, Andheri (West)
Bombay - 400 061, INDIA

This dissertation was typed by the author.